This is a repository copy of *Search for singly produced vectorlike top partners in multilepton final states with 139 fb−1 of pp collision data at s =13 TeV with the ATLAS detector*.

White Rose Research Online URL for this paper:
https://eprints.whiterose.ac.uk/215557/

Version: Published Version

eprints@whiterose.ac.uk
https://eprints.whiterose.ac.uk/

Search for singly produced vectorlike top partners in multilepton final states with 139 fb^{-1} of pp collision data at $\sqrt{s} = 13$ TeV with the ATLAS detector

G. Aad *et al.*[*]

(ATLAS Collaboration)

A search for the single production of a vectorlike top partner (T) with mass greater than 1 TeV decaying into a Z boson and a top quark is presented, using the full Run 2 dataset corresponding to 139 fb^{-1} of pp collisions at $\sqrt{s} = 13$ TeV, collected in 2015–2018 with the ATLAS detector at the Large Hadron Collider. The targeted final state is characterized by the presence of a pair of electrons or muons with opposite-sign charges which form a Z-boson candidate, as well as by the presence of b-tagged jets and forward jets. Events with exactly two or at least three leptons are categorized into two independently optimized analysis channels. No significant excess above the background expectation is observed and the results from the two channels are statistically combined to set exclusion limits at 95% confidence level on the masses and couplings of T. The results are interpreted in several benchmark scenarios to set limits on the mass and universal coupling strength (κ) of the vectorlike quark. For singlet T quarks, κ values between 0.22 and 0.64 are excluded for masses between 1000 and 1975 GeV. For T quarks in the doublet scenario, where the production cross section is much lower, κ values between 0.54 and 0.88 are excluded for masses between 1000 and 1425 GeV.

I. INTRODUCTION

The discovery of the Higgs boson by the ATLAS and CMS experiments at the Large Hadron Collider (LHC) [1,2] was a major milestone for the Standard Model (SM), the framework for understanding the fundamental constituents of our universe and their interactions. While finding the Higgs boson completed the SM, this model leaves many questions unaddressed about the physical nature of our universe. One of these questions is about the measured Higgs boson mass—specifically, the many orders of magnitude that separate it from the Planck scale, requiring quadratically divergent finely tuned corrections [3]. These large corrections are mitigated in some beyond Standard Model(BSM) theories. Vectorlike quarks (VLQs), colored spin-$\frac{1}{2}$ fermions with identical electroweak (EW) representation for both left and right chiralities, are predicted by a large subset of these theories [4–13]. The usual four VLQ species are denoted by $X_{+\frac{5}{3}}, T_{+\frac{2}{3}}, B_{-\frac{1}{3}}$ and $Y_{-\frac{4}{3}}$, where the subscript indicates the electric charge of the corresponding particle. Their renormalizable EW representation consists of (T) or (B) singlets, (X, T), (T, B), or (B, Y) doublets and

(X, T, B) or (T, B, Y) triplets. In most representations, they couple to the SM quarks via an exchange of charged ($W^{\pm}$) or neutral (Z, H) bosons. The interaction of the VLQs with the SM quarks can be summarized with the following simplified Lagrangian [14]:

$$\mathcal{L} = \sum_{Q,q,\zeta} \left[\frac{g_w}{2c_W} \tilde{\kappa}_\zeta^{Qq} \bar{Q} \slashed{Z} P_\zeta q + \frac{g_w}{\sqrt{2}} \kappa_\zeta^{Qq} \bar{Q} \slashed{W} P_\zeta q - \hat{\kappa}_\zeta^{Qq} H \bar{Q} P_\zeta q \right] + \text{H.c.}, \tag{1}$$

where Q represents a VLQ, ζ represents the chirality with P_ζ being the corresponding projection operator, q represents a SM quark of up or down type, and the electroweak couplings $\tilde{\kappa}_\zeta^{Qq}, \kappa_\zeta^{Qq}$, and $\hat{\kappa}_\zeta^{Qq}$ determine the coupling strengths between Q and q when mediated by the Z, W, and H bosons respectively. The mass hierarchy of the SM quarks suggests that VLQs interact predominantly with the third-generation SM quarks [15,16]. Hence, VLQ interactions with lighter generations are set to zero in the simplified representation of Eq. (1) and the VLQ species T and B are referred to as top and bottom partners respectively in the following discussion.

At the LHC, the dominant modes of VLQ production are pair and single production. During Run 1 (2010–2012) of the LHC, the VLQ searches at center-of-mass energies of $\sqrt{s} = 7$ and 8 TeV typically probed VLQ masses lower than 1 TeV where VLQ pair production dominates [16].
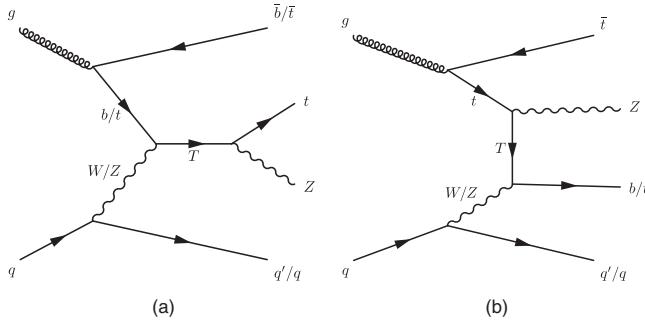
FIG. 1.   Illustrative (a) *s*-channel and (b) *t*-channel Feynman diagrams for $WTZt$ and $ZTZt$ processes.

Since the pair production of VLQs proceeds through QCD interactions, the cross section under the narrow-width approximation only depends on the VLQ mass and not on the species nor its EW representation. No significant excess was observed by the Run 1 searches looking for pair production of VLQs and lower exclusion limits on VLQ mass were reported in the range of approximately 600–1000 GeV, depending on the search [17–22]. The searches for single production of T or B also reported similar limits in Run 1 for a range of couplings probed in the singlet and doublet benchmarks [19,23].

Run 2 (2015–2018) searches at $\sqrt{s} = 13$ TeV for pair production of top and bottom partners from ATLAS and CMS have set lower limits on the VLQ masses in the range of 800–1400 GeV [24–34]. Since the single production of VLQs can have a larger cross section at high masses for reasonably large couplings [16], the Run 2 searches are increasingly focusing on this production mode [35–45]. However, unlike pair production, single production of VLQs is mediated by electroweak processes. Both the kinematics and cross sections of the single VLQ processes depend on the representation and the choice of couplings that determine the relative strength of these particles interacting with SM quarks and vector/Higgs bosons.

This paper focuses on the search for a singly produced T decaying to a Z boson and a top quark using the complete Run 2 dataset collected by the ATLAS detector. As shown in Fig. 1, the electroweak interaction can produce a T in the *s*- and *t*-channel topologies. These processes are referred to as $WTZt$ and $ZTZt$ processes, where the first W or Z refers to the vector boson scattered off of the incoming parton, T refers to the VLQ exchanged in the intermediate stage, and Zt refers to the production of the Z boson and t quark. The $WTZt$ mode dominates in the singlet representation of T since the smaller coupling between the T and the Z boson and the kinematically disfavored $g \to t\bar{t}$ splitting suppress the contribution from $ZTZt$. On the other hand, the latter is the dominant mode in the doublet representation since the T's coupling with the W boson is suppressed by the mass diagonalization matrix [16]. A model-independent approach [46–48] that allows probing a wide range of couplings for

the W, Z, and H-mediated interactions of these heavy quarks is adopted in this search.

The analysis is performed across two channels spanning decays of T quarks with mass in the range between 1.0 and 2.7 TeV. The dilepton (2ℓ) channel selects events with exactly one pair of opposite-sign leptons, i.e. electrons or muons and a hadronically decaying top quark in the final state. The trilepton (3ℓ) channel requires, in addition to the pair of opposite-sign leptons, at least a third lepton from a leptonically decaying top quark. The reconstructed Z-boson from the pair of leptons is expected to have large transverse momentum while the hadronic decay of the boosted top quark in the 2ℓ channel would constitute wide-radius jet signatures. These results improve on a previous ATLAS search [35] with a data sample corresponding to an integrated luminosity of 36.1 fb^{-1}, by benefiting from the larger data sample of 139 fb^{-1}, improved kinematic selections and introducing a method to identify hadronically decaying top quarks.

The paper is organized as follows. Section II provides a brief overview of the ATLAS detector. The data and simulated background and signal samples are described in Sec. III. Section IV describes the object definition while event selection, categorization, and the analysis strategy are outlined in Sec. V. The systematic uncertainties are discussed in Sec. VI. Results obtained from this search are reported in Sec. VII and conclusions are presented in Sec. VIII.

II. ATLAS DETECTOR

The ATLAS detector [49] at the LHC covers nearly the entire solid angle around the collision point.[1] It consists of an inner tracking detector surrounded by a thin super-conducting solenoid, electromagnetic and hadronic calorimeters, and a muon spectrometer incorporating three large superconducting air-core toroidal magnets.

The inner-detector system (ID) is immersed in a 2 T axial magnetic field and provides charged-particle tracking in the range of $|\eta| < 2.5$. The high-granularity silicon pixel detector covers the vertex region and typically provides four measurements per track, the first hit normally being in the insertable B-layer (IBL) installed before Run 2 [50]. It is followed by the silicon microstrip tracker (SCT), which usually provides eight measurements per track. These silicon detectors are complemented by the transition radiation tracker (TRT), which enables radially extended track

---

[1]ATLAS uses a right-handed coordinate system with its origin at the nominal interaction point (IP) in the center of the detector and the z-axis along the beam pipe. The x-axis points from the IP to the center of the LHC ring, while the y-axis points upward. Cylindrical coordinates (r, ϕ) are used in the transverse plane, ϕ being the azimuthal angle around the z-axis. The pseudorapidity is defined in terms of the polar angle θ as $\eta = -\ln\tan(\theta/2)$. Angular distance ($\Delta R$) is defined as $\Delta R \equiv \sqrt{(\Delta\eta)^2 + (\Delta\phi)^2}$.

reconstruction up to $|\eta| = 2.0$. The TRT also provides electron identification information based on the fraction of hits (typically 30 in total) above a higher energy-deposit threshold corresponding to transition radiation.

The calorimeter system covers the pseudorapidity range of $|\eta| < 4.9$. Within the region $|\eta| = 3.2$, electromagnetic calorimetry is provided by barrel and end cap high-granularity lead/liquid-argon (LAr) calorimeters, with an additional thin LAr presampler covering $|\eta| < 1.8$ to correct for energy loss in material upstream of the calorimeters. Hadron calorimetry is provided by the steel/scintillator-tile calorimeter, segmented into three barrel structures within $|\eta| = 1.7$, and two copper/LAr hadron end cap calorimeters. The solid angle coverage is completed with forward copper/LAr and tungsten/LAr calorimeter modules optimized for electromagnetic and hadronic energy measurements respectively.

The muon spectrometer (MS) comprises separate trigger and high-precision tracking chambers measuring the deflection of muons in a magnetic field generated by the superconducting air-core toroidal magnets. The field integral of the toroids ranges between 2.0 and 6.0 T m across most of the detector. Three layers of precision chambers, each consisting of layers of monitored drift tubes, cover the region $|\eta| < 2.7$, complemented by cathode-strip chambers in the forward region, where the background is highest. The muon trigger system covers the range of $|\eta| < 2.4$ with resistive-plate chambers in the barrel, and thin-gap chambers in the end cap regions.

Interesting events are selected by the first-level trigger system implemented in custom hardware, followed by selections made by algorithms implemented in the software-based high-level trigger (HLT) [51]. The first-level trigger reduces the incoming data rate from the 40 MHz bunch crossings to a design value of 100 kHz, which is further reduced by the HLT to record events to disk at a rate of about 1 kHz.

An extensive software suite [52] is used in data simulation, in the reconstruction and analysis of real and simulated data, in detector operations, and in the trigger and data acquisition systems of the experiment.

III. DATA AND SIMULATED EVENT SAMPLES

The data sample was collected by the ATLAS detector in proton–proton (pp) collisions at a center-of-mass energy of $\sqrt{s} = 13$ TeV during Run 2 with all detector subsystems operational and with the LHC operating in stable beam conditions with 25 ns bunch spacing. The dataset corresponds to an integrated luminosity of 139 fb^{-1} with an average of about 34 simultaneous interactions per bunch crossing (pileup).

All of the nominal Monte Carlo (MC) simulation samples used in the analysis were processed with the ATLAS simulation framework [53], using a detailed simulation based on Geant4 [54]. The effect of pileup was modeled by overlaying the simulated hard-scattering event with inelastic pp events generated with PYTHIA 8.186 [55] using the NNPDF2.3LO set of parton distribution functions (PDF) [56] and the A3 set of tuned parameters (tune) [57]. The pileup is reweighted in the MC event samples to match the pileup conditions in data.

The nominal MC sample for Z boson production with jets ($Z + $ jets) was generated with Sherpa 2.2.1 [58] and the nominal diboson (VV) sample was generated with Sherpa 2.2.2. Both the samples were generated using the NNPDF3.0 [59] next-to-next-to-leading-order (NNLO) PDF set. The $Z + $ jets sample includes events generated with up to two partons at next-to-leading-order (NLO) and up to four partons at leading-order (LO) and is normalized to the NNLO cross section [60]. The VV sample is normalized to the Sherpa NLO cross section and includes $q\bar{q}$-initiated events with up to one parton at NLO and up to three partons at LO and gg-initiated processes simulated using LO matrix elements for up to one additional jet. For both samples, COMIX [61] and OpenLoops [62–64] were used and the matrix element (ME) was merged with the Sherpa parton shower [65] according to the MEPS@NLO prescription [66–69]. To estimate modeling uncertainties for these backgrounds, additional samples were produced with MadGraph5_aMC@NLO2.2.3 [70], using the NNPDF3.0NLO PDF set and interfaced to PYTHIA 8.210 [71] with the A14 tune [72] and the NNPDF2.3LO PDF for showering. In the 2ℓ channel, the simulated $Z + $ jets events are categorized into $Z + $ Light Flavor (LF) and $Z + $ Heavy Flavor (HF) events in accordance with the absence or presence of heavy flavor jets in the MC generator record of these simulated events in the kinematic acceptance defined in Secs. IV and V. An additional set of $Z + $ jets events was generated with Sherpa 2.2.11 to compare the modeling of the $Z + $ jets background in the 2ℓ channel.

The nominal $t\bar{t}$ background sample uses the POWHEG method [73,74] implemented in POWHEG BOX v2 [75,76] with the NNPDF3.0NNLO PDF set. POWHEG BOX was interfaced with PYTHIA 8.230 with the A14 tune for showering and hadronization. The sample is normalized to the NNLO cross section in QCD including resummation of next-to-next-to-leading-logarithmic (NNLL) soft gluon terms calculated with Top++ [77–83]. For the evaluation of modeling uncertainties, samples were produced with the same matrix element generator as the nominal sample, but Herwig 7 was used with the H7-UE-MMHT tune [84] for showering and hadronization. To assess the uncertainty in the matching of NLO matrix elements to the parton shower, additional samples were generated with MadGraph5_aMC@NLO 2.6.0 and the NNPDF3.0NNLO PDF set, interfaced with PYTHIA 8.230 using the same showering configuration as the nominal sample.

The nominal sample for $t\bar{t}$ production with a vector boson ($t\bar{t} + W$ and $t\bar{t} + Z$) was generated with MadGraph5_aMC@NLO 2.3.3 interfaced with PYTHIA 8.210 for showering

and hadronization, using the NNPDF2.3LO PDF set and the A14 tune. These events were normalized to the NLO cross sections calculated with MadGraph5_aMC@NLO [85,86]. To evaluate modeling uncertainties, alternative samples were produced where either the A14 tune was varied or Herwig 7 was used with the H7-UE-MMHT tune for the showering. Additional samples were produced using Sherpa 2.2.1 to evaluate the uncertainty due to the choice of matrix element generator. The production of $t\bar{t}t\bar{t}$ and $t\bar{t}WW$ events was modeled using the MadGraph5_aMC@NLO generator at LO with the NNPDF 3.1NLO PDF, interfaced with PYTHIA 8.230 using the A14 tune and the NNPDF2.3LO PDF set. These samples were normalized to cross sections calculated with NLO QCD and EW corrections [85]. These four processes are merged into a single process labeled $t\bar{t} + X$ in which the contribution from $t\bar{t} + Z$ dominates due to the requirement of an opposite-sign same-flavor (OS-SF) lepton pair with an invariant mass close to that of a Z boson in the final state.

The single-top-quark processes were simulated with POWHEG BOX [87,88] using the NNPDF3.0NLO PDF set and interfaced to PYTHIA 8.234 with the A14 tune. The samples are normalized to their respective NLO QCD cross sections [89,90] for the t-channel and s-channel, and with additional NNLL soft gluon terms for Wt production [91–93]. The production of tZq and tWZ events was modeled using the MadGraph5_aMC@NLO generator at NLO with the NNPDF3.0NLO PDF and interfaced with PYTHIA 8.212 using the A14 tune and the NNPDF2.3LO PDF set. The diagram-removal scheme [94] was used in the generation of Wt and tWZ events to address their overlaps with $t\bar{t}$ and $t\bar{t} + Z$ samples. These samples were also merged into a single process labeled as single-top.

Signal samples for the $WTZt$ and $ZTZt$ processes were generated at LO using MadGraph5_aMC@NLO with the Universal FeynRules Output (UFO) model [95] from Ref. [14], interfaced with PYTHIA 8.244 and using the NNPDF3.0LO PDF set and the A14 tune. This model uses the four-flavor scheme. Top partner samples were obtained for various masses, ranging from 1.0 TeV and 2.7 TeV in steps of 100 GeV. For each mass point, the coupling strength κ was varied between 0.1 and 1.0 with a step of 0.05 (0.1) for couplings less (greater) than 0.5. The relative strength of the three coupling modes were obtained from $\vec{\xi} = (\xi_W, \xi_Z, \xi_H) = (0.5, 0.25, 0.25)$.[2] The MC samples were produced for a subset of the mass and coupling points. Those samples were used for other masses and couplings by implementing an event-by-event matrix element

---

[2] The parameterization of VLQ Lagrangian in terms of the κ and $\vec{\xi}$ parameters was introduced in Ref. [47] and is used for the interpretation of the search presented in this paper. Its conversion to the coupling convention in Eq. (1) is obtained by doing a one-to-one mapping of the tree level couplings in the Lagrangian. The ξ_W, ξ_Z, ξ_H parameters satisfy the constraint $\xi_W + \xi_Z + \xi_H = 1$ and asymptotically represent the branching ratios of T decaying into Wb, Zt, and Ht in the narrow-width limit.

reweighting [96]. While the left- and right-handed couplings dominate in the singlet and doublet representations of T, the current analysis was found to be insensitive to the choice of chirality for the signal MC generation and all signal samples were generated using the left-handed couplings. The signal samples were normalized to the NLO cross section calculated with the narrow-width approximation [97]. Due to the requirement of at least one jet containing a b-hadron in the signal region the kinematic differences between the 4 flavor scheme and 5 flavor scheme are expected to be small. However, since the top partner can have large width based on the choice of coupling, additional correction factors were applied to evaluate the cross section at finite width [98]. The contribution from the nonresonant t-channel diagram was also taken into account [99].

IV. OBJECT RECONSTRUCTION

Events are required to have at least one vertex with at least two tracks with transverse momentum $p_T > 0.5$ GeV. The primary vertex (PV) is defined as the one with the largest Σp_T^2, where the sum is performed over all the tracks matched to the vertex.

Electrons are reconstructed from energy clusters in the EM calorimeter matched with ID tracks and must fulfill the *tight likelihood* identification criteria [100]. Electrons are calibrated [100] and required to have $p_T > 28$ GeV and to be reconstructed within $|\eta| = 2.47$, excluding the calorimeter barrel–end cap transition regions ($1.37 < |\eta| < 1.52$). A high acceptance for the expected signal events is maintained by not applying an isolation requirement to electron candidates beyond those implicit in the trigger requirements, which are explained in Sec. V. Furthermore, the track matched with the candidate electron is required to have a longitudinal impact parameter with respect to the PV which satisfies $|z_0 \cdot \sin\theta| < 0.5$ mm and a transverse impact parameter with respect to the beamline (d_0) with a significance $|d_0|/\sigma(d_0) < 5$.

Muons are reconstructed [101] from combined tracks in the MS and the ID and must fulfill the *medium* identification criteria [101]. Muons are calibrated and required to have $p_T > 28$ GeV and to be reconstructed within $|\eta| = 2.5$. Muon candidates must also satisfy the track-based isolation requirements defined by the *FixedCutTightTrackOnly* working point [101]. This isolation requirement does not significantly reduce the acceptance. This working point uses the scalar sum of the p_T of all tracks that are inside of a cone of size $\Delta R = \min\{0.3, 10 \text{ GeV}/p_T(\mu)\}$ around the muon candidate, where $p_T(\mu)$ is the candidate muon p_T. The track matched with the muon candidate under consideration is excluded from the sum. The muon is selected if this sum is less than 15% of $p_T(\mu)$. Finally, muon candidates are required to have a matched track with $|z_0 \cdot \sin\theta| < 0.5$ mm and a significance $|d_0|/\sigma(d_0) < 3$.

Jets are reconstructed from particle-flow objects [102] using the anti-k_t algorithm [103,104] with a radius

parameter of $R = 0.4$. Jets are calibrated to the particle level from a combination of simulation-based corrections and measurements in data [105] and are required to fulfill $p_T > 25$ GeV for $|\eta| < 2.5$ and $p_T > 35$ GeV for $2.5 < |\eta| < 4.5$. These two jet categories are respectively called central and forward jets. To reduce jet contributions from pileup, a "jet vertex tagger" algorithm using a two-dimensional likelihood discriminant [106] is applied to jets with $|\eta| < 2.4$ and $p_T < 60$ GeV. The DL1r algorithm [107] is used to identify jets in the central region ($|\eta| < 2.5$) containing b-hadrons (b-tagging) with a working point corresponding to a b-tagging efficiency in simulated $t\bar{t}$ events of 77%, a c-jet rejection factor of ∼6, and a light-jet rejection factor of ∼192.

The missing transverse momentum [108], with magnitude E_T^{miss}, is defined as the negative vectorial sum of the transverse momenta of all the calibrated reconstructed lepton and jet candidates in the event and includes a "soft term" with contributions from tracks emanating from the PV but not matched with any of the reconstructed objects.

A procedure to remove potential overlaps between reconstructed lepton and jet candidates is performed sequentially as follows. First, any electron sharing an ID track with one of the muons is removed. Next, any jet within $\Delta R = 0.2$ of an electron is removed, followed by the removal of electrons within $\Delta R = 0.4$ of any remaining jet. Then any jet with at most two tracks with $p_T > 0.5$ GeV within $\Delta R = 0.2$ of a muon is removed, unless it is b-tagged. At the end of the procedure, any muon within $\Delta R = \min\{0.4, 0.04 + 10\text{ GeV}/p_T(\mu)\}$ of any remaining jet is removed.

To identify hadronically decaying boosted top-quark jets, variable-radius reclustered jets (vRC jets) are reconstructed using the variable-radius jet algorithm [109] from calibrated jets with $R = 0.4$ where the effective radius of the jet cone is chosen as $R_0 = \frac{2m_t}{p_T}$, m_t and p_T representing the mass of the top quark and the jet transverse momentum respectively. These vRC jets are known to provide stable top-tagging performance for a wide range of jet p_T [110]. The vRC jets are called top-tagged (top-vetoed) if the vRC jet mass is greater (less) than 140 GeV. Top-tagged and top-vetoed jets are required to have $p_T > 200$ GeV and to contain at least two $R = 0.4$ jets as jet constituents when their transverse momentum is less than 700 GeV.

V. EVENT SELECTION

A common initial event selection is performed for both the 2ℓ and 3ℓ channels where events are required to have passed the single lepton trigger selections [51,111,112]. For muons, triggers with a p_T threshold of 20 GeV (26 GeV) in 2015 (2016–2018) and isolation requirements, are combined in logical OR with triggers with a 50 GeV p_T threshold with no isolation requirement. A complementary barrel region only trigger with a 60 GeV p_T threshold is

added for the 2017–2018 data taking period. Similarly, electron triggers with isolation and identification requirements (tight likelihood identification in 2016–18, with a less restrictive requirement in 2015) and p_T thresholds of 24–26 GeV are combined with triggers with higher p_T thresholds between 120 GeV and 140 GeV, less restrictive identification criteria, and no isolation requirements.

Events are additionally required to have at least one OS-SF lepton pair with the transverse momentum of each lepton being greater than 28 GeV. The pair of OS-SF leptons with invariant mass $m(\ell\ell)$ closest to the mass of the Z-boson (m_Z) is identified as the Z-boson candidate. Based on the expected hadronic activity of the signal topologies, events are also required to have at least one vRC jet (in the 2ℓ channel) or at least two central jets (in the 3ℓ channel).

A. Dilepton channel

The preselection of events for the 2ℓ channel (2ℓPS) requires the Z-boson candidate to have an invariant mass satisfying $|m(\ell\ell) - m_Z| < 10$ GeV. Given that the search is sensitive to energetic final-state objects, additional background reduction is achieved by requiring the Z-boson candidate to have a transverse momentum $[p_T(\ell\ell)]$ of at least 200 GeV and the scalar sum of transverse momenta of jets in the event, denoted by H_T, to be at least 300 GeV. Since signal events are expected to contain a hadronically decaying boosted top quark, events without any vRC jets are rejected. The four momentum of the leading vRC jet (J), defined as the vRC jet with the highest p_T, is combined with that of the Z-boson candidate to obtain an estimate of the mass of T, $m_{\ell\ell J}$. To reduce sensitivity to VLQ pair-production and to allow for a consistent phenomenological interpretation of observed data counts, a requirement of $H_T + E_T^{miss} < m_{\ell\ell J}$ is also placed on preselection events [35].

The main background for the 2ℓ channel is comprised of $Z + $ jets events, with minor contributions from VV and $t\bar{t}$ processes. Measurements of differential cross sections have recently shown that the current simulations of $Z + $ jets processes overestimate both the upper tail of the H_T spectrum and the cross section at high jet multiplicities [113]. This leads to discrepancies in the shapes of the $H_T + E_T^{miss}$ and jet multiplicity spectra between the data and expected background in the kinematic regimes relevant for this search. Data-driven reweighting factors are therefore used to correct the observed discrepancies in these processes. These corrections are derived using the following procedure.

To improve the background modeling, a reweighting factor is extracted for the $Z + $ jets samples by comparing data with simulated events in the 2ℓPS region for the jet multiplicity and $H_T + E_T^{miss}$ distributions. These reweighting factors are separately derived for 2ℓPS events with and without b-tagged jets. Since the shapes of the $Z + $ LF and
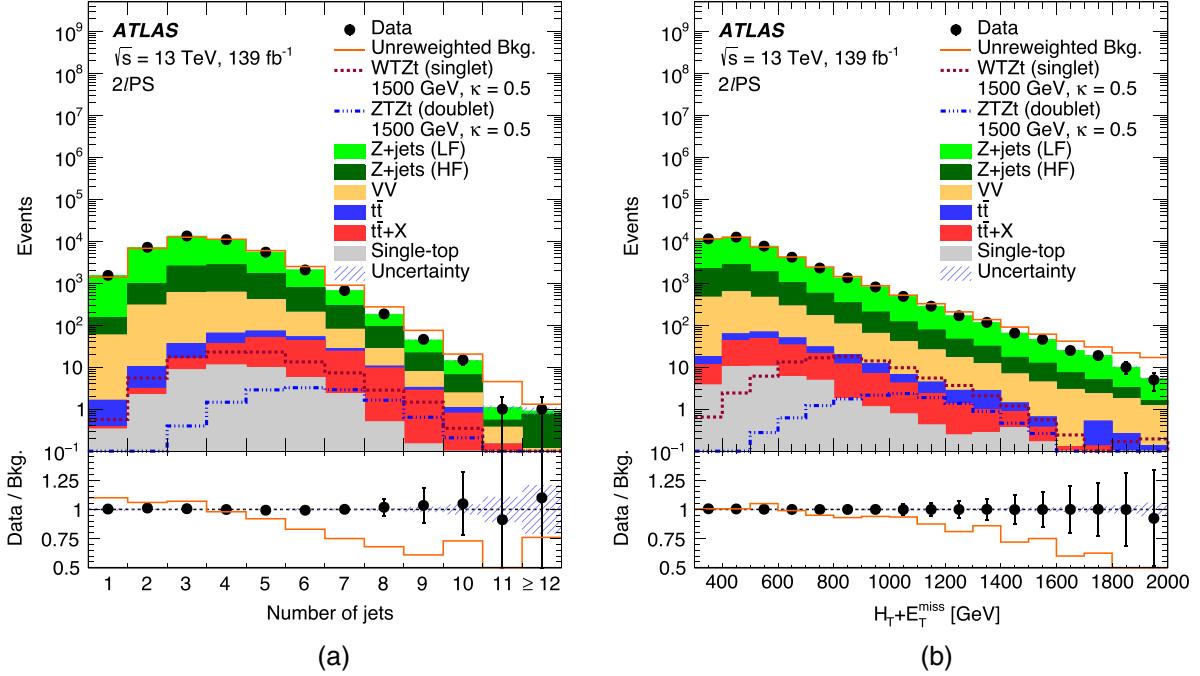
FIG. 2.   Distributions of (a) jet multiplicity and (b) $H_T + E_T^{miss}$ in the 2ℓPS region after reweighting. The overlaid solid line shows the total background prediction before the reweighting and the corresponding data-over-background ratio in the bottom panel. The red and blue dotted lines show the signal contributions from $WTZt$ and $ZTZt$ processes with $M_T = 1.5$ TeV and $\kappa = 0.5$ in the singlet and doublet representations respectively. The last bin in each distribution contains the overflow.

$Z + $ HF samples were found to be similar in these regions, these factors are applied on the $Z + $ jets template obtained by combining these samples together. The reweighting function is defined bin-by-bin by the formula

$$R_{Z+jets}(x) = \frac{\text{Data}(x) - \text{MC}^{non\text{-}Z+jets}(x)}{\text{MC}^{Z+jets}(x)}, \qquad (2)$$

where x represents the binning in each kinematic variable. After reweighting in jet multiplicity, a second reweighting is applied on $H_T + E_T^{miss}$ using Eq. (2). The joint reweighting factors are applied on an event-by-event basis to estimate the MC contribution of $Z + $ jets events for this channel. The jet multiplicity and $H_T + E_T^{miss}$ distributions in the 2ℓPS region are shown in Fig. 2. In the bins of jet multiplicity and $H_T + E_T^{miss}$ distributions, the contribution of non-Z-jets processes is less than 15% before reweighting. The predicted signal contribution is also quite small. For a benchmark $WTZt$ process with $M_T = 1.5$ TeV and $\kappa = 0.5$ in the singlet representation, the bin-by-bin signal-over-background ratio (S/B) varies between 4–7% for most bins and is always less than 9%.

Figure 3 shows the distributions of the key kinematic variables for the expected background and benchmark signal processes in the 2ℓPS region. Events with a singly produced T have a distinctive signature with a forward jet scattering off of a vector boson from one of the incoming

partons. Events are additionally expected to have b-tagged jets. Hence, in addition to the preselection, the signal-enriched kinematic phase space, called the *signal region* (2ℓSR), requires events with at least one forward jet, at least one b-tagged jet, and at least one top-tagged jet, as shown in Table I. The distribution of the transverse momentum of the Z-boson candidate, $p_T(\ell\ell)$, was the variable that offered maximum sensitivity and, hence, is used as the final discriminant in this channel to perform the statistical fit described in Sec. VII.

Three control regions (CRs) are defined to improve the background modeling and reduce its uncertainties. Two validation regions (VRs) are defined to validate the background prediction in the distribution of the final discriminant. The event selection criteria for these regions are summarized in Table I. Each of the control regions is obtained by inverting exactly two of the three jet cuts of the 2ℓSR shown in Table I. The regions 2ℓCR1, 2ℓCR2, and 2ℓCR3 are defined to have the same selection as 2ℓSR in multiplicities of forward jets, b-tagged jets, and top-tagged jets respectively. The inversion of the requirement of the presence of top-tagged jets requires the presence of at least one top-vetoed tagged jet. Both the validation regions are required to have at least one top-tagged jet to maintain their kinematic similarity with the signal region. Identified as 2ℓVR1 and 2ℓVR2, they are made orthogonal to the 2ℓSR by requiring zero b-tagged jets and zero forward jets respectively.
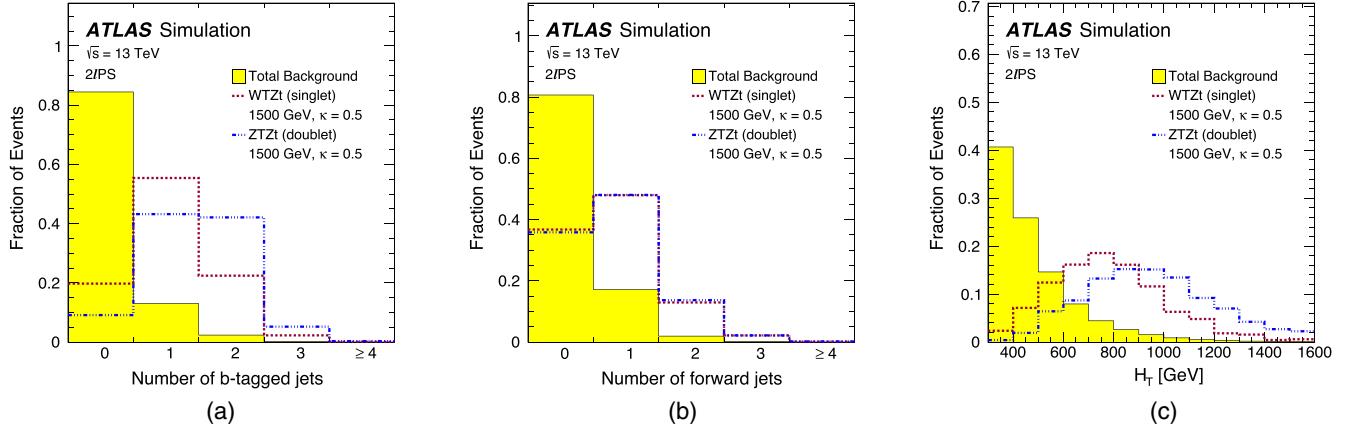
FIG. 3.   Simulated distributions of (a) b-tagged jet multiplicity, (b) forward jet multiplicity, and (c) H_T for total background (solid area) and benchmark signal processes (dashed lines) in the 2ℓPS region before reweighting is performed in jet multiplicity and $H_T + E_T^{\text{miss}}$ distributions. Each distribution is separately normalized to unit area. The signal contributions are from $WTZt$ and $ZTZt$ processes with $M_T = 1.5$ TeV and $\kappa = 0.5$ in the singlet and doublet representations respectively. The last bin in each distribution contains the overflow.

B. Trilepton channel

As the name of the channel suggests, events with at least three leptons passing the preselection are selected. Although the selection is inclusive of events with four or more leptons, their overall contribution is quite small ($< 5\%$). The lepton with highest p_T that does not comprise the Z-boson candidate is labeled as the third lepton (ℓ_3) in this channel. The main sources of background are diboson processes and $t\bar{t} + X$, the latter being primarily composed of $t\bar{t} + Z$ and other small contributions from $t\bar{t} + W$ and $t\bar{t}t\bar{t}$ processes. Minor contributions result from background processes like single-top and $Z +$ jets. To improve the quality of MC background modeling, a data-driven reweighting factor is determined for the VV and $t\bar{t} + X$ samples in this channel. This reweighting is performed for the central jet multiplicity distribution for events passing the 3ℓPS criteria. These events are classified into separate regions according to the presence or absence of b-tagged jets in the event. A pair of simultaneous linear equations can be formulated for these two sets of data and MC distributions:

$$n_{0,i}^{\text{data}} = \alpha_i^{VV} n_{0,i}^{VV} + \alpha_i^{ttX} n_{0,i}^{ttX} + n_{0,i}^{\text{others}},$$

$$n_{1,i}^{\text{data}} = \alpha_i^{VV} n_{1,i}^{VV} + \alpha_i^{ttX} n_{1,i}^{ttX} + n_{1,i}^{\text{others}}, \qquad (3)$$

where n^{data} denotes the data yield and n^{VV}, n^{ttX}, and n^{others} denote the predicted yields from VV, $t\bar{t} + X$, and other backgrounds respectively. The subscripts $0/1$ refer to events with $0/ \geq 1$ b-tagged jets and the index i runs over the bins of the central jet multiplicity distribution. The $(\alpha_i^{VV}, \alpha_i^{ttX})$ factors for each bin are obtained by simultaneously solving the pair of equations in Eq. (3) and applied to estimate the MC contributions of VV and $t\bar{t} + X$ processes. The central jet multiplicity distribution in the 3ℓPS is shown in Fig. 4. In the regions where the reweighting factors are derived, the overall contribution of the minor backgrounds is up to 29%, reaching a bin-by-bin maximum of 37%. The predicted signal contributions in these regions are small. For a benchmark $WTZt$ process with $M_T = 1.5$ TeV and $\kappa = 0.5$ in the singlet representation, the bin-by-bin S/B is less than 2%.

Figure 5 shows distributions of some of the kinematic variables for the expected background and benchmark

TABLE I.   Summary of selections applied to define the control, validation, and signal regions for the 2ℓ channel.

|	2ℓCR1	2ℓCR2	2ℓCR3	2ℓVR1	2ℓVR2	2ℓSR
Preselection		= 2 OS-SF leptons with $\|m(\ell\ell) - m_Z\| < 10$ GeV $p_T(\ell\ell) > 200$ GeV, $H_T > 300$ GeV ≥ 1 vRC jet $H_T + E_T^{\text{miss}} < m_{\ell\ell J}$				
Forward jets	≥ 1	0	0	≥ 1	0	≥ 1
b-tagged jets	0	≥ 1	0	0	≥ 1	≥ 1
Top-tagged jets	$\cdots$	$\cdots$	≥ 1	≥ 1	≥ 1	≥ 1
Top-vetoed jets	≥ 1	≥ 1	$\cdots$	$\cdots$	$\cdots$	$\cdots$
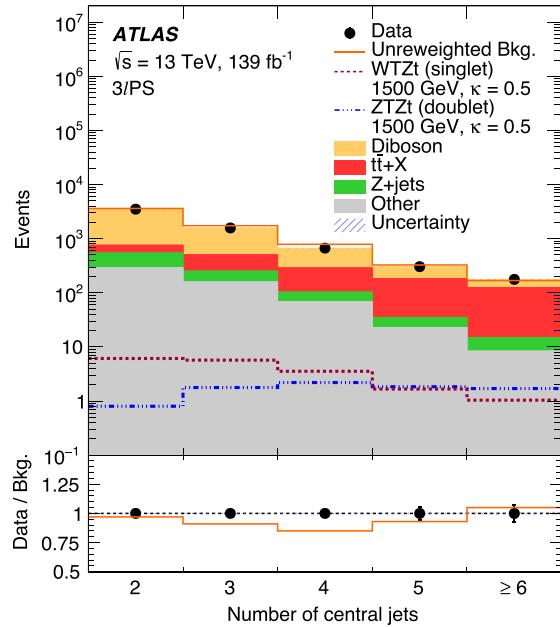
FIG. 4. Distribution of central jet multiplicity in the 3ℓPS region after reweighting. The overlaid solid line shows the total background prediction before the reweighting and the corresponding data-over-background ratio in the bottom panel. The red and blue dotted lines show the signal contributions from *WTZt* and *ZTZt* processes with $M_T = 1.5$ TeV and $\kappa = 0.5$ in singlet and doublet representations respectively.

signal processes in the 3ℓPS region. Exploiting the distinctive signature of signal events, which are expected to have b-tagged and forward jets, the signal region in this channel (3ℓSR) requires events to have at least one of each of these jet types. To further increase the signal-to-background ratio, additional requirements are applied on

the Z-boson candidate p_T, $p_T(\ell\ell) > 300$ GeV and the leading lepton p_T, $\max(p_T(\ell)) > 200$ GeV. The decay products of T, the Z boson and the top-quark, are expected to have large angular separation between them. Requiring the azimuthal separation of the Z candidate from the third lepton ($\Delta\phi(Z, \ell_3)$) to be at least $\frac{\pi}{2}$ significantly improves the signal purity in the signal region [Fig. 5(c)]. For similar reasons, the azimuthal separation between the Z candidate and the leading b-tagged jet, defined as the b-tagged jet with the largest p_T which is expected to emerge from the decay of the top quark, is required to satisfy $\Delta\phi(Z, b_{\text{lead}}) > \frac{\pi}{2}$.

Finally, to allow for a consistent phenomenological interpretation, the product of H_T and jet multiplicity, $H_T \cdot n(\text{jets})$, is required to be less than 6 TeV in the signal region to reduce potential contamination from pair production of VLQs [35].

The statistical analysis in this channel also uses $p_T(\ell\ell)$ as the final discriminant. Three control regions and one validation region are defined in this channel. The diboson control region (3ℓVV) is defined by rejecting events with any b-tagged jet. The mixed control region (3ℓMixed) and the $t\bar{t} + X$ control region (3ℓttX), are defined by accepting events with exactly one b-tagged jet and at least two b-tagged jets respectively. To maintain orthogonality with the signal region, both regions reject events with forward jets and require $\Delta\phi(Z, \ell_3) < 2.6$. Finally, a validation region (3ℓVR) is defined to validate the background modeling by requiring the same set of selections on the b-tagged jet and forward jet multiplicities as the signal region, but made orthogonal to it by requiring that at least one of the $\Delta\phi$ requirements is reversed, i.e., $\Delta\phi(Z, \ell_3) < \frac{\pi}{2}$ or $\Delta\phi(Z, b_{\text{lead}}) < \frac{\pi}{2}$. The definitions of these regions are summarized in Table II.
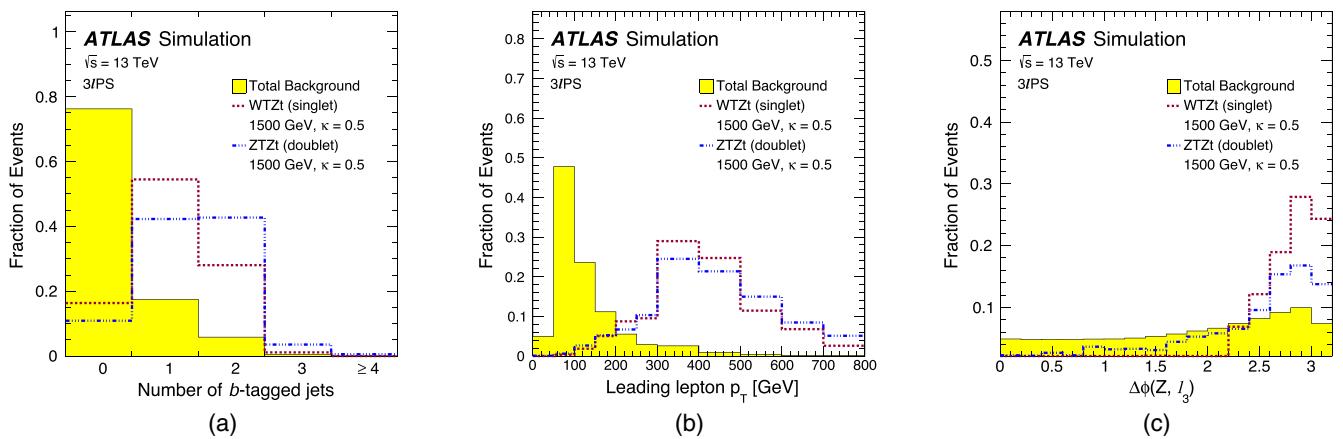
FIG. 5. Simulated distributions of (a) b-tagged jet multiplicity, (b) p_T of the leading lepton, and (c) $\Delta\phi$ between the Z candidate and the third lepton for total background (solid area) and benchmark signal processes (dashed lines) in the 3ℓPS region before reweighting is performed in the central jet multiplicity distribution. Each distribution is separately normalized to unit area. The signal contributions are from *WTZt* and *ZTZt* processes with $M_T = 1.5$ TeV and $\kappa = 0.5$ in the singlet and doublet representations respectively. The last bin in each distribution contains the overflow.

TABLE II.　Summary of selections applied to define the control, validation, and signal regions for the 3ℓ channel.

	3ℓVV	3ℓMixed	3ℓttX	3ℓVR	3ℓSR
Preselection			≥ 3 leptons ≥ 1 pair of OS-SF leptons with $|m(\ell\ell) - m_Z| < 10$ GeV ≥ 2 central jets		
b-tagged jets	0	1	≥ 2	≥ 1	≥ 1
Forward jets	$\cdots$	0	0	≥ 1	≥ 1
$\Delta\phi$ selections	$\cdots$	$\Delta\phi(Z, \ell_3) < 2.6$	$\Delta\phi(Z, \ell_3) < 2.6$	$\Delta\phi(Z, \ell_3) < \frac{\pi}{2}$ or $\Delta\phi(Z, b_{\text{lead}}) < \frac{\pi}{2}$	$\Delta\phi(Z, \ell_3) > \frac{\pi}{2}$ and $\Delta\phi(Z, b_{\text{lead}}) > \frac{\pi}{2}$
Other selections	$\cdots$	$\cdots$	$\cdots$	$\cdots$	$\max(p_{\text{T}}(\ell)) > 200$ GeV $p_{\text{T}}(\ell\ell) > 300$ GeV $H_{\text{T}} \cdot n(\text{jets}) < 6$ TeV

VI. SYSTEMATIC UNCERTAINTIES

Uncertainties from experimental and theoretical sources are introduced in the normalization or shape of the final discriminant in the two analysis channels. Experimental uncertainties include effects on the electron energy scale and energy resolution, the muon momentum scale and resolution, and uncertainties in the data-to-MC correction factors for the electron and muon trigger, reconstruction, identification, and isolation efficiencies [100,101]. Jet energy scale and resolution uncertainties are also included, as obtained from studies in data and simulation [105]. Flavor-tagging uncertainties include uncertainties in the b-jet tagging, c-jet mistagging, and light-jet mistagging efficiencies, and uncertainties due to extrapolations to regions not covered by the data used for the efficiency measurements [114–116]. Subdominant uncertainties include uncertainties related to the soft term in the $E_{\text{T}}^{\text{miss}}$ calculation [117] and to the $E_{\text{T}}^{\text{miss}}$ energy scale and resolution, uncertainties in the reweighting of the MC event samples to match the pileup conditions in data and a 1.7% [118] uncertainty in the integrated luminosity of the 2015–2018 data sample, obtained using the LUCID-2 detector [119] for the primary luminosity measurements.

Theoretical uncertainties include cross section and other modeling uncertainties for all background samples. The cross section uncertainties considered are between 5–6% for the $Z + \text{jets}$, $t\bar{t}$, and VV samples [77,120,121] and between 10–12% for the $t\bar{t} + Z$ sample [122]. Uncertainties associated with missing higher orders are estimated by varying the renormalization and factorization scales by factors of 0.5 and 2 and then, constructing upward and downward varying envelopes by considering the largest positive and negative fluctuation on a bin-by-bin basis. PDF uncertainties when comparing distributions obtained with events generated with different PDF sets are obtained using the PDF4LHC recommendations [123]. For the 2ℓ channel, the $Z + \text{jets}$ scale and PDF variations are decorrelated between $Z + \text{LF}$ and $Z + \text{HF}$ events. For the 3ℓ channel, the VV scale-variation uncertainties are broken down into their normalization and shape components, and

treated as uncorrelated across regions with different b-jet multiplicities.

Uncertainties due to the choice of generator or showering algorithm are estimated by comparing additional samples from alternative generators. Generator uncertainties for $t\bar{t} + X$ are obtained from comparing the nominal MadGraph5_aMC@NLO samples with the alternative Sherpa samples. For the 3ℓ channel where $Z + \text{jets}$ is a minor background and mainly contributes via jets misidentified as leptons, generator uncertainties are estimated by comparing nominal samples with alternative MadGraph5_aMC@NLO samples and only taking the shape difference into account. For the 2ℓ channel where $Z + \text{jets}$ is the main background, generator uncertainties are taken into account by comparing the Sherpa 2.2.1 sample with the Sherpa 2.2.11 sample where an independent reweighting based on jet multiplicity and $H_{\text{T}} + E_{\text{T}}^{\text{miss}}$ distribution, as explained in Sec. VA, is applied on the latter. To estimate the uncertainties due to the modeling of initial-state radiation, final-state radiation, and the choice of parton shower algorithm, either additional event weights for the nominal samples or alternative MC samples were produced. These uncertainties were calculated by comparing the nominal MC distribution with the distributions obtained from these additional event weights or the alternative samples.

A conservative uncertainty of 30% on the fraction of VV and $Z + \text{jets}$ events with heavy-flavor jets is applied in both the channels. This uncertainty is based on variations of the factorization and renormalization scales and the multijet merging scale [124]. Also, a shape uncertainty is introduced in the 3ℓ channel for VV and $t\bar{t} + \text{X}$ by comparing the distributions before and after implementing jet multiplicity based reweighting explained in Sec. V B. In the 2ℓ channel, bin-by-bin variations in the reweighting factors due to the statistical fluctuations in the MC samples are calculated and these variations are used to obtain upward and downward fluctuating envelopes for the fit distributions. Shape uncertainties extracted from these fluctuations are applied on the $Z + \text{jets}$ samples for the light and heavy-flavor components.

Events with jets misidentified as leptons can potentially arise in the 2ℓ channel mainly from the $t\bar{t}$ process and in the 3ℓ channel from the $t\bar{t}$ or $Z+$ jets processes. After the $m(\ell\ell)$ and $p_T(\ell\ell)$ cuts, these contributions are estimated to be less than 2% in the signal regions. Following the prescription in Ref. [35], a conservative 25% uncertainty is applied on the normalization of the $t\bar{t}$ ($t\bar{t}$ and $Z+$ jets) events in the 2ℓ (3ℓ) channel. This uncertainty is decorrelated across the control and signal regions in the 2ℓ and 3ℓ channels.

VII. STATISTICAL ANALYSIS AND RESULTS

A binned profile likelihood fit in the discriminating variable $p_T(\ell\ell)$ is performed in both channels to test if the data is compatible with the background-only hypothesis. The uncertainties are introduced in the likelihood as nuisance parameters (NP), which are constrained using Gaussian priors. Additional NPs are included to take into account the statistical uncertainties in each bin for each event category due to the limited size of the simulated samples [125]. The likelihood function $L(\mu, \vec{\theta})$ is constructed as a
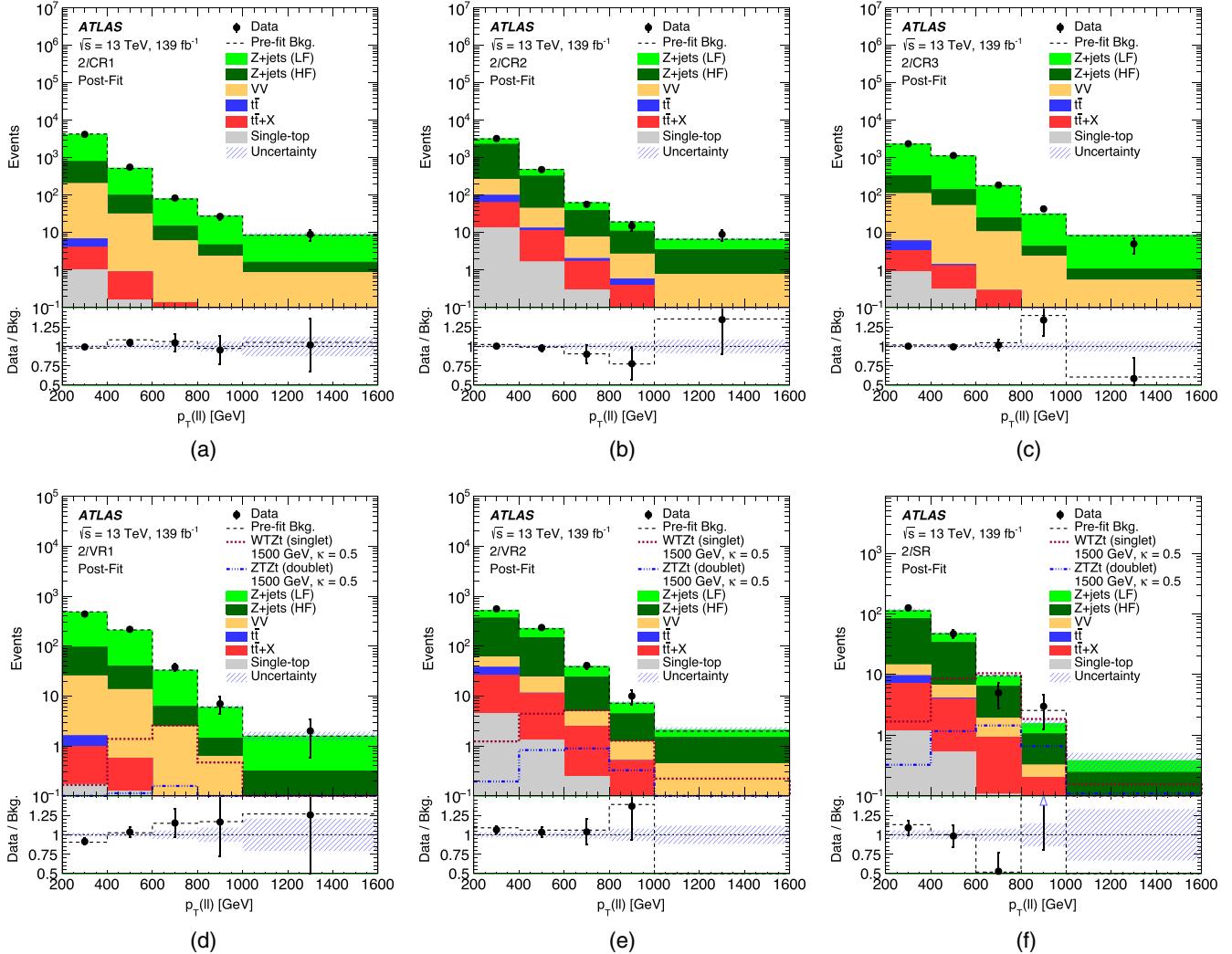
FIG. 6. Distribution of the final discriminant, $p_T(\ell\ell)$, for the 2ℓ channel in the control regions (a) 2ℓCR1, (b) 2ℓCR2, (c) 2ℓCR3, the validation regions (d) 2ℓVR1, (e) 2ℓVR2, and the signal region (f) 2ℓSR. The distributions are shown after the background-only fit in the 2ℓ channel. The black, dashed line shows the total prefit background distribution and the corresponding data-over-background ratio in the bottom panel. The blue arrows in the bottom panel indicate points that are outside the vertical range of the figure. The overlaid red and blue dotted lines in (d)–(f) show the expected signal contributions in the corresponding regions from $WTZt$ and $ZTZt$ processes with $M_T = 1.5$ TeV and $\kappa = 0.5$ in singlet and doublet representations respectively. Expected signal contributions in the control regions are negligible. The last bin in each distribution contains the overflow.

product of Poisson probabilities for each bin of the discriminating variable in the control and signal regions,

$$L(\mu, \vec{\theta}) = \Pi_{i=1}^{N_{\text{bins}}} \text{Pois}(n_i^{\text{data}}|b_i + \mu s_i) \times P(\vec{\theta}), \quad (4)$$

where N_{bins} is the total number of bins in control and signal regions. The parameters, $n_i^{\text{data}}, b_i, s_i$, represent the number of observed data, expected background and signal events respectively in the ith bin. The product of prior distributions for the NPs, $(\vec{\theta})$, is given by $P(\vec{\theta})$. The expected number of events in each bin depends on these NPs as well as the signal strength, μ, which acts as a scaling factor for the signal cross section.

The background and signal templates are fitted to the observed data to obtain the best estimate of signal and background contributions in the control and signal regions. The fitted values of $\mu, \vec{\theta}$ are propagated to the validation regions to test the quality of the fit and the corresponding background modeling. The background-only *post-fit* distributions, obtained by maximizing the likelihood function in Eq. (4) with a fixed choice of $\mu = 0$, are shown for the 2ℓ and 3ℓ control, validation, and signal regions in Figs. 6 and 7 respectively. The expected prefit signal yields for the $WTZt$ and $ZTZt$ processes with $M_T = 1.5$ TeV and $\kappa = 0.5$ for the singlet and doublet representations of T are also shown in these figures. The contribution of different
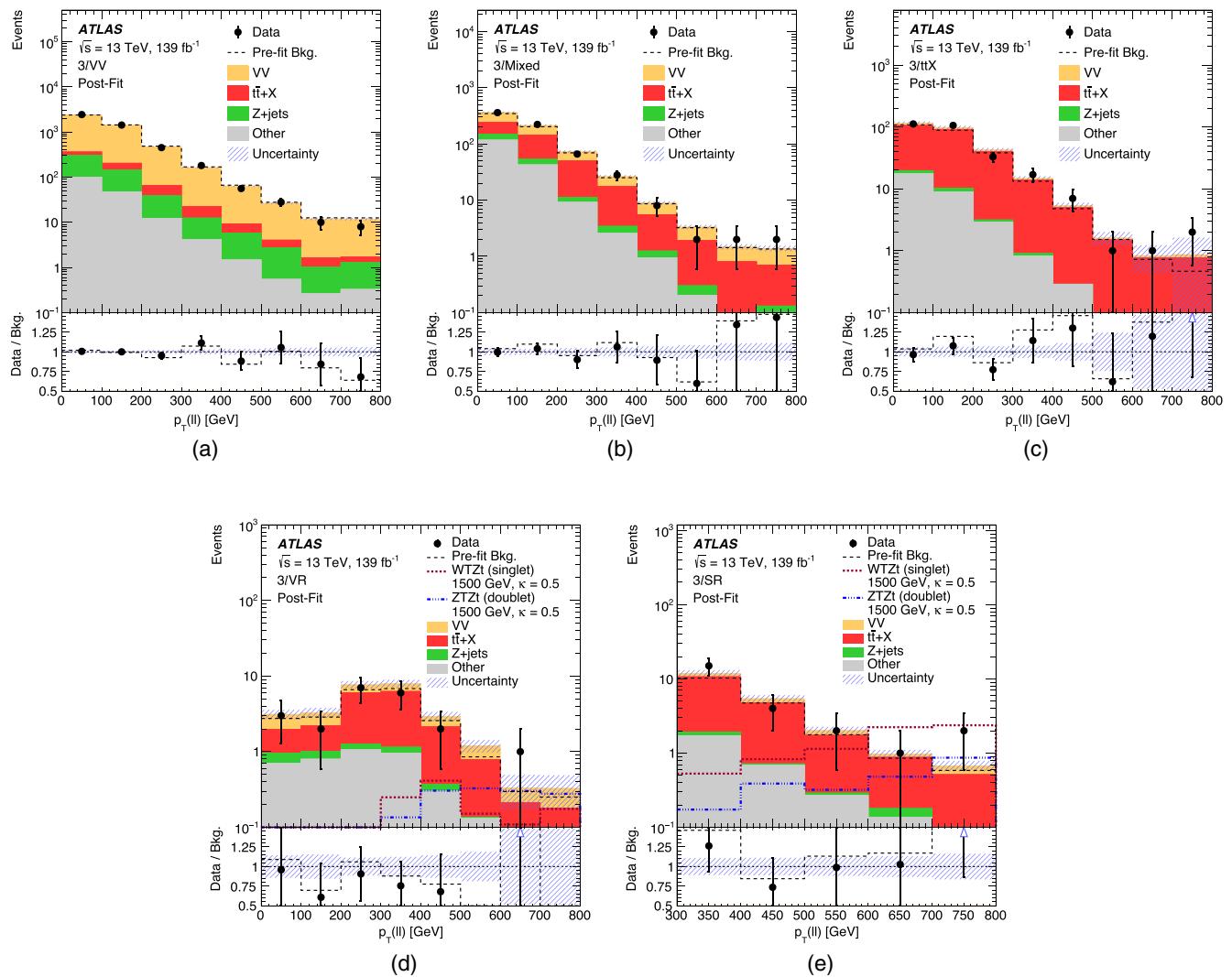
FIG. 7. Distribution of the final discriminant, $p_T(\ell\ell)$, for the 3ℓ channel in the control regions (a) 3ℓVV, (b) 3ℓMixed, (c) 3ℓttX, the validation region (d) 3ℓVR, and the signal region (e) 3ℓSR. The distributions are shown after the background-only fit in the 3ℓ channel. The black, dashed line shows the total prefit background distribution and the corresponding data-over-background ratio in the bottom panel. The blue arrows in the bottom panel indicate points that are outside the vertical range of the figure. The overlaid red and blue dotted lines in (d) and (e) show the expected signal contributions in the corresponding regions from $WTZt$ and $ZTZt$ processes with $M_T = 1.5$ TeV and $\kappa = 0.5$ in singlet and doublet representations respectively. Expected signal contributions in the control regions are negligible. The last bin in each distribution contains the overflow.

TABLE III. Observed number of events in data and post-fit number of background events in the control, validation, and signal regions for the 2ℓ channel. The fit was performed under a background-only hypothesis. Statistical uncertainties from the limited size of MC samples and systematic uncertainties are added in quadrature. Systematic uncertainties take the correlations among nuisance parameters into account. The *WTZt* and *ZTZt* signal yields correspond to prefit yields.

	2ℓCR1	2ℓCR2	2ℓCR3	2ℓVR1	2ℓVR2	2ℓSR
WTZt (singlet) $M_T = 1.5$ TeV, $\kappa = 0.5$	3.9 ± 0.5	9.8 ± 0.9	3.6 ± 0.5	4.7 ± 0.6	12.4 ± 1.1	22.8 ± 1.7
ZTZt (doublet) $M_T = 1.5$ TeV, $\kappa = 0.5$	0.34 ± 0.04	1.64 ± 0.16	0.19 ± 0.04	0.32 ± 0.05	2.28 ± 0.22	3.72 ± 0.24
Z + jets (LF)	3980 ± 90	1170 ± 110	3220 ± 80	589 ± 16	258 ± 27	48 ± 6
Z + jets (HF)	660 ± 60	2330 ± 140	330 ± 50	101 ± 9	452 ± 28	103 ± 10
VV	238 ± 35	206 ± 25	169 ± 26	40 ± 6	40 ± 7	8.7 ± 1.6
$t\bar{t}$	2.8 ± 3.4	38 ± 20	2.8 ± 1.9	0.6 ± 0.6	12 ± 5	2.6 ± 1.6
$t\bar{t}$ + X	3.9 ± 1.0	61 ± 23	3.8 ± 0.8	1.34 ± 0.28	34 ± 12	10 ± 4
Single-top	1.23 ± 0.17	15.6 ± 1.8	1.27 ± 0.15	0.33 ± 0.09	6.1 ± 0.8	1.85 ± 0.26
Total background	4886 ± 70	3821 ± 60	3727 ± 60	732 ± 16	802 ± 24	174 ± 9
Data	4887	3818	3735	704	846	181

background processes, expected signal yields, and observed data in different regions for the 2ℓ and 3ℓ channels are summarized in Tables III and IV respectively. The post-fit background contribution shows reasonable agreement in all regions with the observed data within the uncertainties.

To test whether the observed data is compatible with the background-only hypothesis, tests are performed with RooStats [126] with statistical models implemented using RooFit [127] and HistFactory [128]. No significant excess over the background expectation is observed. Hence, the results were used to set upper limits on the top partner total production cross section $\sigma(WTZt + ZTZt)$ at 95%

confidence level (CL) using the CL$_s$ method [129,130]. These limits were calculated with the asymptotic approximation [131] of the test statistic and validated against the limits obtained using pseudoexperiments for benchmark signal samples with $M_T = 1200$, 1500, and 2100 GeV. For all these benchmarks, the expected and observed limits obtained from pseudoexperiments at 95% CL agreed with the limits obtained using the asymptotic approximation within 5%. The largest difference, close to 30%, in the results obtained with the two methods was observed in the -1σ and -2σ bands for the 2100 GeV mass point.

The overall impact of the systematic uncertainties introduced in Sec. VI on the final result is found to be

TABLE IV. Observed number of events in data and post-fit number of background events in the control, validation, and signal regions for the 3ℓ channel. The fit was performed under a background-only hypothesis. Statistical uncertainties from the limited size of MC samples and systematic uncertainties are added in quadrature. Systematic uncertainties take the correlations among nuisance parameters into account. The *WTZt* and *ZTZt* signal yields correspond to prefit yields.

	3ℓVV	3ℓMixed	3ℓttX	3ℓVR	3ℓSR
WTZt (singlet) $M_T = 1.5$ TeV, $\kappa = 0.5$	3.2 ± 0.4	0.85 ± 0.19	0.58 ± 0.14	1.21 ± 0.24	8.3 ± 0.8
ZTZt (doublet) $M_T = 1.5$ TeV, $\kappa = 0.5$	0.84 ± 0.24	0.68 ± 0.12	0.40 ± 0.12	2.0 ± 0.8	2.04 ± 0.32
VV	3920 ± 160	230 ± 40	21 ± 4	7.1 ± 1.5	2.4 ± 0.5
$t\bar{t}$ + X	156 ± 27	245 ± 28	225 ± 20	14.9 ± 2.5	15.4 ± 2.2
Z + jets	350 ± 120	45 ± 13	3.8 ± 1.5	1.0 ± 0.4	0.31 ± 0.11
$t\bar{t}$	82 ± 30	93 ± 16	5 ± 6	0.9 ± 1.1	0.005 ± 0.007
Single-top	63.1 ± 2.6	77.9 ± 1.6	25.8 ± 0.8	2.99 ± 0.17	2.88 ± 0.17
VVV	22.6 ± 1.2	1.22 ± 0.09	0.087 ± 0.012	0.078 ± 0.015	0.023 ± 0.004
Total background	4594 ± 70	692 ± 26	281 ± 16	27.0 ± 3.0	21.0 ± 2.2
Data	4590	690	279	21	24
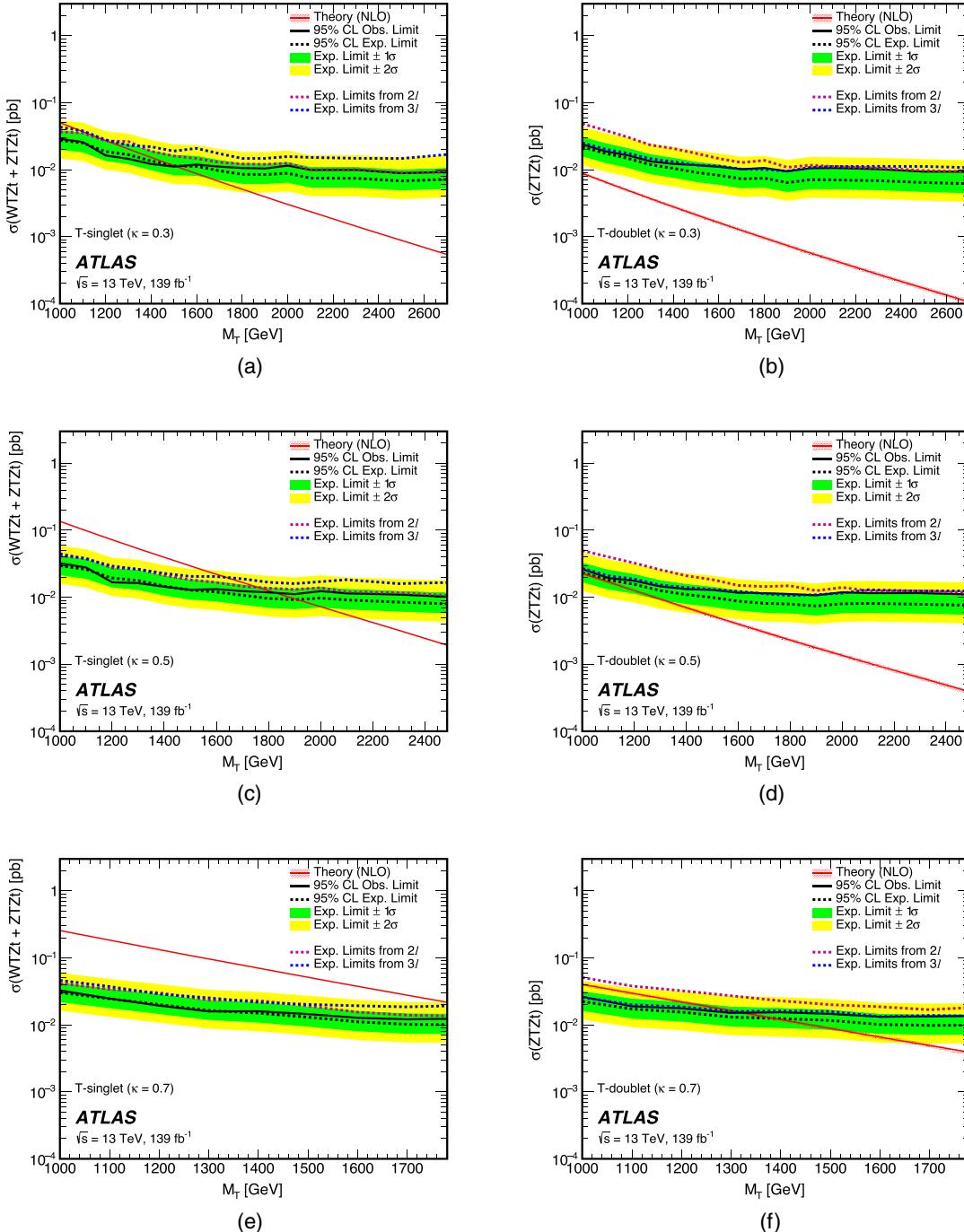
FIG. 8. Observed (solid black line) and expected (dashed black line) limits calculated at 95% CL on total cross section of the $WTZt$ and $ZTZt$ processes as a function of the T mass for a choice of coupling $\kappa = 0.3$ (top row), $\kappa = 0.5$ (middle row), and $\kappa = 0.7$ (bottom row) for singlet (left column) and doublet (right column) representations. Expected limits calculated at 95% CL by independently fitting the 2ℓ and 3ℓ channels are shown as overlaid blue and red dotted lines respectively. The green (yellow) band is the 68% (95%) confidence interval around the median expected limit. The solid red line shows the theory prediction for the NLO cross section, with the surrounding shaded band representing the corresponding uncertainty. The mass range in these figures is restricted to ensure that the relative decay width $\frac{\Gamma_T}{M_T}$ is limited to less than 50%.
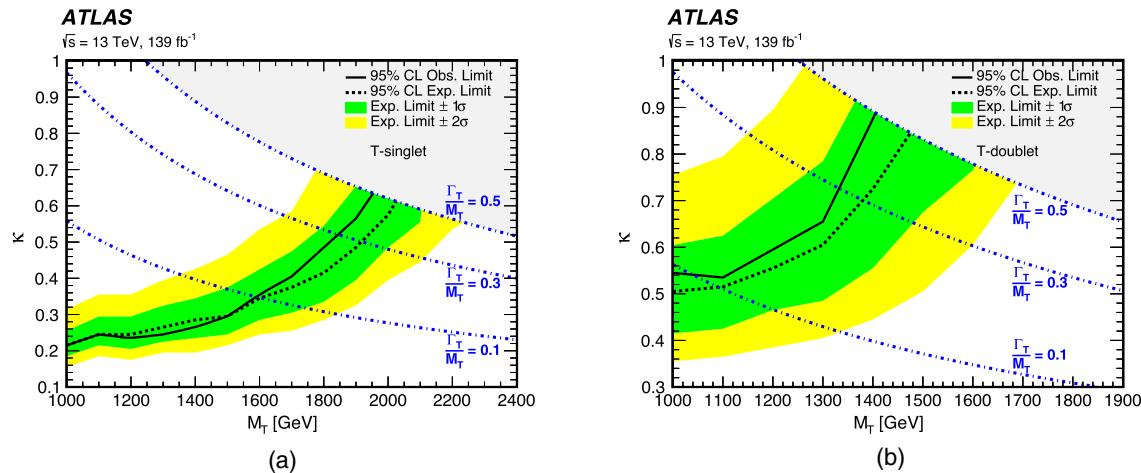
FIG. 9. Observed (solid black line) and expected (dashed black line) limits calculated at 95% CL on the top partner coupling as a function of the T mass for (a) singlet and (b) doublet representations. The shaded regions represent the parametric space with $\frac{\Gamma_T}{M_T} > 50\%$. The green (yellow) band is the 68% (95%) confidence interval around the median expected limit. The dotted lines represent contours of equal values in $\frac{\Gamma_T}{M_T}$.

small. Considering only statistical uncertainties, the limits on the total cross section of the $WTZt$ and $ZTZt$ processes are reduced by less than 14%.

Given that the signal efficiencies for the $WTZt$ and $ZTZt$ signal modes can be different, limits were independently calculated for different combinations of top partner mass, coupling, and branching ratios, under the assumption that $\xi_Z = \xi_H$. The latter is motivated by the Goldstone equivalence theorem [132], which states that the asymptotic branching ratios of T decaying into Zt and Ht become similar in the large M_T limit under the narrow-width approximation.

To maximize the sensitivity of the search, the results from both channels were statistically combined. All

experimental uncertainties are treated as fully correlated across the channels while the theoretical and modeling uncertainties are taken to be uncorrelated. The corresponding limits on the signal strength translate into limits on the total cross section of the $WTZt$ and $ZTZt$ processes for the corresponding choice of coupling and branching ratio. Limits corresponding to $\kappa = 0.3$, 0.5, and 0.7 for the singlet and doublet representations are shown in Fig. 8. The combined expected limit is significantly stronger than limits obtained independently from the 2ℓ and 3ℓ channels. For the singlet representation with $\kappa = 0.5$, top partner masses less than 1825 GeV are excluded. The doublet representation only receives contribution from the $ZTZt$ process that has a much smaller cross section because of the
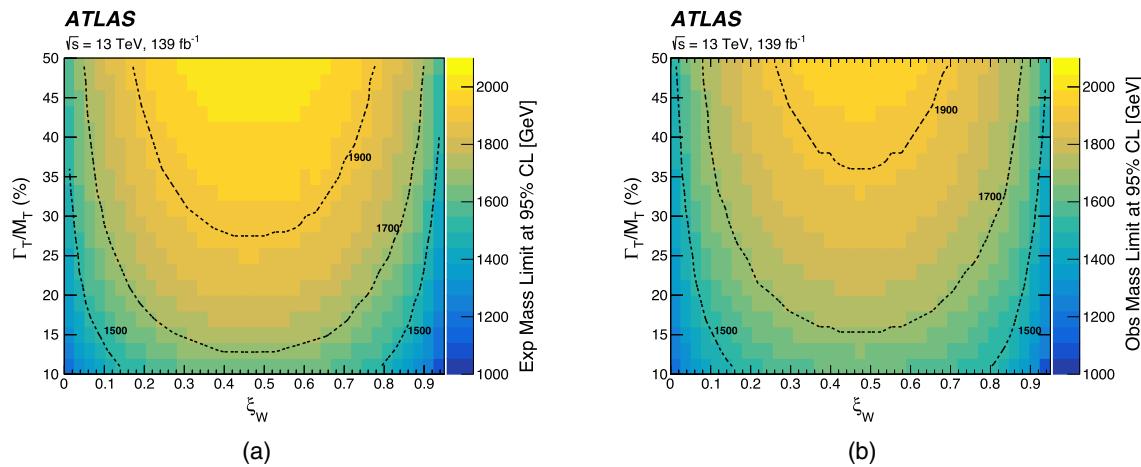

FIG. 10. (a) Expected and (b) observed upper limits calculated at 95% CL on the excluded top partner mass as a function of its relative decay width $\left(\frac{\Gamma_T}{M_T}\right)$ and the relative coupling parameter ξ_W with the assumption of $\xi_Z = \xi_H = \frac{1-\xi_W}{2}$. The dotted contour lines represent exclusion limits of equal mass in units of GeV.

suppressed matrix element contribution from the gluon splitting into $t\bar{t}$ (Fig. 1). Hence, the doublet exclusion limits are found to be considerably weaker than the singlet limits and none of the considered T masses are excluded for $\kappa \leq 0.5$.

The cross section limits calculated for different choices of coupling can be reinterpreted as limits on the plane of (M_T, κ), as shown in Figs. 9(a) and 9(b) for the singlet and doublet representations only. Following the prescription of Ref. [133], this interpretation is only applied for the parametric subspace where the top partner's relative decay width, $\frac{\Gamma_T}{M_T}$ is smaller than 50%. The correction factors for finite width and nonresonant contributions [98,99] are also valid for the same parametric subspace. Hence, the limits in Fig. 9 beyond $\frac{\Gamma_T}{M_T} > 50\%$ are omitted for phenomenological consistency.

To further generalize the interpretation of the search results for any possible combination of top partner branching ratios, the semi-analytical interpretation strategy presented in Ref. [98] was adopted in Fig. 10 to represent the excluded top partner mass as a function of its relative decay width and ξ_W, the asymptotic branching ratio for the $T \rightarrow Wb$ decay mode. The ξ parameters for the other two decay modes are determined by the constraint $\xi_Z = \xi_H = \frac{1-\xi_W}{2}$.

VIII. CONCLUSION

A search for the production of a single vectorlike quark T with electric charge $\frac{2}{3}e$ and mass greater than 1 TeV in a final state with a leptonically decaying Z boson and a top quark is presented. Two orthogonal channels with two or at least three leptons are separately optimized and their results are statistically combined to obtain the final result. No significant excess over the background expectation is observed, and therefore 95% CL upper limits on the inclusive single-T cross section are derived for different choices of T mass and couplings. These results are interpreted in terms of limits on the T mass and coupling for different electroweak representations and generalized branching ratio scenarios. For the singlet representation, κ values are excluded between 0.22 and 0.64 for masses of T between 1000 and 1975 GeV. The exclusion range for the doublet representation spans κ values between 0.54 and 0.88 for masses of T between 1000 and 1425 GeV. These limits significantly improve on the previous limits obtained from the 2015–16 data sample. The strongest exclusion is observed for singlet representation with $\xi_W \approx 0.5$ where masses up to 1975 GeV are excluded at relative decay width of $\frac{\Gamma_T}{M_T} = 0.5$ for the top partner. The exclusion of singlet T production with mass and coupling of 1.8 (1.6) TeV and

0.70 (0.35), corresponding to a decay width of 30% (10%), provides the strongest limits from the LHC in these parameter regions.

[1] ATLAS Collaboration, Observation of a new particle in the search for the Standard Model Higgs boson with the ATLAS detector at the LHC, Phys. Lett. B **716,** 1 (2012).

[2] CMS Collaboration, Observation of a new boson at a mass of 125 GeV with the CMS experiment at the LHC, Phys. Lett. B **716,** 30 (2012).

[3] L. Susskind, Dynamics of spontaneous symmetry breaking in the Weinberg-Salam theory, Phys. Rev. D **20,** 2619 (1979).

[4] F. Del Aguila and M. J. Bowick, The possibility of new fermions with $\Delta I = 0$ mass, Nucl. Phys. **B224,** 107 (1983).

[5] D. B. Kaplan, H. Georgi, and S. Dimopoulos, Composite Higgs scalars, Phys. Lett. **136B,** 187 (1984).

[6] K. Agashe, R. Contino, and A. Pomarol, The minimal composite Higgs model, Nucl. Phys. **B719,** 165 (2005).

[7] R. Contino, L. Da Rold, and A. Pomarol, Light custodians in natural composite Higgs models, Phys. Rev. D **75,** 055014 (2007).

[8] N. Arkani-Hamed, A. Cohen, E. Katz, and A. Nelson, The littlest Higgs, J. High Energy Phys. 07 (2002) 034.

[9] Y. Hosotani, S. Noda, and K. Takenaga, Dynamical gauge-Higgs unification in the electroweak theory, Phys. Lett. B **607,** 276 (2005).

[10] I. Antoniadis, K. Benakli, and M. Quirós, Finite Higgs mass without supersymmetry, New J. Phys. **3,** 20 (2001).

[11] T. Appelquist, H.-C. Cheng, and B. A. Dobrescu, Bounds on universal extra dimensions, Phys. Rev. D **64,** 035002 (2001).

[12] F. Del Aguila, L. Ametller, G. L. Kane, and J. Vidal, Vector-like fermion and standard Higgs production at hadron colliders, Nucl. Phys. **B334,** 1 (1990).

[13] J. Aguilar-Saavedra, Identifying top partners at LHC, J. High Energy Phys. 11 (2009) 030.

[14] B. Fuks and H.-S. Shao, QCD next-to-leading-order predictions matched to parton showers for vector-like quark models, Eur. Phys. J. C **77,** 135 (2017).

[15] Y. Okada and L. Panizzi, LHC signatures of vector-like quarks, Adv. High Energy Phys. **2013,** 364936 (2013).

[16] J. A. Aguilar-Saavedra, R. Benbrik, S. Heinemeyer, and M. Pérez-Victoria, Handbook of vectorlike quarks: Mixing and single production, Phys. Rev. D **88,** 094010 (2013).

[17] ATLAS Collaboration, Search for production of vector-like quark pairs and of four top quarks in the lepton-plus-jets final state in pp collisions at $\sqrt{s} = 8$ TeV with the ATLAS detector, J. High Energy Phys. 08 (2015) 105.

[18] ATLAS Collaboration, Search for vectorlike B quarks in events with one isolated lepton, missing transverse momentum, and jets at $\sqrt{s} = 8$ TeV with the ATLAS detector, Phys. Rev. D **91,** 112011 (2015).

[19] ATLAS Collaboration, Search for pair and single production of new heavy quarks that decay to a Z boson and a third-generation quark in pp collisions at $\sqrt{s} = 8$ TeV with the ATLAS detector, J. High Energy Phys. 11 (2014) 104.

[20] CMS Collaboration, Search for vectorlike charge 2/3 T quarks in proton–proton collisions at $\sqrt{(s)} = 8$ TeV, Phys. Rev. D **93,** 012003 (2016).

[21] CMS Collaboration, Search for pair-produced vectorlike B quarks in proton–proton collisions at $\sqrt{s} = 8$ TeV, Phys. Rev. D **93,** 112009 (2016).

[22] CMS Collaboration, Search for top-quark partners with charge 5/3 in the same-sign dilepton final state, Phys. Rev. Lett. **112,** 171801 (2014).

[23] ATLAS Collaboration, Search for single production of vector-like quarks decaying into Wb in pp collisions at $\sqrt{s} = 8$ TeV with the ATLAS detector, Eur. Phys. J. C **76,** 442 (2016).

[24] ATLAS Collaboration, Search for pair production of up-type vector-like quarks and for four-top-quark events in final states with multiple b-jets with the ATLAS detector, J. High Energy Phys. 07 (2018) 089.

[25] ATLAS Collaboration, Search for pair production of heavy vector-like quarks decaying to high-p_T W bosons and b quarks in the lepton-plus-jets final state in pp collisions at $\sqrt{s} = 13$ TeV with the ATLAS detector, J. High Energy Phys. 10 (2017) 141.

[26] ATLAS Collaboration, Search for pair production of vector-like top quarks in events with one lepton, jets, and missing transverse momentum in $\sqrt{s} = 13$ TeV pp collisions with the ATLAS detector, J. High Energy Phys. 08 (2017) 052.

[27] ATLAS Collaboration, Search for new phenomena in events with same-charge leptons and b-jets in pp collisions at $\sqrt{s} = 13$ TeV with the ATLAS detector, J. High Energy Phys. 12 (2018) 039.

[28] ATLAS Collaboration, Search for pair production of heavy vector-like quarks decaying into hadronic final states in pp collisions at $\sqrt{s} = 13$ TeV with the ATLAS detector, Phys. Rev. D **98,** 092005 (2018).

[29] ATLAS Collaboration, Combination of the searches for pair-produced vector-like partners of the third-generation quarks at $\sqrt{s} = 13$ TeV with the ATLAS detector, Phys. Rev. Lett. **121,** 211801 (2018).

[30] ATLAS Collaboration, Search for pair-production of vector-like quarks in pp collision events at $\sqrt{s} = 13$ TeV with at least one leptonically decaying Z boson and a third-generation quark with the ATLAS detector, Phys. Lett. B **843,** 138019 (2023).

[31] CMS Collaboration, Search for pair production of vector-like T and B quarks in single-lepton final states using boosted jet substructure techniques at $\sqrt{s} = 13$ TeV, J. High Energy Phys. 11 (2017) 085.

[32] CMS Collaboration, Search for pair production of vector-like quarks in the $bW\bar{b}W$ channel from proton–proton collisions at $\sqrt{s} = 13$ TeV, Phys. Lett. B **779,** 82 (2018).

[33] CMS Collaboration, Search for vector-like T and B quark pairs in final states with leptons at $\sqrt{s} = 13$ TeV, J. High Energy Phys. 08 (2018) 177.

[34] CMS Collaboration, Search for pair production of vector-like quarks in leptonic final states in proton-proton collisions at $\sqrt{s} = 13$ TeV, J. High Energy Phys. 07 (2023) 020.

[35] ATLAS Collaboration, Search for pair- and single-production of vector-like quarks in final states with at least one Z boson decaying into a pair of electrons or muons in pp collision data collected with the ATLAS detector, Phys. Rev. D **98,** 112010 (2018).

[36] ATLAS Collaboration, Search for pair- and single-production of vector-like quarks in final states with at least one Z boson decaying into a pair of electrons or

muons in pp collision data collected with the ATLAS detector, J. High Energy Phys. 05 (2019) 164.

[37] ATLAS Collaboration, Search for large missing transverse momentum in association with one top-quark in proton–proton collisions at $\sqrt{s} = 13$ TeV with the ATLAS detector, J. High Energy Phys. 05 (2019) 041.

[38] CMS Collaboration, Search for single production of a vector-like T quark decaying to a Z boson and a top quark in proton–proton collisions at $\sqrt{s} = 13$ TeV, Phys. Lett. B **781**, 574 (2018).

[39] CMS Collaboration, Search for single production of vector-like quarks decaying to a top quark and a W boson in proton–proton collisions at $\sqrt{s} = 13$ TeV, Eur. Phys. J. C **79**, 90 (2019).

[40] CMS Collaboration, Search for single production of vector-like quarks decaying to a b quark and a Higgs boson, J. High Energy Phys. 06 (2018) 031.

[41] CMS Collaboration, Search for electroweak production of a vector-like T quark using fully hadronic final states, J. High Energy Phys. 01 (2020) 036.

[42] CMS Collaboration, Search for single production of a vector-like T quark decaying to a top quark and a Z boson in the final state with jets and missing transverse momentum at $\sqrt{s} = 13$ TeV, J. High Energy Phys. 05 (2022) 093.

[43] CMS Collaboration, Search for a vector-like quark $T' \rightarrow tH$ via the diphoton decay mode of the Higgs boson in proton-proton collisions at $\sqrt{s} = 13$ TeV, J. High Energy Phys. 09 (2023) 057.

[44] ATLAS Collaboration, Search for single production of a vectorlike T quark decaying into a Higgs boson and top quark with fully hadronic final states using the ATLAS detector, Phys. Rev. D **105**, 092012 (2022).

[45] ATLAS Collaboration, Search for single production of vector-like T quarks decaying into Ht or Zt in pp collisions at $\sqrt{s} = 13$ TeV with the ATLAS detector, J. High Energy Phys. 08 (2023) 153.

[46] A. Atre, G. Azuelos, M. Carena, T. Han, E. Ozcan, J. Santiago, and G. Unel, Model-independent searches for new quarks at the LHC, J. High Energy Phys. 08 (2011) 080.

[47] M. Buchkremer, G. Cacciapaglia, A. Deandrea, and L. Panizzi, Model-independent framework for searches of top partners, Nucl. Phys. **B876**, 376 (2013).

[48] O. Matsedonskyi, G. Panico, and A. Wulzer, On the interpretation of top partners searches, J. High Energy Phys. 12 (2014) 097.

[49] ATLAS Collaboration, The ATLAS experiment at the CERN Large Hadron Collider, J. Instrum. **3**, S08003 (2008).

[50] B. Abbott et al., Production and integration of the ATLAS insertable B-layer, J. Instrum. **13**, T05008 (2018).

[51] ATLAS Collaboration, Performance of the ATLAS trigger system in 2015, Eur. Phys. J. C **77**, 317 (2017).

[52] ATLAS Collaboration, The ATLAS Collaboration software and firmware, Report No. ATL-SOFT-PUB-2021-001, 2021, https://cds.cern.ch/record/2767187.

[53] ATLAS Collaboration, The ATLAS simulation infrastructure, Eur. Phys. J. C **70**, 823 (2010).

[54] S. Agostinelli et al., Geant4—A simulation toolkit, Nucl. Instrum. Methods Phys. Res., Sect. A **506**, 250 (2003).

[55] T. Sjöstrand, S. Mrenna, and P. Skands, A brief introduction to PYTHIA 8.1, Comput. Phys. Commun. **178**, 852 (2008).

[56] R. D. Ball et al. (NNPDF Collaboration), Parton distributions with LHC data, Nucl. Phys. **B867**, 244 (2013).

[57] ATLAS Collaboration, The PYTHIA 8 A3 tune description of ATLAS minimum bias and inelastic measurements incorporating the Donnachie–Landshoff diffractive model, Report No. ATL-PHYS-PUB-2016-017, 2016, https://cds.cern.ch/record/2206965.

[58] E. Bothmann et al., Event generation with Sherpa 2.2, SciPost Phys. **7**, 034 (2019).

[59] R. D. Ball et al. (The NNPDF Collaboration), Parton distributions for the LHC run II, J. High Energy Phys. 04 (2015) 040.

[60] C. Anastasiou, L. Dixon, K. Melnikov, and F. Petriello, High-precision QCD at hadron colliders: Electroweak gauge boson rapidity distributions at next-to-next-to leading order, Phys. Rev. D **69**, 094008 (2004).

[61] T. Gleisberg and S. Höche, COMIX, A new matrix element generator, J. High Energy Phys. 12 (2008) 039.

[62] F. Buccioni, J.-N. Lang, J. M. Lindert, P. Maierhöfer, S. Pozzorini, H. Zhang, and M. F. Zoller, OpenLoops 2, Eur. Phys. J. C **79**, 866 (2019).

[63] F. Cascioli, P. Maierhöfer, and S. Pozzorini, Scattering amplitudes with open loops, Phys. Rev. Lett. **108**, 111601 (2012).

[64] A. Denner, S. Dittmaier, and L. Hofer, Collier: A Fortran-based complex one-loop library in extended regularizations, Comput. Phys. Commun. **212**, 220 (2017).

[65] S. Schumann and F. Krauss, A parton shower algorithm based on Catani–Seymour dipole factorisation, J. High Energy Phys. 03 (2008) 038.

[66] S. Höche, F. Krauss, M. Schönherr, and F. Siegert, A critical appraisal of NLO + PS matching methods, J. High Energy Phys. 09 (2012) 049.

[67] S. Höche, F. Krauss, M. Schönherr, and F. Siegert, QCD matrix elements + parton showers. The NLO case, J. High Energy Phys. 04 (2013) 027.

[68] S. Catani, F. Krauss, B. R. Webber, and R. Kuhn, QCD matrix elements + parton showers, J. High Energy Phys. 11 (2001) 063.

[69] S. Höche, F. Krauss, S. Schumann, and F. Siegert, QCD matrix elements and truncated showers, J. High Energy Phys. 05 (2009) 053.

[70] J. Alwall, R. Frederix, S. Frixione, V. Hirschi, F. Maltoni, O. Mattelaer, H.-S. Shao, T. Stelzer, P. Torrielli, and M. Zaro, The automated computation of tree-level and next-to-leading order differential cross sections, and their matching to parton shower simulations, J. High Energy Phys. 07 (2014) 079.

[71] T. Sjöstrand, S. Ask, J. R. Christiansen, R. Corke, N. Desai, P. Ilten, S. Mrenna, S. Prestel, C. O. Rasmussen, and P. Z. Skands, An introduction to PYTHIA 8.2, Comput. Phys. Commun. **191**, 159 (2015).

[72] ATLAS Collaboration, ATLAS PYTHIA 8 tunes to 7 TeV data, Report No. ATL-PHYS-PUB-2014-021, 2014, https://cds.cern.ch/record/1966419.

[73] P. Nason, A new method for combining NLO QCD with shower Monte Carlo algorithms, J. High Energy Phys. 11 (2004) 040.

[74] S. Frixione, P. Nason, and C. Oleari, Matching NLO QCD computations with parton shower simulations: The POWHEG method, J. High Energy Phys. 11 (2007) 070.

[75] S. Alioli, P. Nason, C. Oleari, and E. Re, A general framework for implementing NLO calculations in shower Monte Carlo programs: The POWHEG BOX, J. High Energy Phys. 06 (2010) 043.

[76] J. M. Campbell, R. K. Ellis, P. Nason, and E. Re, Top-pair production and decay at NLO matched with parton showers, J. High Energy Phys. 04 (2015) 114.

[77] M. Czakon and A. Mitov, TOP++: A program for the calculation of the top-pair cross section at hadron colliders, Comput. Phys. Commun. **185,** 2930 (2014).

[78] M. Czakon, P. Fiedler, and A. Mitov, Total top-quark pair-production cross section at hadron colliders through $O(\alpha_S^4)$, Phys. Rev. Lett. **110,** 252004 (2013).

[79] M. Beneke, P. Falgari, S. Klein, and C. Schwinn, Hadronic top-quark pair production with NNLL threshold resummation, Nucl. Phys. **B855,** 695 (2012).

[80] M. Cacciari, M. Czakon, M. Mangano, A. Mitov, and P. Nason, Top-pair production at hadron colliders with next-to-next-to-leading logarithmic soft-gluon resummation, Phys. Lett. B **710,** 612 (2012).

[81] M. Czakon and A. Mitov, NNLO corrections to top pair production at hadron colliders: The quark-gluon reaction, J. High Energy Phys. 01 (2013) 080.

[82] M. Czakon and A. Mitov, NNLO corrections to top-pair production at hadron colliders: The all-fermionic scattering channels, J. High Energy Phys. 12 (2012) 054.

[83] P. Bärnreuther, M. Czakon, and A. Mitov, Percent-level-precision physics at the Tevatron: Next-to-next-to-leading order QCD corrections to $q\bar{q} \to t\bar{t} + X$, Phys. Rev. Lett. **109,** 132001 (2012).

[84] J. Bellm *et al.*, Herwig 7.0/Herwig++ 3.0 release note, Eur. Phys. J. C **76,** 196 (2016).

[85] R. Frederix, D. Pagani, and M. Zaro, Large NLO corrections in $t\bar{t}W^{\pm}$ and $t\bar{t}t\bar{t}$ hadroproduction from supposedly subleading EW contributions, J. High Energy Phys. 02 (2018) 031.

[86] S. Frixione, V. Hirschi, D. Pagani, H.-S. Shao, and M. Zaro, Electroweak and QCD corrections to top-pair hadroproduction in association with heavy bosons, J. High Energy Phys. 06 (2015) 184.

[87] R. Frederix, E. Re, and P. Torrielli, Single-top *t*-channel hadroproduction in the four-flavour scheme with POWHEG and aMC@NLO, J. High Energy Phys. 09 (2012) 130.

[88] E. Re, Single-top *Wt*-channel production matched with parton showers using the POWHEG method, Eur. Phys. J. C **71,** 1547 (2011).

[89] M. Aliev, H. Lacker, U. Langenfeld, S. Moch, P. Uwer, and M. Wiedermann, HATHOR—Hadronic top and heavy quarks cross section calculator, Comput. Phys. Commun. **182,** 1034 (2011).

[90] P. Kant, O. M. Kind, T. Kintscher, T. Lohse, T. Martini, S. Mölbitz, P. Rieck, and P. Uwer, HatHor for single top-quark production: Updated predictions and uncertainty estimates for single top-quark production in hadronic collisions, Comput. Phys. Commun. **191,** 74 (2015).

[91] N. Kidonakis, Next-to-next-to-leading-order collinear and soft gluon corrections for *t*-channel single top quark production, Phys. Rev. D **83,** 091503 (2011).

[92] N. Kidonakis, Two-loop soft anomalous dimensions for single top quark associated production with a W^- or H^-, Phys. Rev. D **82,** 054018 (2010).

[93] N. Kidonakis, Next-to-next-to-leading logarithm resummation for *s*-channel single top quark production, Phys. Rev. D **81,** 054028 (2010).

[94] S. Frixione, E. Laenen, P. Motylinski, C. White, and B. R. Webber, Single-top hadroproduction in association with a *W* boson, J. High Energy Phys. 07 (2008) 029.

[95] C. Degrande, C. Duhr, B. Fuks, D. Grellscheid, O. Mattelaer, and T. Reiter, UFO–The universal FEYNRULES output, Comput. Phys. Commun. **183,** 1201 (2012).

[96] O. Mattelaer, On the maximal use of Monte Carlo samples: Re-weighting events at NLO accuracy, Eur. Phys. J. C **76,** 1 (2016).

[97] G. Cacciapaglia, A. Carvalho, A. Deandrea, T. Flacke, B. Fuks, D. Majumder, L. Panizzi, and H.-S. Shao, Next-to-leading-order predictions for single vector-like quark production at the LHC, Phys. Lett. B **793,** 206 (2019).

[98] A. Roy, N. Nikiforou, N. Castro, and T. Andeen, Novel interpretation strategy for searches of singly produced vectorlike quarks at the LHC, Phys. Rev. D **101,** 115027 (2020).

[99] A. Roy and T. Andeen, Non-resonant diagrams for single production of top and bottom partners, Phys. Lett. B **833,** 137330 (2022).

[100] ATLAS Collaboration, Electron and photon performance measurements with the ATLAS detector using the 2015–2017 LHC proton–proton collision data, J. Instrum. **14,** P12006 (2019).

[101] ATLAS Collaboration, Muon reconstruction and identification efficiency in ATLAS using the full Run 2 *pp* collision data set at $\sqrt{s} = 13$ TeV, Eur. Phys. J. C **81,** 578 (2021).

[102] ATLAS Collaboration, Jet reconstruction and performance using particle flow with the ATLAS detector, Eur. Phys. J. C **77,** 466 (2017).

[103] M. Cacciari, G. P. Salam, and G. Soyez, The anti-k_t jet clustering algorithm, J. High Energy Phys. 04 (2008) 063.

[104] M. Cacciari, G. P. Salam, and G. Soyez, FASTJET user manual, Eur. Phys. J. C **72,** 1896 (2012).

[105] ATLAS Collaboration, Jet energy scale and resolution measured in proton–proton collisions at $\sqrt{s} = 13$ TeV with the ATLAS detector, Eur. Phys. J. C **81,** 689 (2021).

[106] ATLAS Collaboration, Performance of pile-up mitigation techniques for jets in *pp* collisions at $\sqrt{s} = 8$ TeV using the ATLAS detector, Eur. Phys. J. C **76,** 581 (2016).

[107] ATLAS Collaboration, ATLAS flavour-tagging algorithms for the LHC Run 2 *pp* collision dataset, Eur. Phys. J. C **83,** 681 (2023).

[108] ATLAS Collaboration, E_T^{miss} performance in the ATLAS detector using 2015–2016 LHC *pp* collisions, Report

No. ATLAS-CONF-2018-023, 2018, https://cds.cern.ch/record/2625233.

[109] D. Krohn, J. Thaler, and L.-T. Wang, Jets with variable R, J. High Energy Phys. 06 (2009) 059.

[110] T. Lapsien, R. Kogler, and J. Haller, A new tagger for hadronically decaying heavy particles at the LHC, Eur. Phys. J. C **76,** 600 (2016).

[111] ATLAS Collaboration, Performance of the ATLAS muon triggers in Run 2, J. Instrum. **15,** P09015 (2020).

[112] ATLAS Collaboration, Performance of electron and photon triggers in ATLAS during LHC Run 2, Eur. Phys. J. C **80,** 47 (2020).

[113] ATLAS Collaboration, ATLAS simulation of boson plus jets processes in Run 2, Report No. ATL-PHYS-PUB-2017-006, 2017, https://cds.cern.ch/record/2261937.

[114] ATLAS Collaboration, ATLAS b-jet identification performance and efficiency measurement with $t\bar{t}$ events in pp collisions at $\sqrt{s} = 13$ TeV, Eur. Phys. J. C **79,** 970 (2019).

[115] ATLAS Collaboration, Measurement of the c-jet mistagging efficiency in $t\bar{t}$ events using pp collision data at $\sqrt{s} = 13$ TeV collected with the ATLAS detector, Eur. Phys. J. C **82,** 95 (2021).

[116] ATLAS Collaboration, Calibration of the light-flavour jet mistagging efficiency of the b-tagging algorithms with $Z + $ jets events using 139 fb^{-1} of ATLAS proton-proton collision data at $\sqrt{s} = 13$ TeV, Eur. Phys. J. C **83,** 728 (2023).

[117] ATLAS Collaboration, Performance of missing transverse momentum reconstruction with the ATLAS detector using proton–proton collisions at $\sqrt{s} = 13$ TeV, Eur. Phys. J. C **78,** 903 (2018).

[118] ATLAS Collaboration, Luminosity determination in pp collisions at $\sqrt{s} = 13$ TeV using the ATLAS detector at the LHC, Report No. ATLAS-CONF-2019-021, 2019, https://cds.cern.ch/record/2677054.

[119] G. Avoni et al., The new LUCID-2 detector for luminosity measurement and monitoring in ATLAS, J. Instrum. **13,** P07017 (2018).

[120] ATLAS Collaboration, Measurements of the production cross section of a Z boson in association with jets in pp collisions at $\sqrt{s} = 13$ TeV with the ATLAS detector, Eur. Phys. J. C **77,** 361 (2017).

[121] J. M. Campbell and R. K. Ellis, Update on vector boson pair production at hadron colliders, Phys. Rev. D **60,** 113006 (1999).

[122] ATLAS Collaboration, Measurements of the inclusive and differential production cross sections of a top-quark-antiquark pair in association with a Z boson at $\sqrt{s} = 13$ TeV with the ATLAS detector, Eur. Phys. J. C **81,** 737 (2021).

[123] J. Butterworth et al., PDF4LHC recommendations for LHC Run II, J. Phys. G **43,** 023001 (2016).

[124] ATLAS Collaboration, Measurement of Higgs boson decay into b-quarks in associated production with a top-quark pair in pp collisions at $\sqrt{s} = 13$ TeV with the ATLAS detector, J. High Energy Phys. 06 (2021) 097.

[125] R. Barlow and C. Beeston, Fitting using finite Monte Carlo samples, Comput. Phys. Commun. **77,** 219 (1993).

[126] L. Moneta et al., The RooStats project, Proc. Sci. ACAT2010 (**2010**) 057 [arXiv:1009.1003].

[127] W. Verkerke and D. Kirkby, The RooFit toolkit for data modeling, arXiv:physics/0306116.

[128] K. Cranmer, G. Lewis, L. Moneta, A. Shibata, and W. Verkerke, HistFactory: A tool for creating statistical models for use with RooFit and RooStats, Technical Report No. CERN-OPEN-2012-016, 2012, https://cds.cern.ch/record/1456844.

[129] T. Junk, Confidence level computation for combining searches with small statistics, Nucl. Instrum. Methods Phys. Res., Sect. A **434,** 435 (1999).

[130] A. L. Read, Presentation of search results: The CL_S technique, J. Phys. G **28,** 2693 (2002).

[131] G. Cowan, K. Cranmer, E. Gross, and O. Vitells, Asymptotic formulae for likelihood-based tests of new physics, Eur. Phys. J. C **71,** 1554 (2011); **73,** 2501(E) (2013).

[132] M. S. Chanowitz and M. K. Gaillard, The TeV physics of strongly interacting W's and Z's, Nucl. Phys. **B261,** 379 (1985).

[133] A. Deandrea, T. Flacke, B. Fuks, L. Panizzi, and H.-S. Shao, Single production of vector-like quarks: The effects of large width, interference and NLO corrections, J. High Energy Phys. 08 (2021) 107.

[134] ATLAS Collaboration, ATLAS computing acknowledgements, Report No. ATL-SOFT-PUB-2023-001, 2023, https://cds.cern.ch/record/2869272.

G. Aad,[102] B. Abbott,[120] K. Abeling,[55] N. J. Abicht,[49] S. H. Abidi,[29] A. Aboulhorma,[35e] H. Abramowicz,[151] H. Abreu,[150] Y. Abulaiti,[117] A. C. Abusleme Hoffman,[137a] B. S. Acharya,[69a,69b,b] C. Adam Bourdarios,[4] L. Adamczyk,[86a] L. Adamek,[155] S. V. Addepalli,[26] M. J. Addison,[101] J. Adelman,[115] A. Adiguzel,[21c] T. Adye,[134] A. A. Affolder,[136] Y. Afik,[36] M. N. Agaras,[13] J. Agarwala,[73a,73b] A. Aggarwal,[100] C. Agheorghiesei,[27c] A. Ahmad,[36] F. Ahmadov,[38,c] W. S. Ahmed,[104] S. Ahuja,[95] X. Ai,[62a] G. Aielli,[76a,76b] M. Ait Tamlihat,[35e] B. Aitbenchikh,[35a] I. Aizenberg,[169] M. Akbiyik,[100] T. P. A. Åkesson,[98] A. V. Akimov,[37] D. Akiyama,[168] N. N. Akolkar,[24] K. Al Khoury,[41] G. L. Alberghi,[23b] J. Albert,[165] P. Albicocco,[53] G. L. Albouy,[60] S. Alderweireldt,[52] M. Aleksa,[36] I. N. Aleksandrov,[38] C. Alexa,[27b] T. Alexopoulos,[10] A. Alfonsi,[114] F. Alfonsi,[23b] M. Algren,[56] M. Alhroob,[120] B. Ali,[132] H. M. J. Ali,[91] S. Ali,[148] S. W. Alibocus,[92] M. Aliev,[37] G. Alimonti,[71a] W. Alkakhi,[55] C. Allaire,[66] B. M. M. Allbrooke,[146] J. F. Allen,[52] C. A. Allendes Flores,[137f] P. P. Allport,[20] A. Aloisio,[72a,72b] F. Alonso,[90] C. Alpigiani,[138] M. Alvarez Estevez,[99] A. Alvarez Fernandez,[100]

M. Alves Cardoso,[56] M. G. Alviggi,[72a,72b] M. Aly,[101] Y. Amaral Coutinho,[83b] A. Ambler,[104] C. Amelung,[36] M. Amerl,[101] C. G. Ames,[109] D. Amidei,[106] S. P. Amor Dos Santos,[130a] K. R. Amos,[163] V. Ananiev,[125] C. Anastopoulos,[139] T. Andeen,[11] J. K. Anders,[36] S. Y. Andrean,[47a,47b] A. Andreazza,[71a,71b] S. Angelidakis,[9] A. Angerami,[41,d] A. V. Anisenkov,[37] A. Annovi,[74a] C. Antel,[56] M. T. Anthony,[139] E. Antipov,[145] M. Antonelli,[53] D. J. A. Antrim,[17a] F. Anulli,[75a] M. Aoki,[84] T. Aoki,[153] J. A. Aparisi Pozo,[163] M. A. Aparo,[146] L. Aperio Bella,[48] C. Appelt,[18] A. Apyan,[26] N. Aranzabal,[36] C. Arcangeletti,[53] A. T. H. Arce,[51] E. Arena,[92] J-F. Arguin,[108] S. Argyropoulos,[54] J.-H. Arling,[48] O. Arnaez,[4] H. Arnold,[114] Z. P. Arrubarrena Tame,[109] G. Artoni,[75a,75b] H. Asada,[111] K. Asai,[118] S. Asai,[153] N. A. Asbah,[61] J. Assahsah,[35d] K. Assamagan,[29] R. Astalos,[28a] S. Atashi,[160] R. J. Atkin,[33a] M. Atkinson,[162] N. B. Atlay,[18] H. Atmani,[62b] P. A. Atmasiddha,[106] K. Augsten,[132] S. Auricchio,[72a,72b] A. D. Auriol,[20] V. A. Austrup,[101] G. Avolio,[36] K. Axiotis,[56] G. Azuelos,[108,e] D. Babal,[28b] H. Bachacou,[135] K. Bachas,[152,f] A. Bachiu,[34] F. Backman,[47a,47b] A. Badea,[61] P. Bagnaia,[75a,75b] M. Bahmani,[18] A. J. Bailey,[163] V. R. Bailey,[162] J. T. Baines,[134] L. Baines,[94] C. Bakalis,[10] O. K. Baker,[172] E. Bakos,[15] D. Bakshi Gupta,[8] R. Balasubramanian,[114] E. M. Baldin,[37] P. Balek,[86a] E. Ballabene,[23b,23a] F. Balli,[135] L. M. Baltes,[63a] W. K. Balunas,[32] J. Balz,[100] E. Banas,[87] M. Bandieramonte,[129] A. Bandyopadhyay,[24] S. Bansal,[24] L. Barak,[151] M. Barakat,[48] E. L. Barberio,[105] D. Barberis,[57b,57a] M. Barbero,[102] G. Barbour,[96] K. N. Barends,[33a] T. Barillari,[110] M-S. Barisits,[36] T. Barklow,[143] P. Baron,[122] D. A. Baron Moreno,[101] A. Baroncelli,[62a] G. Barone,[29] A. J. Barr,[126] J. D. Barr,[96] L. Barranco Navarro,[47a,47b] F. Barreiro,[99] J. Barreiro Guimarães da Costa,[14a] U. Barron,[151] M. G. Barros Teixeira,[130a] S. Barsov,[37] F. Bartels,[63a] R. Bartoldus,[143] A. E. Barton,[91] P. Bartos,[28a] A. Basan,[100] M. Baselga,[49] A. Bassalat,[66,g] M. J. Basso,[156a] C. R. Basson,[101] R. L. Bates,[59] S. Batlamous,[35e] J. R. Batley,[32] B. Batool,[141] M. Battaglia,[136] D. Battulga,[18] M. Bauce,[75a,75b] M. Bauer,[36] P. Bauer,[24] L. T. Bazzano Hurrell,[30] J. B. Beacham,[51] T. Beau,[127] P. H. Beauchemin,[158] F. Becherer,[54] P. Bechtle,[24] H. P. Beck,[19,h] K. Becker,[167] A. J. Beddall,[82] V. A. Bednyakov,[38] C. P. Bee,[145] L. J. Beemster,[15] T. A. Beermann,[36] M. Begalli,[83d] M. Begel,[29] A. Behera,[145] J. K. Behr,[48] J. F. Beirer,[55] F. Beisiegel,[24] M. Belfkir,[159] G. Bella,[151] L. Bellagamba,[23b] A. Bellerive,[34] P. Bellos,[20] K. Beloborodov,[37] N. L. Belyaev,[37] D. Benchekroun,[35a] F. Bendebba,[35a] Y. Benhammou,[151] M. Benoit,[29] J. R. Bensinger,[26] S. Bentvelsen,[114] L. Beresford,[48] M. Beretta,[53] E. Bergeaas Kuutmann,[161] N. Berger,[4] B. Bergmann,[132] J. Beringer,[17a] G. Bernardi,[5] C. Bernius,[143] F. U. Bernlochner,[24] F. Bernon,[36,102] T. Berry,[95] P. Berta,[133] A. Berthold,[50] I. A. Bertram,[91] S. Bethke,[110] A. Betti,[75a,75b] A. J. Bevan,[94] M. Bhamjee,[33c] S. Bhatta,[145] D. S. Bhattacharya,[166] P. Bhattarai,[26] V. S. Bhopatkar,[121] R. Bi,[29,i] R. M. Bianchi,[129] G. Bianco,[23b,23a] O. Biebel,[109] R. Bielski,[123] M. Biglietti,[77a] T. R. V. Billoud,[132] M. Bindi,[55] A. Bingul,[21b] C. Bini,[75a,75b] A. Biondini,[92] C. J. Birch-sykes,[101] G. A. Bird,[20,134] M. Birman,[169] M. Biros,[133] T. Bisanz,[49] E. Bisceglie,[43b,43a] D. Biswas,[141] A. Bitadze,[101] K. Bjørke,[125] I. Bloch,[48] C. Blocker,[26] A. Blue,[59] U. Blumenschein,[94] J. Blumenthal,[100] G. J. Bobbink,[114] V. S. Bobrovnikov,[37] M. Boehler,[54] B. Boehm,[166] D. Bogavac,[36] A. G. Bogdanchikov,[37] C. Bohm,[47a] V. Boisvert,[95] P. Bokan,[48] T. Bold,[86a] M. Bomben,[5] M. Bona,[94] M. Boonekamp,[135] C. D. Booth,[95] A. G. Borbély,[59] I. S. Bordulev,[37] H. M. Borecka-Bielska,[108] L. S. Borgna,[96] G. Borissov,[91] D. Bortoletto,[126] D. Boscherini,[23b] M. Bosman,[13] J. D. Bossio Sola,[36] K. Bouaouda,[35a] N. Bouchhar,[163] J. Boudreau,[129] E. V. Bouhova-Thacker,[91] D. Boumediene,[40] R. Bouquet,[5] A. Boveia,[119] J. Boyd,[36] D. Boye,[29] I. R. Boyko,[38] J. Bracinik,[20] N. Brahimi,[62d] G. Brandt,[171] O. Brandt,[32] F. Braren,[48] B. Brau,[103] J. E. Brau,[123] R. Brener,[169] L. Brenner,[114] R. Brenner,[161] S. Bressler,[169] D. Britton,[59] D. Britzger,[110] I. Brock,[24] G. Brooijmans,[41] W. K. Brooks,[137f] E. Brost,[29] L. M. Brown,[165,j] L. E. Bruce,[61] T. L. Bruckler,[126] P. A. Bruckman de Renstrom,[87] B. Brüers,[48] D. Bruncko,[28b,a] A. Bruni,[23b] G. Bruni,[23b] M. Bruschi,[23b] N. Bruscino,[75a,75b] T. Buanes,[16] Q. Buat,[138] D. Buchin,[110] A. G. Buckley,[59] M. K. Bugge,[125] O. Bulekov,[37] B. A. Bullard,[143] S. Burdin,[92] C. D. Burgard,[49] A. M. Burger,[40] B. Burghgrave,[8] O. Burlayenko,[54] J. T. P. Burr,[32] C. D. Burton,[11] J. C. Burzynski,[142] E. L. Busch,[41] V. Büscher,[100] P. J. Bussey,[59] J. M. Butler,[25] C. M. Buttar,[59] J. M. Butterworth,[96] W. Buttinger,[134] C. J. Buxo Vazquez,[107] A. R. Buzykaev,[37] G. Cabras,[23b] S. Cabrera Urbán,[163] L. Cadamuro,[66] D. Caforio,[58] H. Cai,[129] Y. Cai,[14a,14e] V. M. M. Cairo,[36] O. Cakir,[3a] N. Calace,[36] P. Calafiura,[17a] G. Calderini,[127] P. Calfayan,[68] G. Callea,[59] L. P. Caloba,[83b] D. Calvet,[40] S. Calvet,[40] T. P. Calvet,[102] M. Calvetti,[74a,74b] R. Camacho Toro,[127] S. Camarda,[36] D. Camarero Munoz,[26] P. Camarri,[76a,76b] M. T. Camerlingo,[72a,72b] D. Cameron,[125] C. Camincher,[165] M. Campanelli,[96] A. Camplani,[42]

V. Canale[72a,72b] A. Canesse[104] M. Cano Bret[80] J. Cantero[163] Y. Cao[162] F. Capocasa[26] M. Capua[43b,43a] A. Carbone[71a,71b] R. Cardarelli[76a] J. C. J. Cardenas[8] F. Cardillo[163] T. Carli[36] G. Carlino[72a] J. I. Carlotto[13] B. T. Carlson[129,k] E. M. Carlson[165,156a] L. Carminati[71a,71b] A. Carnelli[135] M. Carnesale[75a,75b] S. Caron[113] E. Carquin[137f] S. Carrá[71a,71b] G. Carratta[23b,23a] F. Carrio Argos[33g] J. W. S. Carter[155] T. M. Carter[52] M. P. Casado[13,l] M. Caspar[48] E. G. Castiglia[172] F. L. Castillo[4] L. Castillo Garcia[13] V. Castillo Gimenez[163] N. F. Castro[130a,130e] A. Catinaccio[36] J. R. Catmore[125] V. Cavaliere[29] N. Cavalli[23b,23a] V. Cavasinni[74a,74b] Y. C. Cekmecelioglu[48] E. Celebi[21a] F. Celli[126] M. S. Centonze[70a,70b] K. Cerny[122] A. S. Cerqueira[83a] A. Cerri[146] L. Cerrito[76a,76b] F. Cerutti[17a] B. Cervato[141] A. Cervelli[23b] G. Cesarini[53] S. A. Cetin[82] Z. Chadi[35a] D. Chakraborty[115] M. Chala[130f] J. Chan[170] W. Y. Chan[153] J. D. Chapman[32] E. Chapon[135] B. Chargeishvili[149b] D. G. Charlton[20] T. P. Charman[94] M. Chatterjee[19] C. Chauhan[133] S. Chekanov[6] S. V. Chekulaev[156a] G. A. Chelkov[38,m] A. Chen[106] B. Chen[151] B. Chen[165] H. Chen[14c] H. Chen[29] J. Chen[62c] J. Chen[142] M. Chen[126] S. Chen[153] S. J. Chen[14c] X. Chen[62c] X. Chen[14b,n] Y. Chen[62a] C. L. Cheng[170] H. C. Cheng[64a] S. Cheong[143] A. Cheplakov[38] E. Cheremushkina[48] E. Cherepanova[114] R. Cherkaoui El Moursli[35e] E. Cheu[7] K. Cheung[65] L. Chevalier[135] V. Chiarella[53] G. Chiarelli[74a] N. Chiedde[102] G. Chiodini[70a] A. S. Chisholm[20] A. Chitan[27b] M. Chitishvili[163] M. V. Chizhov[38] K. Choi[11] A. R. Chomont[75a,75b] Y. Chou[103] E. Y. S. Chow[114] T. Chowdhury[33g] K. L. Chu[169] M. C. Chu[64a] X. Chu[14a,14e] J. Chudoba[131] J. J. Chwastowski[87] D. Cieri[110] K. M. Ciesla[86a] V. Cindro[93] A. Ciocio[17a] F. Cirotto[72a,72b] Z. H. Citron[169,o] M. Citterio[71a] D. A. Ciubotaru[27b] B. M. Ciungu[155] A. Clark[56] P. J. Clark[52] J. M. Clavijo Columbie[48] S. E. Clawson[48] C. Clement[47a,47b] J. Clercx[48] L. Clissa[23b,23a] Y. Coadou[102] M. Cobal[69a,69c] A. Coccaro[57b] R. F. Coelho Barrue[130a] R. Coelho Lopes De Sa[103] S. Coelli[71a] H. Cohen[151] A. E. C. Coimbra[71a,71b] B. Cole[41] J. Collot[60] P. Conde Muiño[130a,130g] M. P. Connell[33c] S. H. Connell[33c] I. A. Connelly[59] E. I. Conroy[126] F. Conventi[72a,p] H. G. Cooke[20] A. M. Cooper-Sarkar[126] A. Cordeiro Oudot Choi[127] F. Cormier[164] L. D. Corpe[40] M. Corradi[75a,75b] F. Corriveau[104,q] A. Cortes-Gonzalez[18] M. J. Costa[163] F. Costanza[4] D. Costanzo[139] B. M. Cote[119] G. Cowan[95] K. Cranmer[170] D. Cremonini[23b,23a] S. Crépé-Renaudin[60] F. Crescioli[127] M. Cristinziani[141] M. Cristoforetti[78a,78b] V. Croft[114] J. E. Crosby[121] G. Crosetti[43b,43a] A. Cueto[99] T. Cuhadar Donszelmann[160] H. Cui[14a,14e] Z. Cui[7] W. R. Cunningham[59] F. Curcio[43b,43a] P. Czodrowski[36] M. M. Czurylo[63b] M. J. Da Cunha Sargedas De Sousa[62a] J. V. Da Fonseca Pinto[83b] C. Da Via[101] W. Dabrowski[86a] T. Dado[49] S. Dahbi[33g] T. Dai[106] C. Dallapiccola[103] M. Dam[42] G. D'amen[29] V. D'Amico[109] J. Damp[100] J. R. Dandoy[128] M. F. Daneri[30] M. Danninger[142] V. Dao[36] G. Darbo[57b] S. Darmora[6] S. J. Das[29,i] S. D'Auria[71a,71b] C. David[156b] T. Davidek[133] B. Davis-Purcell[34] I. Dawson[94] H. A. Day-hall[132] K. De[8] R. De Asmundis[72a] N. De Biase[48] S. De Castro[23b,23a] N. De Groot[113] P. de Jong[114] H. De la Torre[107] A. De Maria[14c] A. De Salvo[75a] U. De Sanctis[76a,76b] A. De Santo[146] J. B. De Vivie De Regie[60] D. V. Dedovich[38] J. Degens[114] A. M. Deiana[44] F. Del Corso[23b,23a] J. Del Peso[99] F. Del Rio[63a] F. Deliot[135] C. M. Delitzsch[49] M. Della Pietra[72a,72b] D. Della Volpe[56] A. Dell'Acqua[36] L. Dell'Asta[71a,71b] M. Delmastro[4] P. A. Delsart[60] S. Demers[172] M. Demichev[38] S. P. Denisov[37] L. D'Eramo[40] D. Derendarz[87] F. Derue[127] P. Dervan[92] K. Desch[24] C. Deutsch[24] F. A. Di Bello[57b,57a] A. Di Ciaccio[76a,76b] L. Di Ciaccio[4] A. Di Domenico[75a,75b] C. Di Donato[72a,72b] A. Di Girolamo[36] G. Di Gregorio[5] A. Di Luca[78a,78b] B. Di Micco[77a,77b] R. Di Nardo[77a,77b] C. Diaconu[102] M. Diamantopoulou[34] F. A. Dias[114] T. Dias Do Vale[142] M. A. Diaz[137a,137b] F. G. Diaz Capriles[24] M. Didenko[163] E. B. Diehl[106] L. Diehl[54] S. Díez Cornell[48] C. Diez Pardos[141] C. Dimitriadi[161,24,161] A. Dimitrievska[17a] J. Dingfelder[24] I-M. Dinu[27b] S. J. Dittmeier[63b] F. Dittus[36] F. Djama[102] T. Djobava[149b] J. I. Djuvsland[16] C. Doglioni[101,98] J. Dolejsi[133] Z. Dolezal[133] M. Donadelli[83c] B. Dong[107] J. Donini[40] A. D'Onofrio[77a,77b] M. D'Onofrio[92] J. Dopke[134] A. Doria[72a] N. Dos Santos Fernandes[130a] M. T. Dova[90] A. T. Doyle[59] M. A. Draguet[126] E. Dreyer[169] I. Drivas-koulouris[10] A. S. Drobac[158] M. Drozdova[56] D. Du[62a] T. A. du Pree[114] F. Dubinin[37] M. Dubovsky[28a] E. Duchovni[169] G. Duckeck[109] O. A. Ducu[27b] D. Duda[52] A. Dudarev[36] E. R. Duden[26] M. D'uffizi[101] L. Duflot[66] M. Dührssen[36] C. Dülsen[171] A. E. Dumitriu[27b] M. Dunford[63a] S. Dungs[49] K. Dunne[47a,47b] A. Duperrin[102] H. Duran Yildiz[3a] M. Düren[58] A. Durglishvili[149b] B. L. Dwyer[115] G. I. Dyckes[17a] M. Dyndal[86a] S. Dysch[101] B. S. Dziedzic[87] Z. O. Earnshaw[146] G. H. Eberwein[126] B. Eckerova[28a] S. Eggebrecht[55] M. G. Eggleston[51] E. Egidio Purcino De Souza[127]

L. F. Ehrke[56] G. Eigen[16] K. Einsweiler[17a] T. Ekelof[161] P. A. Ekman[98] S. El Farkh[35b] Y. El Ghazali[35b] H. El Jarrari[35e,148] A. El Moussaouy[35a] V. Ellajosyula[161] M. Ellert[161] F. Ellinghaus[171] A. A. Elliot[94] N. Ellis[36] J. Elmsheuser[29] M. Elsing[36] D. Emeliyanov[134] Y. Enari[153] I. Ene[17a] S. Epari[13] J. Erdmann[49] P. A. Erland[87] M. Errenst[171] M. Escalier[66] C. Escobar[163] E. Etzion[151] G. Evans[130a] H. Evans[68] L. S. Evans[95] M. O. Evans[146] A. Ezhilov[37] S. Ezzarqtouni[35a] F. Fabbri[59] L. Fabbri[23b,23a] G. Facini[96] V. Fadeyev[136] R. M. Fakhrutdinov[37] S. Falciano[75a] L. F. Falda Ulhoa Coelho[36] P. J. Falke[24] J. Faltova[133] C. Fan[162] Y. Fan[14a] Y. Fang[14a,14e] M. Fanti[71a,71b] M. Faraj[69a,69b] Z. Farazpay[97] A. Farbin[8] A. Farilla[77a] T. Farooque[107] S. M. Farrington[52] F. Fassi[35e] D. Fassouliotis[9] M. Faucci Giannelli[76a,76b] W. J. Fawcett[32] L. Fayard[66] P. Federic[133] P. Federicova[131] O. L. Fedin[37,m] G. Fedotov[37] M. Feickert[170] L. Feligioni[102] D. E. Fellers[123] C. Feng[62b] M. Feng[14b] Z. Feng[114] M. J. Fenton[160] A. B. Fenyuk[37] L. Ferencz[48] R. A. M. Ferguson[91] S. I. Fernandez Luengo[137f] M. J. V. Fernoux[102] J. Ferrando[48] A. Ferrari[161] P. Ferrari[114,113] R. Ferrari[73a] D. Ferrere[56] C. Ferretti[106] F. Fiedler[100] A. Filipčič[93] E. K. Filmer[1] F. Filthaut[113] M. C. N. Fiolhais[130a,130c,r] L. Fiorini[163] W. C. Fisher[107] T. Fitschen[101] P. M. Fitzhugh[135] I. Fleck[141] P. Fleischmann[106] T. Flick[171] L. Flores[128] M. Flores[33d,s] L. R. Flores Castillo[64a] L. Flores Sanz De Acedo[36] F. M. Follega[78a,78b] N. Fomin[16] J. H. Foo[155] B. C. Forland[68] A. Formica[135] A. C. Forti[101] E. Fortin[36] A. W. Fortman[61] M. G. Foti[17a] L. Fountas[9,t] D. Fournier[66] H. Fox[91] P. Francavilla[74a,74b] S. Francescato[61] S. Franchellucci[56] M. Franchini[23b,23a] S. Franchino[63a] D. Francis[36] L. Franco[113] L. Franconi[48] M. Franklin[61] G. Frattari[26] A. C. Freegard[94] W. S. Freund[83b] Y. Y. Frid[151] N. Fritzsche[50] A. Froch[54] D. Froidevaux[36] J. A. Frost[126] Y. Fu[62a] M. Fujimoto[118] E. Fullana Torregrosa[163,a] K. Y. Fung[64a] E. Furtado De Simas Filho[83b] M. Furukawa[153] J. Fuster[163] A. Gabrielli[23b,23a] A. Gabrielli[155] P. Gadow[36] G. Gagliardi[57b,57a] L. G. Gagnon[17a] E. J. Gallas[126] B. J. Gallop[134] K. K. Gan[119] S. Ganguly[153] J. Gao[62a] Y. Gao[52] F. M. Garay Walls[137a,137b] B. Garcia[29,i] C. García[163] A. Garcia Alonso[114] A. G. Garcia Caffaro[172] J. E. García Navarro[163] M. Garcia-Sciveres[17a] G. L. Gardner[128] R. W. Gardner[39] N. Garelli[158] D. Garg[80] R. B. Garg[143,u] J. M. Gargan[52] C. A. Garner[155] S. J. Gasiorowski[138] P. Gaspar[83b] G. Gaudio[73a] V. Gautam[13] P. Gauzzi[75a,75b] I. L. Gavrilenko[37] A. Gavrilyuk[37] C. Gay[164] G. Gaycken[48] E. N. Gazis[10] A. A. Geanta[27b] C. M. Gee[136] C. Gemme[57b] M. H. Genest[60] S. Gentile[75a,75b] S. George[95] W. F. George[20] T. Geralis[46] P. Gessinger-Befurt[36] M. E. Geyik[171] M. Ghneimat[141] K. Ghorbanian[94] A. Ghosal[141] A. Ghosh[160] A. Ghosh[7] B. Giacobbe[23b] S. Giagu[75a,75b] P. Giannetti[74a] A. Giannini[62a] S. M. Gibson[95] M. Gignac[136] D. T. Gil[86b] A. K. Gilbert[86a] B. J. Gilbert[41] D. Gillberg[34] G. Gilles[114] N. E. K. Gillwald[48] L. Ginabat[127] D. M. Gingrich[2,e] M. P. Giordani[69a,69c] P. F. Giraud[135] G. Giugliarelli[69a,69c] D. Giugni[71a] F. Giuli[36] I. Gkialas[9,t] L. K. Gladilin[37] C. Glasman[99] G. R. Gledhill[123] G. Glemža[48] M. Glisic[123] I. Gnesi[43b,v] Y. Go[29,i] M. Goblirsch-Kolb[36] B. Gocke[49] D. Godin[108] B. Gokturk[21a] S. Goldfarb[105] T. Golling[56] M. G. D. Gololo[33g] D. Golubkov[37] J. P. Gombas[107] A. Gomes[130a,130b] G. Gomes Da Silva[141] A. J. Gomez Delegido[163] R. Gonçalo[130a,130c] G. Gonella[123] L. Gonella[20] A. Gongadze[149c] F. Gonnella[20] J. L. Gonski[41] R. Y. González Andana[52] S. González de la Hoz[163] S. Gonzalez Fernandez[13] R. Gonzalez Lopez[92] C. Gonzalez Renteria[17a] R. Gonzalez Suarez[161] S. Gonzalez-Sevilla[56] G. R. Gonzalvo Rodriguez[163] L. Goossens[36] P. A. Gorbounov[37] B. Gorini[36] E. Gorini[70a,70b] A. Gorišek[93] T. C. Gosart[128] A. T. Goshaw[51] M. I. Gostkin[38] S. Goswami[121] C. A. Gottardo[36] M. Gouighri[35b] V. Goumarre[48] A. G. Goussiou[138] N. Govender[33c] I. Grabowska-Bold[86a] K. Graham[34] E. Gramstad[125] S. Grancagnolo[70a,70b] M. Grandi[146] P. M. Gravila[27f] F. G. Gravili[70a,70b] H. M. Gray[17a] M. Greco[70a,70b] C. Grefe[24] I. M. Gregor[48] P. Grenier[143] C. Grieco[13] A. A. Grillo[136] K. Grimm[31] S. Grinstein[13,w] J.-F. Grivaz[66] E. Gross[169] J. Grosse-Knetter[55] C. Grud[106] J. C. Grundy[126] L. Guan[106] W. Guan[29] C. Gubbels[164] J. G. R. Guerrero Rojas[163] G. Guerrieri[69a,69c] F. Guescini[110] R. Gugel[100] J. A. M. Guhit[106] A. Guida[18] T. Guillemin[4] E. Guilloton[167,134] S. Guindon[36] F. Guo[14a,14e] J. Guo[62c] L. Guo[48] Y. Guo[106] R. Gupta[48] S. Gurbuz[24] S. S. Gurdasani[54] G. Gustavino[36] M. Guth[56] P. Gutierrez[120] L. F. Gutierrez Zagazeta[128] C. Gutschow[96] C. Gwenlan[126] C. B. Gwilliam[92] E. S. Haaland[125] A. Haas[117] M. Habedank[48] C. Haber[17a] H. K. Hadavand[8] A. Hadef[100] S. Hadzic[110] J. J. Hahn[141] E. H. Haines[96] M. Haleem[166] J. Haley[121] J. J. Hall[139] G. D. Hallewell[102] L. Halser[19] K. Hamano[165] H. Hamdaoui[35e] M. Hamer[24] G. N. Hamity[52] E. J. Hampshire[95] J. Han[62b] K. Han[62a] L. Han[14c] L. Han[62a] S. Han[17a]

Y. F. Han [155] K. Hanagaki [84] M. Hance [136] D. A. Hangal [41,d] H. Hanif [142] M. D. Hank [128] R. Hankache [101]
J. B. Hansen [42] J. D. Hansen [42] P. H. Hansen [42] K. Hara [157] D. Harada [56] T. Harenberg [171] S. Harkusha [37]
M. L. Harris [103] Y. T. Harris [126] J. Harrison [13] N. M. Harrison [119] P. F. Harrison [167] N. M. Hartman [110]
N. M. Hartmann [109] Y. Hasegawa [140] A. Hasib [52] S. Haug [19] R. Hauser [107] C. M. Hawkes [20] R. J. Hawkings [36]
Y. Hayashi [153] S. Hayashida [111] D. Hayden [107] C. Hayes [106] R. L. Hayes [114] C. P. Hays [126] J. M. Hays [94]
H. S. Hayward [92] F. He [62a] M. He [14a,14e] Y. He [154] Y. He [127] N. B. Heatley [94] V. Hedberg [98] A. L. Heggelund [125]
N. D. Hehir [94] C. Heidegger [54] K. K. Heidegger [54] W. D. Heidorn [81] J. Heilman [34] S. Heim [48] T. Heim [17a]
J. G. Heinlein [128] J. J. Heinrich [123] L. Heinrich [110,x] J. Hejbal [131] L. Helary [48] A. Held [170] S. Hellesund [16]
C. M. Helling [164] S. Hellman [47a,47b] R. C. W. Henderson [91] L. Henkelmann [32] A. M. Henriques Correia [36] H. Herde [98]
Y. Hernández Jiménez [145] L. M. Herrmann [24] T. Herrmann [50] G. Herten [54] R. Hertenberger [109] L. Hervas [36]
M. E. Hesping [100] N. P. Hessey [156a] H. Hibi [85] S. J. Hillier [20] J. R. Hinds [107] F. Hinterkeuser [24] M. Hirose [124]
S. Hirose [157] D. Hirschbuehl [171] T. G. Hitchings [101] B. Hiti [93] J. Hobbs [145] R. Hobincu [27e] N. Hod [169]
M. C. Hodgkinson [139] B. H. Hodkinson [32] A. Hoecker [36] J. Hofer [48] T. Holm [24] M. Holzbock [110]
L. B. A. H. Hommels [32] B. P. Honan [101] J. Hong [62c] T. M. Hong [129] B. H. Hooberman [162] W. H. Hopkins [6]
Y. Horii [111] S. Hou [148] A. S. Howard [93] J. Howarth [59] J. Hoya [6] M. Hrabovsky [122] A. Hrynevich [48]
T. Hryn'ova [4] P. J. Hsu [65] S.-C. Hsu [138] Q. Hu [41] Y. F. Hu [14a,14e] S. Huang [64b] X. Huang [14c] Y. Huang [139,y]
Y. Huang [14a] Z. Huang [101] Z. Hubacek [132] M. Huebner [24] F. Huegging [24] T. B. Huffman [126] C. A. Hugli [48]
M. Huhtinen [36] S. K. Huiberts [16] R. Hulsken [104] N. Huseynov [12,m] J. Huston [107] J. Huth [61] R. Hyneman [143]
G. Iacobucci [56] G. Iakovidis [29] I. Ibragimov [141] L. Iconomidou-Fayard [66] P. Iengo [72a,72b] R. Iguchi [153]
T. Iizawa [84] Y. Ikegami [84] N. Ilic [155] H. Imam [35a] M. Ince Lezki [56] T. Ingebretsen Carlson [47a,47b]
G. Introzzi [73a,73b] M. Iodice [77a] V. Ippolito [75a,75b] R. K. Irwin [92] M. Ishino [153] W. Islam [170] C. Issever [18,48]
S. Istin [21a,z] H. Ito [168] J. M. Iturbe Ponce [64a] R. Iuppa [78a,78b] A. Ivina [169] J. M. Izen [45] V. Izzo [72a] P. Jacka [131,132]
P. Jackson [1] R. M. Jacobs [48] B. P. Jaeger [142] C. S. Jagfeld [109] P. Jain [54] G. Jäkel [171] K. Jakobs [54]
T. Jakoubek [169] J. Jamieson [59] K. W. Janas [86a] A. E. Jaspan [92] M. Javurkova [103] F. Jeanneau [135] L. Jeanty [123]
J. Jejelava [149a,aa] P. Jenni [54,bb] C. E. Jessiman [34] S. Jézéquel [4] C. Jia [62b] J. Jia [145] X. Jia [61] X. Jia [14a,14e] Z. Jia [14c]
Y. Jiang [62a] S. Jiggins [48] J. Jimenez Pena [13] S. Jin [14c] A. Jinaru [27b] O. Jinnouchi [154] P. Johansson [139]
K. A. Johns [7] J. W. Johnson [136] D. M. Jones [32] E. Jones [48] P. Jones [32] R. W. L. Jones [91] T. J. Jones [92]
R. Joshi [119] J. Jovicevic [15] X. Ju [17a] J. J. Junggeburth [36] T. Junkermann [63a] A. Juste Rozas [13,w] M. K. Juzek [87]
S. Kabana [137e] A. Kaczmarska [87] M. Kado [110] H. Kagan [119] M. Kagan [143] A. Kahn [41] A. Kahn [128] C. Kahra [100]
T. Kaji [168] E. Kajomovitz [150] N. Kakati [169] I. Kalaitzidou [54] C. W. Kalderon [29] A. Kamenshchikov [155]
S. Kanayama [154] N. J. Kang [136] D. Kar [33g] K. Karava [126] M. J. Kareem [156b] E. Karentzos [54] I. Karkanias [152]
O. Karkout [114] S. N. Karpov [38] Z. M. Karpova [38] V. Kartvelishvili [91] A. N. Karyukhin [37] E. Kasimi [152]
J. Katzy [48] S. Kaur [34] K. Kawade [140] M. P. Kawale [120] T. Kawamoto [135] E. F. Kay [36] F. I. Kaya [158]
S. Kazakos [107] V. F. Kazanin [37] Y. Ke [145] J. M. Keaveney [33a] R. Keeler [165] G. V. Kehris [61] J. S. Keller [34]
A. S. Kelly [96] J. J. Kempster [146] K. E. Kennedy [41] P. D. Kennedy [100] O. Kepka [131] B. P. Kerridge [167] S. Kersten [171]
B. P. Kerševan [93] S. Keshri [66] L. Keszeghova [28a] S. Ketabchi Haghighat [155] M. Khandoga [127] A. Khanov [121]
A. G. Kharlamov [37] T. Kharlamova [37] E. E. Khoda [138] T. J. Khoo [18] G. Khoriauli [166] J. Khubua [149b]
Y. A. R. Khwaira [66] A. Kilgallon [123] D. W. Kim [47a,47b] Y. K. Kim [39] N. Kimura [96] A. Kirchhoff [55] C. Kirfel [24]
F. Kirfel [24] J. Kirk [134] A. E. Kiryunin [110] C. Kitsaki [10] O. Kivernyk [24] M. Klassen [63a] C. Klein [34] L. Klein [166]
M. H. Klein [106] M. Klein [92] S. B. Klein [56] U. Klein [92] P. Klimek [36] A. Klimentov [29] T. Klioutchnikova [36]
P. Kluit [114] S. Kluth [110] E. Kneringer [79] T. M. Knight [155] A. Knue [54] R. Kobayashi [88] S. F. Koch [126]
M. Kocian [143] P. Kodyš [133] D. M. Koeck [123] P. T. Koenig [24] T. Koffas [34] M. Kolb [135] I. Koletsou [4]
T. Komarek [122] K. Köneke [54] A. X. Y. Kong [1] T. Kono [118] N. Konstantinidis [96] B. Konya [98] R. Kopeliansky [68]
S. Koperny [86a] K. Korcyl [87] K. Kordas [152,cc] G. Koren [151] A. Korn [96] S. Korn [55] I. Korolkov [13] N. Korotkova [37]
B. Kortman [114] O. Kortner [110] S. Kortner [110] W. H. Kostecka [115] V. V. Kostyukhin [141] A. Kotsokechagia [135]
A. Kotwal [51] A. Koulouris [36] A. Kourkoumeli-Charalampidi [73a,73b] C. Kourkoumelis [9] E. Kourlitis [110,x]
O. Kovanda [146] R. Kowalewski [165] W. Kozanecki [135] A. S. Kozhin [37] V. A. Kramarenko [37] G. Kramberger [93]
P. Kramer [100] M. W. Krasny [127] A. Krasznahorkay [36] J. W. Kraus [171] J. A. Kremer [100] T. Kresse [50]
J. Kretzschmar [92] K. Kreul [18] P. Krieger [155] S. Krishnamurthy [103] M. Krivos [133] K. Krizka [20] K. Kroeninger [49]

H. Kroha,[110] J. Kroll,[131] J. Kroll,[128] K. S. Krowpman,[107] U. Kruchonak,[38] H. Krüger,[24] N. Krumnack,[81] M. C. Kruse,[51] J. A. Krzysiak,[87] O. Kuchinskaia,[37] S. Kuday,[3a] S. Kuehn,[36] R. Kuesters,[54] T. Kuhl,[48] V. Kukhtin,[38] Y. Kulchitsky,[37,m] S. Kuleshov,[137d,137b] M. Kumar,[33g] N. Kumari,[102] A. Kupco,[131] T. Kupfer,[49] A. Kupich,[37] O. Kuprash,[54] H. Kurashige,[85] L. L. Kurchaninov,[156a] O. Kurdysh,[66] Y. A. Kurochkin,[37] A. Kurova,[37] M. Kuze,[154] A. K. Kvam,[103] J. Kvita,[122] T. Kwan,[104] N. G. Kyriacou,[106] L. A. O. Laatu,[102] C. Lacasta,[163] F. Lacava,[75a,75b] H. Lacker,[18] D. Lacour,[127] N. N. Lad,[96] E. Ladygin,[38] B. Laforge,[127] T. Lagouri,[137e] S. Lai,[55] I. K. Lakomiec,[86a] N. Lalloue,[60] J. E. Lambert,[165,j] S. Lammers,[68] W. Lampl,[7] C. Lampoudis,[152,cc] A. N. Lancaster,[115] E. Lançon,[29] U. Landgraf,[54] M. P. J. Landon,[94] V. S. Lang,[54] R. J. Langenberg,[103] O. K. B. Langrekken,[125] A. J. Lankford,[160] F. Lanni,[36] K. Lantzsch,[24] A. Lanza,[73a] A. Lapertosa,[57b,57a] J. F. Laporte,[135] T. Lari,[71a] F. Lasagni Manghi,[23b] M. Lassnig,[36] V. Latonova,[131] A. Laudrain,[100] A. Laurier,[150] S. D. Lawlor,[95] Z. Lawrence,[101] M. Lazzaroni,[71a,71b] B. Le,[101] E. M. Le Boulicaut,[51] B. Leban,[93] A. Lebedev,[81] M. LeBlanc,[36] F. Ledroit-Guillon,[60] A. C. A. Lee,[96] S. C. Lee,[148] S. Lee,[47a,47b] T. F. Lee,[92] L. L. Leeuw,[33c] H. P. Lefebvre,[95] M. Lefebvre,[165] C. Leggett,[17a] G. Lehmann Miotto,[36] M. Leigh,[56] W. A. Leight,[103] W. Leinonen,[113] A. Leisos,[152,dd] M. A. L. Leite,[83c] C. E. Leitgeb,[48] R. Leitner,[133] K. J. C. Leney,[44] T. Lenz,[24] S. Leone,[74a] C. Leonidopoulos,[52] A. Leopold,[144] C. Leroy,[108] R. Les,[107] C. G. Lester,[32] M. Levchenko,[37] J. Levêque,[4] D. Levin,[106] L. J. Levinson,[169] M. P. Lewicki,[87] D. J. Lewis,[4] A. Li,[5] B. Li,[62b] C. Li,[62a] C-Q. Li,[62c] H. Li,[62a] H. Li,[62b] H. Li,[14c] H. Li,[62b] K. Li,[138] L. Li,[62c] M. Li,[14a,14e] Q. Y. Li,[62a] S. Li,[14a,14e] S. Li,[62d,62c,ee] T. Li,[5,ff] X. Li,[104] Z. Li,[126] Z. Li,[104] Z. Li,[92] Z. Li,[14a,14e] Z. Liang,[14a] M. Liberatore,[135,gg] B. Liberti,[76a] K. Lie,[64c] J. Lieber Marin,[83b] H. Lien,[68] K. Lin,[107] R. E. Lindley,[7] J. H. Lindon,[2] A. Linss,[48] E. Lipeles,[128] A. Lipniacka,[16] A. Lister,[164] J. D. Little,[4] B. Liu,[14a] B. X. Liu,[142] D. Liu,[62d,62c] J. B. Liu,[62a] J. K. K. Liu,[32] K. Liu,[62d,62c] M. Liu,[62a] M. Y. Liu,[62a] P. Liu,[14a] Q. Liu,[62d,138,62c] X. Liu,[62a] Y. Liu,[14d,14e] Y. L. Liu,[106] Y. W. Liu,[62a] J. Llorente Merino,[142] S. L. Lloyd,[94] E. M. Lobodzinska,[48] P. Loch,[7] S. Loffredo,[76a,76b] T. Lohse,[18] K. Lohwasser,[139] E. Loiacono,[48] M. Lokajicek,[131,a] J. D. Lomas,[20] J. D. Long,[162] I. Longarini,[160] L. Longo,[70a,70b] R. Longo,[162] I. Lopez Paz,[67] A. Lopez Solis,[48] J. Lorenz,[109] N. Lorenzo Martinez,[4] A. M. Lory,[109] G. Löschcke Centeno,[146] O. Loseva,[37] X. Lou,[47a,47b] X. Lou,[14a,14e] A. Lounis,[66] J. Love,[6] P. A. Love,[91] G. Lu,[14a,14e] M. Lu,[80] S. Lu,[128] Y. J. Lu,[65] H. J. Lubatti,[138] C. Luci,[75a,75b] F. L. Lucio Alves,[14c] A. Lucotte,[60] F. Luehring,[68] I. Luise,[145] O. Lukianchuk,[66] O. Lundberg,[144] B. Lund-Jensen,[144] N. A. Luongo,[123] M. S. Lutz,[151] D. Lynn,[29] H. Lyons,[92] R. Lysak,[131] E. Lytken,[98] V. Lyubushkin,[38] T. Lyubushkina,[38] M. M. Lyukova,[145] H. Ma,[29] K. Ma,[62a] L. L. Ma,[62b] Y. Ma,[121] D. M. Mac Donell,[165] G. Maccarrone,[53] J. C. MacDonald,[100] R. Madar,[40] W. F. Mader,[50] J. Maeda,[85] T. Maeno,[29] M. Maerker,[50] H. Maguire,[139] V. Maiboroda,[135] A. Maio,[130a,130b,130d] K. Maj,[86a] O. Majersky,[48] S. Majewski,[123] N. Makovec,[66] V. Maksimovic,[15] B. Malaescu,[127] Pa. Malecki,[87] V. P. Maleev,[37] F. Malek,[60] M. Mali,[93] D. Malito,[95,hh] U. Mallik,[80] S. Maltezos,[10] S. Malyukov,[38] J. Mamuzic,[13] G. Mancini,[53] G. Manco,[73a,73b] J. P. Mandalia,[94] I. Mandić,[93] L. Manhaes de Andrade Filho,[83a] I. M. Maniatis,[169] J. Manjarres Ramos,[102,ii] D. C. Mankad,[169] A. Mann,[109] B. Mansoulie,[135] S. Manzoni,[36] A. Marantis,[152,dd] G. Marchiori,[5] M. Marcisovsky,[131] C. Marcon,[71a,71b] M. Marinescu,[20] M. Marjanovic,[120] E. J. Marshall,[91] Z. Marshall,[17a] S. Marti-Garcia,[163] T. A. Martin,[167] V. J. Martin,[52] B. Martin dit Latour,[16] L. Martinelli,[75a,75b] M. Martinez,[13,w] P. Martinez Agullo,[163] V. I. Martinez Outschoorn,[103] P. Martinez Suarez,[13] S. Martin-Haugh,[134] V. S. Martoiu,[27b] A. C. Martyniuk,[96] A. Marzin,[36] D. Mascione,[78a,78b] L. Masetti,[100] T. Mashimo,[153] J. Masik,[101] A. L. Maslennikov,[37] L. Massa,[23b] P. Massarotti,[72a,72b] P. Mastrandrea,[74a,74b] A. Mastroberardino,[43b,43a] T. Masubuchi,[153] T. Mathisen,[161] J. Matousek,[133] N. Matsuzawa,[153] J. Maurer,[27b] B. Maček,[93] D. A. Maximov,[37] R. Mazini,[148] I. Maznas,[152] M. Mazza,[107] S. M. Mazza,[136] E. Mazzeo,[71a,71b] C. Mc Ginn,[29] J. P. Mc Gowan,[104] S. P. Mc Kee,[106] E. F. McDonald,[105] A. E. McDougall,[114] J. A. Mcfayden,[146] R. P. McGovern,[128] G. Mchedlidze,[149b] R. P. Mckenzie,[33g] T. C. Mclachlan,[48] D. J. Mclaughlin,[96] K. D. McLean,[165] S. J. McMahon,[134] P. C. McNamara,[105] C. M. Mcpartland,[92] R. A. McPherson,[165,q] S. Mehlhase,[109] A. Mehta,[92] D. Melini,[150] B. R. Mellado Garcia,[33g] A. H. Melo,[55] F. Meloni,[48] A. M. Mendes Jacques Da Costa,[101] H. Y. Meng,[155] L. Meng,[91] S. Menke,[110] M. Mentink,[36] E. Meoni,[43b,43a] C. Merlassino,[126] L. Merola,[72a,72b] C. Meroni,[71a,71b] G. Merz,[106] O. Meshkov,[37] J. Metcalfe,[6] A. S. Mete,[6] C. Meyer,[68] J-P. Meyer,[135] R. P. Middleton,[134] L. Mijović,[52] G. Mikenberg,[169] M. Mikestikova,[131] M. Mikuž,[93] H. Mildner,[100] A. Milic,[36]

C. D. Milke[44] D. W. Miller[39] L. S. Miller[34] A. Milov[169] D. A. Milstead,[47a,47b] T. Min,[14c] A. A. Minaenko[37]
I. A. Minashvili,[149b] L. Mince[59] A. I. Mincer,[117] B. Mindur,[86a] M. Mineev,[38] Y. Mino[88] L. M. Mir,[13]
M. Miralles Lopez[163] M. Mironova,[17a] A. Mishima,[153] M. C. Missio,[113] T. Mitani,[168] A. Mitra,[167]
V. A. Mitsou,[163] O. Miu[155] P. S. Miyagawa,[94] Y. Miyazaki,[89] A. Mizukami,[84] T. Mkrtchyan,[63a] M. Mlinarevic,[96]
T. Mlinarevic,[96] M. Mlynarikova,[36] S. Mobius,[19] K. Mochizuki,[108] P. Moder,[48] P. Mogg,[109]
A. F. Mohammed,[14a,14e] S. Mohapatra,[41] G. Mokgatitswane,[33g] L. Moleri,[169] B. Mondal,[141] S. Mondal,[132]
K. Mönig,[48] E. Monnier,[102] L. Monsonis Romero,[163] J. Montejo Berlingen,[13,84] M. Montella,[119]
F. Montereali,[77a,77b] F. Monticelli,[90] S. Monzani,[69a,69c] N. Morange,[66] A. L. Moreira De Carvalho,[130a]
M. Moreno Llácer,[163] C. Moreno Martinez,[56] P. Morettini,[57b] S. Morgenstern,[36] M. Morii,[61] M. Morinaga,[153]
A. K. Morley,[36] F. Morodei,[75a,75b] L. Morvaj,[36] P. Moschovakos,[36] B. Moser,[36] M. Mosidze,[149b] T. Moskalets,[54]
P. Moskvitina,[113] J. Moss,[31,jj] E. J. W. Moyse,[103] O. Mtintsilana,[33g] S. Muanza,[102] J. Mueller,[129]
D. Muenstermann,[91] R. Müller,[19] G. A. Mullier,[161] A. J. Mullin,[32] J. J. Mullin,[128] D. P. Mungo,[155]
D. Munoz Perez,[163] F. J. Munoz Sanchez,[101] M. Murin,[101] W. J. Murray,[167,134] A. Murrone,[71a,71b] J. M. Muse,[120]
M. Muškinja,[17a] C. Mwewa,[29] A. G. Myagkov,[37,m] A. J. Myers,[8] A. A. Myers,[129] G. Myers,[68] M. Myska,[132]
B. P. Nachman,[17a] O. Nackenhorst,[49] A. Nag,[50] K. Nagai,[126] K. Nagano,[84] J. L. Nagle,[29,i] E. Nagy,[102]
A. M. Nairz,[36] Y. Nakahama,[84] K. Nakamura,[84] K. Nakkalil,[5] H. Nanjo,[124] R. Narayan,[44] E. A. Narayanan,[112]
I. Naryshkin,[37] M. Naseri,[34] S. Nasri,[159] C. Nass,[24] G. Navarro,[22a] J. Navarro-Gonzalez,[163] R. Nayak,[151]
A. Nayaz,[18] P. Y. Nechaeva,[37] F. Nechansky,[48] L. Nedic,[126] T. J. Neep,[20] A. Negri,[73a,73b] M. Negrini,[23b]
C. Nellist,[114] C. Nelson,[104] K. Nelson,[106] S. Nemecek,[131] M. Nessi,[36,kk] M. S. Neubauer,[162] F. Neuhaus,[100]
J. Neundorf,[48] R. Newhouse,[164] P. R. Newman,[20] C. W. Ng,[129] Y. W. Y. Ng,[48] B. Ngair,[35e] H. D. N. Nguyen,[108]
R. B. Nickerson,[126] R. Nicolaidou,[135] J. Nielsen,[136] M. Niemeyer,[55] J. Niermann,[55,36] N. Nikiforou,[36]
V. Nikolaenko,[37,m] I. Nikolic-Audit,[127] K. Nikolopoulos,[20] P. Nilsson,[29] I. Ninca,[48] H. R. Nindhito,[56]
G. Ninio,[151] A. Nisati,[75a] N. Nishu,[2] R. Nisius,[110] J-E. Nitschke,[50] E. K. Nkadimeng,[33g] S. J. Noacco Rosende,[90]
T. Nobe,[153] D. L. Noel,[32] T. Nommensen,[147] M. B. Norfolk,[139] R. R. B. Norisam,[96] B. J. Norman,[34] J. Novak,[93]
T. Novak,[48] L. Novotny,[132] R. Novotny,[112] L. Nozka,[122] K. Ntekas,[160] N. M. J. Nunes De Moura Junior,[83b]
E. Nurse,[96] J. Ocariz,[127] A. Ochi,[85] I. Ochoa,[130a] S. Oerdek,[161] J. T. Offermann,[39] A. Ogrodnik,[133] A. Oh,[101]
C. C. Ohm,[144] H. Oide,[84] R. Oishi,[153] M. L. Ojeda,[48] Y. Okazaki,[88] M. W. O'Keefe,[92] Y. Okumura,[153]
L. F. Oleiro Seabra,[130a] S. A. Olivares Pino,[137d] D. Oliveira Damazio,[29] D. Oliveira Goncalves,[83a] J. L. Oliver,[160]
A. Olszewski,[87] Ö. O. Öncel,[54] D. C. O'Neil,[142] A. P. O'Neill,[19] A. Onofre,[130a,130e] P. U. E. Onyisi,[11]
M. J. Oreglia,[39] G. E. Orellana,[90] D. Orestano,[77a,77b] N. Orlando,[13] R. S. Orr,[155] V. O'Shea,[59] L. M. Osojnak,[128]
R. Ospanov,[62a] G. Otero y Garzon,[30] H. Otono,[89] P. S. Ott,[63a] G. J. Ottino,[17a] M. Ouchrif,[35d] J. Ouellette,[29]
F. Ould-Saada,[125] M. Owen,[59] R. E. Owen,[134] K. Y. Oyulmaz,[21a] V. E. Ozcan,[21a] N. Ozturk,[8] S. Ozturk,[82]
H. A. Pacey,[32] A. Pacheco Pages,[13] C. Padilla Aranda,[13] G. Padovano,[75a,75b] S. Pagan Griso,[17a] G. Palacino,[68]
A. Palazzo,[70a,70b] S. Palestini,[36] J. Pan,[172] T. Pan,[64a] D. K. Panchal,[11] C. E. Pandini,[114] J. G. Panduro Vazquez,[95]
H. Pang,[14b] P. Pani,[48] G. Panizzo,[69a,69c] L. Paolozzi,[56] C. Papadatos,[108] S. Parajuli,[44] A. Paramonov,[6]
C. Paraskevopoulos,[10] D. Paredes Hernandez,[64b] T. H. Park,[155] M. A. Parker,[32] F. Parodi,[57b,57a] E. W. Parrish,[115]
V. A. Parrish,[52] J. A. Parsons,[41] U. Parzefall,[54] B. Pascual Dias,[108] L. Pascual Dominguez,[151] F. Pasquali,[114]
E. Pasqualucci,[75a] S. Passaggio,[57b] F. Pastore,[95] P. Pasuwan,[47a,47b] P. Patel,[87] U. M. Patel,[51] J. R. Pater,[101]
T. Pauly,[36] J. Pearkes,[143] M. Pedersen,[125] R. Pedro,[130a] S. V. Peleganchuk,[37] O. Penc,[36] E. A. Pender,[52]
H. Peng,[62a] K. E. Penski,[109] M. Penzin,[37] B. S. Peralva,[83d] A. P. Pereira Peixoto,[60] L. Pereira Sanchez,[47a,47b]
D. V. Perepelitsa,[29,i] E. Perez Codina,[156a] M. Perganti,[10] L. Perini,[71a,71b,a] H. Pernegger,[36] O. Perrin,[40]
K. Peters,[48] R. F. Y. Peters,[101] B. A. Petersen,[36] T. C. Petersen,[42] E. Petit,[102] V. Petousis,[132] C. Petridou,[152,cc]
A. Petrukhin,[141] M. Pettee,[17a] N. E. Pettersson,[36] A. Petukhov,[37] K. Petukhova,[133] A. Peyaud,[135] R. Pezoa,[137f]
L. Pezzotti,[36] G. Pezzullo,[172] T. M. Pham,[170] T. Pham,[105] P. W. Phillips,[134] G. Piacquadio,[145] E. Pianori,[17a]
F. Piazza,[71a,71b] R. Piegaia,[30] D. Pietreanu,[27b] A. D. Pilkington,[101] M. Pinamonti,[69a,69c] J. L. Pinfold,[2]
B. C. Pinheiro Pereira,[130a] A. E. Pinto Pinoargote,[135] K. M. Piper,[146] A. Pirttikoski,[56] C. Pitman Donaldson,[96]
D. A. Pizzi,[34] L. Pizzimento,[64b] A. Pizzini,[114] M.-A. Pleier,[29] V. Plesanovs,[54] V. Pleskot,[133] E. Plotnikova,[38]
G. Poddar,[4] R. Poettgen,[98] L. Poggioli,[127] I. Pokharel,[55] S. Polacek,[133] G. Polesello,[73a] A. Poley,[142,156a]
R. Polifka,[132] A. Polini,[23b] C. S. Pollard,[167] Z. B. Pollock,[119] V. Polychronakos,[29] E. Pompa Pacchi,[75a,75b]

D. Ponomarenko[113] L. Pontecorvo[36] S. Popa[27a] G. A. Popeneciu[27d] A. Poreba[36] D. M. Portillo Quintero[156a]
S. Pospisil[132] M. A. Postill[139] P. Postolache[27c] K. Potamianos[167] P. A. Potepa[86a] I. N. Potrap[38] C. J. Potter[32]
H. Potti[1] T. Poulsen[48] J. Poveda[163] M. E. Pozo Astigarraga[36] A. Prades Ibanez[163] J. Pretel[54] D. Price[101]
M. Primavera[70a] M. A. Principe Martin[99] R. Privara[122] T. Procter[59] M. L. Proffitt[138] N. Proklova[128]
K. Prokofiev[64c] G. Proto[110] S. Protopopescu[29] J. Proudfoot[6] M. Przybycien[86a] W. W. Przygoda[86b]
J. E. Puddefoot[139] D. Pudzha[37] D. Pyatiizbyantseva[37] J. Qian[106] D. Qichen[101] Y. Qin[101] T. Qiu[52]
A. Quadt[55] M. Queitsch-Maitland[101] G. Quetant[56] G. Rabanal Bolanos[61] D. Rafanoharana[54] F. Ragusa[71a,71b]
J. L. Rainbolt[39] J. A. Raine[56] S. Rajagopalan[29] E. Ramakoti[37] K. Ran[48,14e] N. P. Rapheeha[33g] H. Rasheed[27b]
V. Raskina[127] D. F. Rassloff[63a] S. Rave[100] B. Ravina[55] I. Ravinovich[169] M. Raymond[36] A. L. Read[125]
N. P. Readioff[139] D. M. Rebuzzi[73a,73b] G. Redlinger[29] A. S. Reed[110] K. Reeves[26] J. A. Reidelsturz[171,ll]
D. Reikher[151] A. Rej[141] C. Rembser[36] A. Renardi[48] M. Renda[27b] M. B. Rendel[110] F. Renner[48]
A. G. Rennie[59] S. Resconi[71a] M. Ressegotti[57b,57a] S. Rettie[36] J. G. Reyes Rivera[107] B. Reynolds[119]
E. Reynolds[17a] O. L. Rezanova[37] P. Reznicek[133] N. Ribaric[91] E. Ricci[78a,78b] R. Richter[110] S. Richter[47a,47b]
E. Richter-Was[86b] M. Ridel[127] S. Ridouani[35d] P. Rieck[117] P. Riedler[36] M. Rijssenbeek[145] A. Rimoldi[73a,73b]
M. Rimoldi[48] L. Rinaldi[23b,23a] T. T. Rinn[29] M. P. Rinnagel[109] G. Ripellino[161] I. Riu[13] P. Rivadeneira[48]
J. C. Rivera Vergara[165] F. Rizatdinova[121] E. Rizvi[94] B. A. Roberts[167] B. R. Roberts[17a] S. H. Robertson[104,q]
M. Robin[48] D. Robinson[32] C. M. Robles Gajardo[137f] M. Robles Manzano[100] A. Robson[59] A. Rocchi[76a,76b]
C. Roda[74a,74b] S. Rodriguez Bosca[63a] Y. Rodriguez Garcia[22a] A. Rodriguez Rodriguez[54]
A. M. Rodríguez Vera[156b] S. Roe[36] J. T. Roemer[160] A. R. Roepe-Gier[136] J. Roggel[171] O. Røhne[125]
R. A. Rojas[103] C. P. A. Roland[68] J. Roloff[29] A. Romaniouk[37] E. Romano[73a,73b] M. Romano[23b]
A. C. Romero Hernandez[162] N. Rompotis[92] L. Roos[127] S. Rosati[75a] B. J. Rosser[39] E. Rossi[126] E. Rossi[72a,72b]
L. P. Rossi[57b] L. Rossini[48] R. Rosten[119] M. Rotaru[27b] B. Rottler[54] C. Rougier[102,ii] D. Rousseau[66]
D. Rousso[32] A. Roy[162] S. Roy-Garand[155] A. Rozanov[102] Y. Rozen[150] X. Ruan[33g] A. Rubio Jimenez[163]
A. J. Ruby[92] V. H. Ruelas Rivera[18] T. A. Ruggeri[1] A. Ruggiero[126] A. Ruiz-Martinez[163] A. Rummler[36]
Z. Rurikova[54] N. A. Rusakovich[38] H. L. Russell[165] G. Russo[75a,75b] J. P. Rutherfoord[7]
S. Rutherford Colmenares[32] K. Rybacki[91] M. Rybar[133] E. B. Rye[125] A. Ryzhov[44] J. A. Sabater Iglesias[56]
P. Sabatini[163] L. Sabetta[75a,75b] H.-W. Sadrozinski[136] F. Safai Tehrani[75a] B. Safarzadeh Samani[146]
M. Safdari[143] S. Saha[165] M. Sahinsoy[110] M. Saimpert[135] M. Saito[153] T. Saito[153] D. Salamani[36]
A. Salnikov[143] J. Salt[163] A. Salvador Salas[13] D. Salvatore[43b,43a] F. Salvatore[146] A. Salzburger[36]
D. Sammel[54] D. Sampsonidis[152,cc] D. Sampsonidou[123] J. Sánchez[163] A. Sanchez Pineda[4]
V. Sanchez Sebastian[163] H. Sandaker[125] C. O. Sander[48] J. A. Sandesara[103] M. Sandhoff[171] C. Sandoval[22b]
D. P. C. Sankey[134] T. Sano[88] A. Sansoni[53] L. Santi[75a,75b] C. Santoni[40] H. Santos[130a,130b] S. N. Santpur[17a]
A. Santra[169] K. A. Saoucha[139] J. G. Saraiva[130a,130d] J. Sardain[7] O. Sasaki[84] K. Sato[157] C. Sauer[63b]
F. Sauerburger[54] E. Sauvan[4] P. Savard[155,e] R. Sawada[153] C. Sawyer[134] L. Sawyer[97] I. Sayago Galvan[163]
C. Sbarra[23b] A. Sbrizzi[23b,23a] T. Scanlon[96] J. Schaarschmidt[138] P. Schacht[110] D. Schaefer[39] U. Schäfer[100]
A. C. Schaffer[66,44] D. Schaile[109] R. D. Schamberger[145] C. Scharf[18] M. M. Schefer[19] V. A. Schegelsky[37]
D. Scheirich[133] F. Schenck[18] M. Schernau[160] C. Scheulen[55] C. Schiavi[57b,57a] E. J. Schioppa[70a,70b]
M. Schioppa[43b,43a] B. Schlag[143,u] K. E. Schleicher[54] S. Schlenker[36] J. Schmeing[171] M. A. Schmidt[171]
K. Schmieden[100] C. Schmitt[100] S. Schmitt[48] L. Schoeffel[135] A. Schoening[63b] P. G. Scholer[54] E. Schopf[126]
M. Schott[100] J. Schovancova[36] S. Schramm[56] F. Schroeder[171] T. Schroer[56] H-C. Schultz-Coulon[63a]
M. Schumacher[54] B. A. Schumm[136] Ph. Schune[135] A. J. Schuy[138] H. R. Schwartz[136] A. Schwartzman[143]
T. A. Schwarz[106] Ph. Schwemling[135] R. Schwienhorst[107] A. Sciandra[136] G. Sciolla[26] F. Scuri[74a]
C. D. Sebastiani[92] K. Sedlaczek[115] P. Seema[18] S. C. Seidel[112] A. Seiden[136] B. D. Seidlitz[41] C. Seitz[48]
J. M. Seixas[83b] G. Sekhniaidze[72a] S. J. Sekula[44] L. Selem[60] N. Semprini-Cesari[23b,23a] D. Sengupta[56]
V. Senthilkumar[163] L. Serin[66] L. Serkin[69a,69b] M. Sessa[76a,76b] H. Severini[120] F. Sforza[57b,57a] A. Sfyrla[56]
E. Shabalina[55] R. Shaheen[144] J. D. Shahinian[128] D. Shaked Renous[169] L. Y. Shan[14a] M. Shapiro[17a]
A. Sharma[36] A. S. Sharma[164] P. Sharma[80] S. Sharma[48] P. B. Shatalov[37] K. Shaw[146] S. M. Shaw[101]
A. Shcherbakova[37] Q. Shen[62c,5] P. Sherwood[96] L. Shi[96] X. Shi[14a] C. O. Shimmin[172] Y. Shimogama[168]
J. D. Shinner[95] I. P. J. Shipsey[126] S. Shirabe[56,kk] M. Shiyakova[38,mm] J. Shlomi[169] M. J. Shochet[39]

J. Shojaii[105] D. R. Shope[125] B. Shrestha[120] S. Shrestha[119,nn] E. M. Shrif[33g] M. J. Shroff[165] P. Sicho[131] A. M. Sickles[162] E. Sideras Haddad[33g] A. Sidoti[23b] F. Siegert[50] Dj. Sijacki[15] R. Sikora[86a] F. Sili[90] J. M. Silva[20] M. V. Silva Oliveira[29] S. B. Silverstein[47a] S. Simion,[66] R. Simoniello[36] E. L. Simpson[59] H. Simpson[146] L. R. Simpson[106] N. D. Simpson,[98] S. Simsek[82] S. Sindhu[55] P. Sinervo[155] S. Singh[155] S. Sinha[48] S. Sinha[101] M. Sioli[23b,23a] I. Siral[36] E. Sitnikova[48] S. Yu. Sivoklokov[37,a] J. Sjölin[47a,47b] A. Skaf[55] E. Skorda[20,oo] P. Skubic[120] M. Slawinska[87] V. Smakhtin,[169] B. H. Smart[134] J. Smiesko[36] S. Yu. Smirnov[37] Y. Smirnov[37] L. N. Smirnova[37,m] O. Smirnova[98] A. C. Smith[41] E. A. Smith[39] H. A. Smith[126] J. L. Smith[92] R. Smith,[143] M. Smizanska[91] K. Smolek[132] A. A. Snesarev[37] S. R. Snider[155] H. L. Snoek[114] S. Snyder[29] R. Sobie[165,q] A. Soffer[151] C. A. Solans Sanchez[36] E. Yu. Soldatov[37] U. Soldevila[163] A. A. Solodkov[37] S. Solomon,[26] A. Soloshenko[38] K. Solovieva[54] O. V. Solovyanov[40] V. Solovyev[37] P. Sommer[36] A. Sonay[13] W. Y. Song[156b] J. M. Sonneveld[114] A. Sopczak[132] A. L. Sopio[96] F. Sopkova[28b] V. Sothilingam,[63a] S. Sottocornola[68] R. Soualah[116b] Z. Soumaimi[35e] D. South[48] S. Spagnolo[70a,70b] M. Spalla[110] D. Sperlich[54] G. Spigo[36] M. Spina[146] S. Spinali[91] D. P. Spiteri[59] M. Spousta[133] E. J. Staats[34] A. Stabile[71a,71b] R. Stamen[63a] M. Stamenkovic[114] A. Stampekis[20] M. Standke[24] E. Stanecka[87] M. V. Stange[50] B. Stanislaus[17a] M. M. Stanitzki[48] B. Stapf[48] E. A. Starchenko[37] G. H. Stark[136] J. Stark[102,ii] D. M. Starko,[156b] P. Staroba[131] P. Starovoitov[63a] S. Stärz[104] R. Staszewski[87] G. Stavropoulos[46] J. Steentoft[161] P. Steinberg[29] B. Stelzer[142,156a] H. J. Stelzer[129] O. Stelzer-Chilton[156a] H. Stenzel[58] T. J. Stevenson[146] G. A. Stewart[36] J. R. Stewart[121] M. C. Stockton[36] G. Stoicea[27b] M. Stolarski[130a] S. Stonjek[110] A. Straessner[50] J. Strandberg[144] S. Strandberg[47a,47b] M. Strauss[120] T. Strebler[102] P. Strizenec[28b] R. Ströhmer[166] D. M. Strom[123] L. R. Strom[48] R. Stroynowski[44] A. Strubig[47a,47b] S. A. Stucci[29] B. Stugu[16] J. Stupak[120] N. A. Styles[48] D. Su[143] S. Su[62a] W. Su[62d] X. Su[62a,66] K. Sugizaki[153] V. V. Sulin[37] M. J. Sullivan[92] D. M. S. Sultan[78a,78b] L. Sultanaliyeva[37] S. Sultansoy[3b] T. Sumida[88] S. Sun[106] S. Sun[170] O. Sunneborn Gudnadottir[161] N. Sur[102] M. R. Sutton[146] H. Suzuki[157] M. Svatos[131] M. Swiatlowski[156a] T. Swirski[166] I. Sykora[28a] M. Sykora[133] T. Sykora[133] D. Ta[100] K. Tackmann,[48,pp] A. Taffard[160] R. Tafirout[156a] J. S. Tafoya Vargas[66] E. P. Takeva[52] Y. Takubo[84] M. Talby[102] A. A. Talyshev[37] K. C. Tam[64b] N. M. Tamir,[151] A. Tanaka[153] J. Tanaka[153] R. Tanaka[66] M. Tanasini[57b,57a] Z. Tao[164] S. Tapia Araya[137f] S. Tapprogge[100] A. Tarek Abouelfadl Mohamed[107] S. Tarem[150] K. Tariq[14a] G. Tarna[102,27b] G. F. Tartarelli[71a] P. Tas[133] M. Tasevsky[131] E. Tassi[43b,43a] A. C. Tate[162] G. Tateno[153] Y. Tayalati[35e,qq] G. N. Taylor[105] W. Taylor[156b] H. Teagle[92] A. S. Tee[170] R. Teixeira De Lima[143] P. Teixeira-Dias[95] J. J. Teoh[155] K. Terashi[153] J. Terron[99] S. Terzo[13] M. Testa[53] R. J. Teuscher[155,q] A. Thaler[79] O. Theiner[56] N. Themistokleous[52] T. Theveneaux-Pelzer[102] O. Thielmann,[171] D. W. Thomas,[95] J. P. Thomas,[20] E. A. Thompson[17a] P. D. Thompson[20] E. Thomson[128] Y. Tian[55] V. Tikhomirov[37,m] Yu. A. Tikhonov[37] S. Timoshenko,[37] D. Timoshyn[133] E. X. L. Ting[1] P. Tipton[172] S. H. Tlou[33g] A. Tnourji[40] K. Todome[23b,23a] S. Todorova-Nova[133] S. Todt,[50] M. Togawa[84] J. Tojo[89] S. Tokár[28a] K. Tokushuku[84] O. Toldaiev[68] R. Tombs[32] M. Tomoto[84,111] L. Tompkins,[143,u] K. W. Topolnicki[86b] E. Torrence[123] H. Torres[102,ii] E. Torró Pastor[163] M. Toscani[30] C. Tosciri[39] M. Tost[11] D. R. Tovey[139] A. Traeet,[16] I. S. Trandafir[27b] T. Trefzger[166] A. Tricoli[29] I. M. Trigger[156a] S. Trincaz-Duvoid[127] D. A. Trischuk[26] B. Trocmé,[60] C. Troncon[71a] L. Truong[33c] M. Trzebinski[87] A. Trzupek[87] F. Tsai[145] M. Tsai[106] A. Tsiamis[152,cc] P. V. Tsiareshka,[37] S. Tsigaridas[156a] A. Tsirigotis[152,dd] V. Tsiskaridze[155] E. G. Tskhadadze,[149a] M. Tsopoulou[152,cc] Y. Tsujikawa[88] I. I. Tsukerman[37] V. Tsulaia[17a] S. Tsuno[84] O. Tsur,[150] K. Tsuri[118] D. Tsybychev[145] Y. Tu[64b] A. Tudorache[27b] V. Tudorache[27b] A. N. Tuna[36] S. Turchikhin[38] I. Turk Cakir[3a] R. Turra[71a] T. Turtuvshin[38,rr] P. M. Tuts[41] S. Tzamarias[152,cc] P. Tzanis[10] E. Tzovara[100] K. Uchida[153] F. Ukegawa[157] P. A. Ulloa Poblete,[137c,137b] E. N. Umaka[29] G. Unal[36] M. Unal[11] A. Undrus[29] G. Unel[160] J. Urban[28b] P. Urquijo[105] G. Usai[8] R. Ushioda[154] M. Usman[108] Z. Uysal[21b] L. Vacavant[102] V. Vacek[132] B. Vachon[104] K. O. H. Vadla[125] T. Vafeiadis[36] A. Vaitkus[96] C. Valderanis[109] E. Valdes Santurio[47a,47b] M. Valente[156a] S. Valentinetti[23b,23a] A. Valero[163] E. Valiente Moreno[163] A. Vallier[102,ii] J. A. Valls Ferrer[163] D. R. Van Arneman[114] T. R. Van Daalen[138] A. Van Der Graaf[49] P. Van Gemmeren[6] M. Van Rijnbach[125,36] S. Van Stroud[96] I. Van Vulpen[114] M. Vanadia[76a,76b] W. Vandelli[36] M. Vandenbroucke[135] E. R. Vandewall[121] D. Vannicola[151] L. Vannoli[57b,57a] R. Vari[75a] E. W. Varnes[7] C. Varni[17b] T. Varol[148] D. Varouchas[66]

L. Varriale[163] K. E. Varvell[147] M. E. Vasile[27b] L. Vaslin,[40] G. A. Vasquez[165] F. Vazeille[40]
T. Vazquez Schroeder[36] J. Veatch[31] V. Vecchio[101] M. J. Veen[103] I. Veliscek[126] L. M. Veloce[155]
F. Veloso[130a,130c] S. Veneziano[75a] A. Ventura[70a,70b] A. Verbytskyi[110] M. Verducci[74a,74b] C. Vergis[24]
M. Verissimo De Araujo[83b] W. Verkerke[114] J. C. Vermeulen[114] C. Vernieri[143] M. Vessella[103] M. C. Vetterli[142,e]
A. Vgenopoulos[152,cc] N. Viaux Maira[137f] T. Vickey[139] O. E. Vickey Boeriu[139] G. H. A. Viehhauser[126]
L. Vigani[63b] M. Villa[23b,23a] M. Villaplana Perez[163] E. M. Villhauer,[52] E. Vilucchi[53] M. G. Vincter[34]
G. S. Virdee[20] A. Vishwakarma[52] A. Visibile,[114] C. Vittori[36] I. Vivarelli[146] V. Vladimirov,[167] E. Voevodina[110]
F. Vogel[109] P. Vokac[132] J. Von Ahnen[48] E. Von Toerne[24] B. Vormwald[36] V. Vorobel[133] K. Vorobev[37]
M. Vos[163] K. Voss[141] J. H. Vossebeld[92] M. Vozak[114] L. Vozdecky[94] N. Vranjes[15]
M. Vranjes Milosavljevic[15] M. Vreeswijk[114] N. K. Vu[62d,62c] R. Vuillermet[36] O. Vujinovic[100] I. Vukotic[39]
S. Wada[157] C. Wagner,[103] J. M. Wagner[17a] W. Wagner[171] S. Wahdan[171] H. Wahlberg[90] R. Wakasa[157]
M. Wakida[111] J. Walder[134] R. Walker[109] W. Walkowiak[141] A. Wall[128] T. Wamorkar[6] A. Z. Wang[170]
C. Wang[100] C. Wang[62c] H. Wang[17a] J. Wang[64a] R.-J. Wang[100] R. Wang[61] R. Wang[6] S. M. Wang[148]
S. Wang[62b] T. Wang[62a] W. T. Wang[80] W. Wang[14a] X. Wang[14c] X. Wang[162] X. Wang[62c] Y. Wang[62d]
Y. Wang[14c] Z. Wang[106] Z. Wang[62d,51,62c] Z. Wang[106] A. Warburton[104] R. J. Ward[20] N. Warrack[59]
A. T. Watson[20] H. Watson[59] M. F. Watson[20] E. Watton[59,134] G. Watts[138] B. M. Waugh[96] C. Weber[29]
H. A. Weber[18] M. S. Weber[19] S. M. Weber[63a] C. Wei[62a] Y. Wei[126] A. R. Weidberg[126] E. J. Weik[117]
J. Weingarten[49] M. Weirich[100] C. Weiser[54] C. J. Wells[48] T. Wenaus[29] B. Wendland[49] T. Wengler[36]
N. S. Wenke,[110] N. Wermes[24] M. Wessels[63a] K. Whalen[123] A. M. Wharton[91] A. S. White[61] A. White[8]
M. J. White[1] D. Whiteson[160] L. Wickremasinghe[124] W. Wiedenmann[170] C. Wiel[50] M. Wielers[134]
C. Wiglesworth[42] D. J. Wilbern[120] H. G. Wilkens[36] D. M. Williams[41] H. H. Williams,[128] S. Williams[32]
S. Willocq[103] B. J. Wilson[101] P. J. Windischhofer[39] F. I. Winkel[30] F. Winklmeier[123] B. T. Winter[54]
J. K. Winter[101] M. Wittgen,[143] M. Wobisch[97] Z. Wolffs[114] R. Wölker[126] J. Wollrath,[160] M. W. Wolter[87]
H. Wolters[130a,130c] A. F. Wongel[48] S. D. Worm[48] B. K. Wosiek[87] K. W. Woźniak[87] S. Wozniewski[55]
K. Wraight[59] C. Wu[20] J. Wu[14a,14e] M. Wu[64a] M. Wu[113] S. L. Wu[170] X. Wu[56] Y. Wu[62a] Z. Wu[135]
J. Wuerzinger,[110,x] T. R. Wyatt[101] B. M. Wynne[52] S. Xella[42] L. Xia[14c] M. Xia[14b] J. Xiang[64c] X. Xiao[106]
M. Xie[62a] X. Xie[62a] S. Xin[14a,14e] J. Xiong[17a] D. Xu[14a] H. Xu[62a] L. Xu[62a] R. Xu[128] T. Xu[106] Y. Xu[14b]
Z. Xu[52] Z. Xu[14a] B. Yabsley[147] S. Yacoob[33a] N. Yamaguchi[89] Y. Yamaguchi[154] E. Yamashita,[153]
H. Yamauchi[157] T. Yamazaki[17a] Y. Yamazaki[85] J. Yan[62c] S. Yan[126] Z. Yan[25] H. J. Yang[62c,62d] H. T. Yang[62a]
S. Yang[62a] T. Yang[64c] X. Yang[62a] X. Yang[14a] Y. Yang[44] Y. Yang[62a] Z. Yang[62a] W-M. Yao[17a] Y. C. Yap[48]
H. Ye[14c] H. Ye[55] J. Ye[44] S. Ye[29] X. Ye[62a] Y. Yeh[96] I. Yeletskikh[38] B. K. Yeo[17b] M. R. Yexley[96]
P. Yin[41] K. Yorita[168] S. Younas[27b] C. J. S. Young[36] C. Young[143] Y. Yu[62a] M. Yuan[106] R. Yuan[62b,ss]
L. Yue[96] M. Zaazoua[62a] B. Zabinski[87] E. Zaid,[52] T. Zakareishvili[149b] N. Zakharchuk[34] S. Zambito[56]
J. A. Zamora Saa[137d,137b] J. Zang[153] D. Zanzi[54] O. Zaplatilek[132] C. Zeitnitz[171] H. Zeng[14a] J. C. Zeng[162]
D. T. Zenger Jr.[26] O. Zenin[37] T. Ženiš[28a] S. Zenz[94] S. Zerradi[35a] D. Zerwas[66] M. Zhai[14a,14e] B. Zhang[14c]
D. F. Zhang[139] J. Zhang[62b] J. Zhang[6] K. Zhang[14a,14e] L. Zhang[14c] P. Zhang[14a,14e] R. Zhang[170] S. Zhang[106]
T. Zhang[153] X. Zhang[62c] X. Zhang[62b] Y. Zhang[62c,5] Y. Zhang[96] Z. Zhang[17a] Z. Zhang[66] H. Zhao[138]
P. Zhao[51] T. Zhao[62b] Y. Zhao[136] Z. Zhao[62a] A. Zhemchugov[38] K. Zheng[162] X. Zheng[62a] Z. Zheng[143]
D. Zhong[162] B. Zhou,[106] H. Zhou[7] N. Zhou[62c] Y. Zhou,[7] C. G. Zhu[62b] J. Zhu[106] Y. Zhu[62c] Y. Zhu[62a]
X. Zhuang[14a] K. Zhukov[37] V. Zhulanov[37] N. I. Zimine[38] J. Zinsser[63b] M. Ziolkowski[141] L. Živković[15]
A. Zoccoli[23b,23a] K. Zoch[56] T. G. Zorbas[139] O. Zormpa[46] W. Zou[41] and L. Zwalinski[36]

(ATLAS Collaboration)

[1]*Department of Physics, University of Adelaide, Adelaide, Australia*
[2]*Department of Physics, University of Alberta, Edmonton, Alberta, Canada*
[3a]*Department of Physics, Ankara University, Ankara, Türkiye*
[3b]*Division of Physics, TOBB University of Economics and Technology, Ankara, Türkiye*
[4]*LAPP, Université Savoie Mont Blanc, CNRS/IN2P3, Annecy, France*
[5]*APC, Université Paris Cité, CNRS/IN2P3, Paris, France*

[6]High Energy Physics Division, Argonne National Laboratory, Argonne, Illinois, USA

[7]Department of Physics, University of Arizona, Tucson, Arizona, USA

[8]Department of Physics, University of Texas at Arlington, Arlington, Texas, USA

[9]Physics Department, National and Kapodistrian University of Athens, Athens, Greece

[10]Physics Department, National Technical University of Athens, Zografou, Greece

[11]Department of Physics, University of Texas at Austin, Austin, Texas, USA

[12]Institute of Physics, Azerbaijan Academy of Sciences, Baku, Azerbaijan

[13]Institut de Física d'Altes Energies (IFAE), Barcelona Institute of Science and Technology, Barcelona, Spain

[14a]Institute of High Energy Physics, Chinese Academy of Sciences, Beijing, China

[14b]Physics Department, Tsinghua University, Beijing, China

[14c]Department of Physics, Nanjing University, Nanjing, China

[14d]School of Science, Shenzhen Campus of Sun Yat-sen University, China

[14e]University of Chinese Academy of Science (UCAS), Beijing, China

[15]Institute of Physics, University of Belgrade, Belgrade, Serbia

[16]Department for Physics and Technology, University of Bergen, Bergen, Norway

[17a]Physics Division, Lawrence Berkeley National Laboratory, Berkeley, California, USA

[17b]University of California, Berkeley, California, USA

[18]Institut für Physik, Humboldt Universität zu Berlin, Berlin, Germany

[19]Albert Einstein Center for Fundamental Physics and Laboratory for High Energy Physics, University of Bern, Bern, Switzerland

[20]School of Physics and Astronomy, University of Birmingham, Birmingham, United Kingdom

[21a]Department of Physics, Bogazici University, Istanbul, Türkiye

[21b]Department of Physics Engineering, Gaziantep University, Gaziantep, Türkiye

[21c]Department of Physics, Istanbul University, Istanbul, Türkiye

[22a]Facultad de Ciencias y Centro de Investigaciónes, Universidad Antonio Nariño, Bogotá, Colombia

[22b]Departamento de Física, Universidad Nacional de Colombia, Bogotá, Colombia

[23a]Dipartimento di Fisica e Astronomia A. Righi, Università di Bologna, Bologna, Italy

[23b]INFN Sezione di Bologna, Bologna, Italy

[24]Physikalisches Institut, Universität Bonn, Bonn, Germany

[25]Department of Physics, Boston University, Boston, Massachusetts, USA

[26]Department of Physics, Brandeis University, Waltham, Massachusetts, USA

[27a]Transilvania University of Brasov, Brasov, Romania

[27b]Horia Hulubei National Institute of Physics and Nuclear Engineering, Bucharest, Romania

[27c]Department of Physics, Alexandru Ioan Cuza University of Iasi, Iasi, Romania

[27d]National Institute for Research and Development of Isotopic and Molecular Technologies, Physics Department, Cluj-Napoca, Romania

[27e]National University of Science and Technology Politechnica, Bucharest, Romania

[27f]West University in Timisoara, Timisoara, Romania

[27g]Faculty of Physics, University of Bucharest, Bucharest, Romania

[28a]Faculty of Mathematics, Physics and Informatics, Comenius University, Bratislava, Slovak Republic

[28b]Department of Subnuclear Physics, Institute of Experimental Physics of the Slovak Academy of Sciences, Kosice, Slovak Republic

[29]Physics Department, Brookhaven National Laboratory, Upton, New York, USA

[30]Universidad de Buenos Aires, Facultad de Ciencias Exactas y Naturales, Departamento de Física, y CONICET, Instituto de Física de Buenos Aires (IFIBA), Buenos Aires, Argentina

[31]California State University, California, USA

[32]Cavendish Laboratory, University of Cambridge, Cambridge, United Kingdom

[33a]Department of Physics, University of Cape Town, Cape Town, South Africa

[33b]iThemba Labs, Western Cape, South Africa

[33c]Department of Mechanical Engineering Science, University of Johannesburg, Johannesburg, South Africa

[33d]National Institute of Physics, University of the Philippines Diliman, Quezon City, Philippines

[33e]University of South Africa, Department of Physics, Pretoria, South Africa

[33f]University of Zululand, KwaDlangezwa, South Africa

[33g]School of Physics, University of the Witwatersrand, Johannesburg, South Africa

[34]Department of Physics, Carleton University, Ottawa, Ontario, Canada

[35a]Faculté des Sciences Ain Chock, Réseau Universitaire de Physique des Hautes Energies—Université Hassan II, Casablanca, Morocco

[35b]Faculté des Sciences, Université Ibn-Tofail, Kénitra, Morocco

[35c]*Faculté des Sciences Semlalia, Université Cadi Ayyad, LPHEA-Marrakech, Morocco*
[35d]*LPMR, Faculté des Sciences, Université Mohamed Premier, Oujda, Morocco*
[35e]*Faculté des sciences, Université Mohammed V, Rabat, Morocco*
[35f]*Institute of Applied Physics, Mohammed VI Polytechnic University, Ben Guerir, Morocco*
[36]*CERN, Geneva, Switzerland*
[37]*Affiliated with an institute covered by a cooperation agreement with CERN*
[38]*Affiliated with an international laboratory covered by a cooperation agreement with CERN*
[39]*Enrico Fermi Institute, University of Chicago, Chicago, Illinois, USA*
[40]*LPC, Université Clermont Auvergne, CNRS/IN2P3, Clermont-Ferrand, France*
[41]*Nevis Laboratory, Columbia University, Irvington, New York, USA*
[42]*Niels Bohr Institute, University of Copenhagen, Copenhagen, Denmark*
[43a]*Dipartimento di Fisica, Università della Calabria, Rende, Italy*
[43b]*INFN Gruppo Collegato di Cosenza, Laboratori Nazionali di Frascati, Frascati, Italy*
[44]*Physics Department, Southern Methodist University, Dallas, Texas, USA*
[45]*Physics Department, University of Texas at Dallas, Richardson, Texas, USA*
[46]*National Centre for Scientific Research "Demokritos", Agia Paraskevi, Greece*
[47a]*Department of Physics, Stockholm University, Stockholm, Sweden*
[47b]*Oskar Klein Centre, Stockholm, Sweden*
[48]*Deutsches Elektronen-Synchrotron DESY, Hamburg and Zeuthen, Germany*
[49]*Fakultät Physik, Technische Universität Dortmund, Dortmund, Germany*
[50]*Institut für Kern- und Teilchenphysik, Technische Universität Dresden, Dresden, Germany*
[51]*Department of Physics, Duke University, Durham, North Carolina, USA*
[52]*SUPA—School of Physics and Astronomy, University of Edinburgh, Edinburgh, United Kingdom*
[53]*INFN e Laboratori Nazionali di Frascati, Frascati, Italy*
[54]*Physikalisches Institut, Albert-Ludwigs-Universität Freiburg, Freiburg, Germany*
[55]*II. Physikalisches Institut, Georg-August-Universität Göttingen, Göttingen, Germany*
[56]*Département de Physique Nucléaire et Corpusculaire, Université de Genève, Genève, Switzerland*
[57a]*Dipartimento di Fisica, Università di Genova, Genova, Italy*
[57b]*INFN Sezione di Genova, Genova, Italy*
[58]*II. Physikalisches Institut, Justus-Liebig-Universität Giessen, Giessen, Germany*
[59]*SUPA—School of Physics and Astronomy, University of Glasgow, Glasgow, United Kingdom*
[60]*LPSC, Université Grenoble Alpes, CNRS/IN2P3, Grenoble INP, Grenoble, France*
[61]*Laboratory for Particle Physics and Cosmology, Harvard University, Cambridge, Massachusetts, USA*
[62a]*Department of Modern Physics and State Key Laboratory of Particle Detection and Electronics, University of Science and Technology of China, Hefei, China*
[62b]*Institute of Frontier and Interdisciplinary Science and Key Laboratory of Particle Physics and Particle Irradiation (MOE), Shandong University, Qingdao, China*
[62c]*School of Physics and Astronomy, Shanghai Jiao Tong University, Key Laboratory for Particle Astrophysics and Cosmology (MOE), SKLPPC, Shanghai, China*
[62d]*Tsung-Dao Lee Institute, Shanghai, China*
[63a]*Kirchhoff-Institut für Physik, Ruprecht-Karls-Universität Heidelberg, Heidelberg, Germany*
[63b]*Physikalisches Institut, Ruprecht-Karls-Universität Heidelberg, Heidelberg, Germany*
[64a]*Department of Physics, Chinese University of Hong Kong, Shatin, N.T., Hong Kong, China*
[64b]*Department of Physics, University of Hong Kong, Hong Kong, China*
[64c]*Department of Physics and Institute for Advanced Study, Hong Kong University of Science and Technology, Clear Water Bay, Kowloon, Hong Kong, China*
[65]*Department of Physics, National Tsing Hua University, Hsinchu, Taiwan*
[66]*IJCLab, Université Paris-Saclay, CNRS/IN2P3, 91405, Orsay, France*
[67]*Centro Nacional de Microelectrónica (IMB-CNM-CSIC), Barcelona, Spain*
[68]*Department of Physics, Indiana University, Bloomington, Indiana, USA*
[69a]*INFN Gruppo Collegato di Udine, Sezione di Trieste, Udine, Italy*
[69b]*ICTP, Trieste, Italy*
[69c]*Dipartimento Politecnico di Ingegneria e Architettura, Università di Udine, Udine, Italy*
[70a]*INFN Sezione di Lecce, Lecce, Italy*
[70b]*Dipartimento di Matematica e Fisica, Università del Salento, Lecce, Italy*
[71a]*INFN Sezione di Milano, Milano, Italy*
[71b]*Dipartimento di Fisica, Università di Milano, Milano, Italy*
[72a]*INFN Sezione di Napoli, Napoli, Italy*
[72b]*Dipartimento di Fisica, Università di Napoli, Napoli, Italy*
[73a]*INFN Sezione di Pavia, Pavia, Italy*

[73b]Dipartimento di Fisica, Università di Pavia, Pavia, Italy
[74a]INFN Sezione di Pisa, Pisa, Italy
[74b]Dipartimento di Fisica E. Fermi, Università di Pisa, Pisa, Italy
[75a]INFN Sezione di Roma, Roma, Italy
[75b]Dipartimento di Fisica, Sapienza Università di Roma, Roma, Italy
[76a]INFN Sezione di Roma Tor Vergata, Roma, Italy
[76b]Dipartimento di Fisica, Università di Roma Tor Vergata, Roma, Italy
[77a]INFN Sezione di Roma Tre, Roma, Italy
[77b]Dipartimento di Matematica e Fisica, Università Roma Tre, Roma, Italy
[78a]INFN-TIFPA, Trento, Italy
[78b]Università degli Studi di Trento, Trento, Italy
[79]Universität Innsbruck, Department of Astro and Particle Physics, Innsbruck, Austria
[80]University of Iowa, Iowa City, Iowa, USA
[81]Department of Physics and Astronomy, Iowa State University, Ames, Iowa, USA
[82]Istinye University, Sariyer, Istanbul, Türkiye
[83a]Departamento de Engenharia Elétrica, Universidade Federal de Juiz de Fora (UFJF),
Juiz de Fora, Brazil
[83b]Universidade Federal do Rio De Janeiro COPPE/EE/IF, Rio de Janeiro, Brazil
[83c]Instituto de Física, Universidade de São Paulo, São Paulo, Brazil
[83d]Rio de Janeiro State University, Rio de Janeiro, Brazil
[84]KEK, High Energy Accelerator Research Organization, Tsukuba, Japan
[85]Graduate School of Science, Kobe University, Kobe, Japan
[86a]AGH University of Krakow, Faculty of Physics and Applied Computer Science, Krakow, Poland
[86b]Marian Smoluchowski Institute of Physics, Jagiellonian University, Krakow, Poland
[87]Institute of Nuclear Physics Polish Academy of Sciences, Krakow, Poland
[88]Faculty of Science, Kyoto University, Kyoto, Japan
[89]Research Center for Advanced Particle Physics and Department of Physics, Kyushu University,
Fukuoka, Japan
[90]Instituto de Física La Plata, Universidad Nacional de La Plata and CONICET, La Plata, Argentina
[91]Physics Department, Lancaster University, Lancaster, United Kingdom
[92]Oliver Lodge Laboratory, University of Liverpool, Liverpool, United Kingdom
[93]Department of Experimental Particle Physics, Jožef Stefan Institute and Department of Physics,
University of Ljubljana, Ljubljana, Slovenia
[94]School of Physics and Astronomy, Queen Mary University of London, London, United Kingdom
[95]Department of Physics, Royal Holloway University of London, Egham, United Kingdom
[96]Department of Physics and Astronomy, University College London, London, United Kingdom
[97]Louisiana Tech University, Ruston, Louisiana, USA
[98]Fysiska institutionen, Lunds universitet, Lund, Sweden
[99]Departamento de Física Teorica C-15 and CIAFF, Universidad Autónoma de Madrid, Madrid, Spain
[100]Institut für Physik, Universität Mainz, Mainz, Germany
[101]School of Physics and Astronomy, University of Manchester, Manchester, United Kingdom
[102]CPPM, Aix-Marseille Université, CNRS/IN2P3, Marseille, France
[103]Department of Physics, University of Massachusetts, Amherst, Massachusetts, USA
[104]Department of Physics, McGill University, Montreal, Quebec, Canada
[105]School of Physics, University of Melbourne, Victoria, Australia
[106]Department of Physics, University of Michigan, Ann Arbor, Michigan, USA
[107]Department of Physics and Astronomy, Michigan State University, East Lansing, Michigan, USA
[108]Group of Particle Physics, University of Montreal, Montreal, Quebec, Canada
[109]Fakultät für Physik, Ludwig-Maximilians-Universität München, München, Germany
[110]Max-Planck-Institut für Physik (Werner-Heisenberg-Institut), München, Germany
[111]Graduate School of Science and Kobayashi-Maskawa Institute, Nagoya University, Nagoya, Japan
[112]Department of Physics and Astronomy, University of New Mexico, Albuquerque, New Mexico, USA
[113]Institute for Mathematics, Astrophysics and Particle Physics, Radboud University/Nikhef,
Nijmegen, Netherlands
[114]Nikhef National Institute for Subatomic Physics and University of Amsterdam, Amsterdam, Netherlands
[115]Department of Physics, Northern Illinois University, DeKalb, Illinois, USA
[116a]New York University Abu Dhabi, Abu Dhabi, United Arab Emirates
[116b]University of Sharjah, Sharjah, United Arab Emirates
[117]Department of Physics, New York University, New York, New York, USA
[118]Ochanomizu University, Otsuka, Bunkyo-ku, Tokyo, Japan

[119]*The Ohio State University, Columbus, Ohio, USA*

[120]*Homer L. Dodge Department of Physics and Astronomy, University of Oklahoma, Norman, Oklahoma, USA*

[121]*Department of Physics, Oklahoma State University, Stillwater, Oklahoma, USA*

[122]*Palacký University, Joint Laboratory of Optics, Olomouc, Czech Republic*

[123]*Institute for Fundamental Science, University of Oregon, Eugene, Oregon, USA*

[124]*Graduate School of Science, Osaka University, Osaka, Japan*

[125]*Department of Physics, University of Oslo, Oslo, Norway*

[126]*Department of Physics, Oxford University, Oxford, United Kingdom*

[127]*LPNHE, Sorbonne Université, Université Paris Cité, CNRS/IN2P3, Paris, France*

[128]*Department of Physics, University of Pennsylvania, Philadelphia, Pennsylvania, USA*

[129]*Department of Physics and Astronomy, University of Pittsburgh, Pittsburgh, Pennsylvania, USA*

[130a]*Laboratório de Instrumentação e Física Experimental de Partículas—LIP, Lisboa, Portugal*

[130b]*Departamento de Física, Faculdade de Ciências, Universidade de Lisboa, Lisboa, Portugal*

[130c]*Departamento de Física, Universidade de Coimbra, Coimbra, Portugal*

[130d]*Centro de Física Nuclear da Universidade de Lisboa, Lisboa, Portugal*

[130e]*Departamento de Física, Universidade do Minho, Braga, Portugal*

[130f]*Departamento de Física Teórica y del Cosmos, Universidad de Granada, Granada, Spain*

[130g]*Departamento de Física, Instituto Superior Técnico, Universidade de Lisboa, Lisboa, Portugal*

[131]*Institute of Physics of the Czech Academy of Sciences, Prague, Czech Republic*

[132]*Czech Technical University in Prague, Prague, Czech Republic*

[133]*Charles University, Faculty of Mathematics and Physics, Prague, Czech Republic*

[134]*Particle Physics Department, Rutherford Appleton Laboratory, Didcot, United Kingdom*

[135]*IRFU, CEA, Université Paris-Saclay, Gif-sur-Yvette, France*

[136]*Santa Cruz Institute for Particle Physics, University of California Santa Cruz, Santa Cruz, California, USA*

[137a]*Departamento de Física, Pontificia Universidad Católica de Chile, Santiago, Chile*

[137b]*Millennium Institute for Subatomic physics at high energy frontier (SAPHIR), Santiago, Chile*

[137c]*Instituto de Investigación Multidisciplinario en Ciencia y Tecnología, y Departamento de Física, Universidad de La Serena, La Serena, Chile*

[137d]*Universidad Andres Bello, Department of Physics, Santiago, Chile*

[137e]*Instituto de Alta Investigación, Universidad de Tarapacá, Arica, Chile*

[137f]*Departamento de Física, Universidad Técnica Federico Santa María, Valparaíso, Chile*

[138]*Department of Physics, University of Washington, Seattle, Washington, USA*

[139]*Department of Physics and Astronomy, University of Sheffield, Sheffield, United Kingdom*

[140]*Department of Physics, Shinshu University, Nagano, Japan*

[141]*Department Physik, Universität Siegen, Siegen, Germany*

[142]*Department of Physics, Simon Fraser University, Burnaby, British Columbia, Canada*

[143]*SLAC National Accelerator Laboratory, Stanford, California, USA*

[144]*Department of Physics, Royal Institute of Technology, Stockholm, Sweden*

[145]*Departments of Physics and Astronomy, Stony Brook University, Stony Brook, New York, USA*

[146]*Department of Physics and Astronomy, University of Sussex, Brighton, United Kingdom*

[147]*School of Physics, University of Sydney, Sydney, Australia*

[148]*Institute of Physics, Academia Sinica, Taipei, Taiwan*

[149a]*E. Andronikashvili Institute of Physics, Iv. Javakhishvili Tbilisi State University, Tbilisi, Georgia*

[149b]*High Energy Physics Institute, Tbilisi State University, Tbilisi, Georgia*

[149c]*University of Georgia, Tbilisi, Georgia*

[150]*Department of Physics, Technion, Israel Institute of Technology, Haifa, Israel*

[151]*Raymond and Beverly Sackler School of Physics and Astronomy, Tel Aviv University, Tel Aviv, Israel*

[152]*Department of Physics, Aristotle University of Thessaloniki, Thessaloniki, Greece*

[153]*International Center for Elementary Particle Physics and Department of Physics, University of Tokyo, Tokyo, Japan*

[154]*Department of Physics, Tokyo Institute of Technology, Tokyo, Japan*

[155]*Department of Physics, University of Toronto, Toronto, Ontario, Canada*

[156a]*TRIUMF, Vancouver, British Columbia, Canada*

[156b]*Department of Physics and Astronomy, York University, Toronto, Ontario, Canada*

[157]*Division of Physics and Tomonaga Center for the History of the Universe, Faculty of Pure and Applied Sciences, University of Tsukuba, Tsukuba, Japan*

[158]*Department of Physics and Astronomy, Tufts University, Medford, Massachusetts, USA*

[159]*United Arab Emirates University, Al Ain, United Arab Emirates*

[160]*Department of Physics and Astronomy, University of California Irvine, Irvine, California, USA*
[161]*Department of Physics and Astronomy, University of Uppsala, Uppsala, Sweden*
[162]*Department of Physics, University of Illinois, Urbana, Illinois, USA*
[163]*Instituto de Física Corpuscular (IFIC), Centro Mixto Universidad de Valencia—CSIC, Valencia, Spain*
[164]*Department of Physics, University of British Columbia, Vancouver, British Columbia, Canada*
[165]*Department of Physics and Astronomy, University of Victoria, Victoria, British Columbia, Canada*
[166]*Fakultät für Physik und Astronomie, Julius-Maximilians-Universität Würzburg, Würzburg, Germany*
[167]*Department of Physics, University of Warwick, Coventry, United Kingdom*
[168]*Waseda University, Tokyo, Japan*
[169]*Department of Particle Physics and Astrophysics, Weizmann Institute of Science, Rehovot, Israel*
[170]*Department of Physics, University of Wisconsin, Madison, Wisconsin, USA*
[171]*Fakultät für Mathematik und Naturwissenschaften, Fachgruppe Physik,*
Bergische Universität Wuppertal, Wuppertal, Germany
[172]*Department of Physics, Yale University, New Haven, Connecticut, USA*

[a]Deceased.
[b]Also at Department of Physics, King's College London, London, United Kingdom.
[c]Also at Institute of Physics, Azerbaijan Academy of Sciences, Baku, Azerbaijan.
[d]Also at Lawrence Livermore National Laboratory, Livermore, California, USA.
[e]Also at TRIUMF, Vancouver, British Columbia, Canada.
[f]Also at Department of Physics, University of Thessaly, Greece.
[g]Also at An-Najah National University, Nablus, Palestine.
[h]Also at Department of Physics, University of Fribourg, Fribourg, Switzerland.
[i]Also at University of Colorado Boulder, Department of Physics, Colorado, Boulder, USA.
[j]Also at Department of Physics and Astronomy, University of Victoria, Victoria, British Columbia, Canada.
[k]Also at Department of Physics, Westmont College, Santa Barbara, California, USA.
[l]Also at Departament de Fisica de la Universitat Autonoma de Barcelona, Barcelona, Spain.
[m]Also at Affiliated with an institute covered by a cooperation agreement with CERN.
[n]Also at The Collaborative Innovation Center of Quantum Matter (CICQM), Beijing, China.
[o]Also at Department of Physics, Ben Gurion University of the Negev, Beer Sheva, Israel.
[p]Also at Università di Napoli Parthenope, Napoli, Italy.
[q]Also at Institute of Particle Physics (IPP), Canada.
[r]Also at Borough of Manhattan Community College, City University of New York, New York, New York, USA.
[s]Also at National Institute of Physics, University of the Philippines Diliman (Philippines), Philippines.
[t]Also at Department of Financial and Management Engineering, University of the Aegean, Chios, Greece.
[u]Also at Department of Physics, Stanford University, Stanford, California, USA.
[v]Also at Centro Studi e Ricerche Enrico Fermi, Italy.
[w]Also at Institucio Catalana de Recerca i Estudis Avancats, ICREA, Barcelona, Spain.
[x]Also at Technical University of Munich, Munich, Germany.
[y]Also at Department of Physics and Astronomy, University of Sheffield, Sheffield, United Kingdom.
[z]Also at Yeditepe University, Physics Department, Istanbul, Türkiye.
[aa]Also at Institute of Theoretical Physics, Ilia State University, Tbilisi, Georgia.
[bb]Also at CERN, Geneva, Switzerland.
[cc]Also at Center for Interdisciplinary Research and Innovation (CIRI-AUTH), Thessaloniki, Greece.
[dd]Also at Hellenic Open University, Patras, Greece.
[ee]Also at Center for High Energy Physics, Peking University, China.
[ff]Also at APC, Université Paris Cité, CNRS/IN2P3, Paris, France.
[gg]Also at IRFU, CEA, Université Paris-Saclay, Gif-sur-Yvette, France.
[hh]Also at Department of Physics, Royal Holloway University of London, Egham, United Kingdom.
[ii]Also at L2IT, Université de Toulouse, CNRS/IN2P3, UPS, Toulouse, France.
[jj]Also at Department of Physics, California State University, Sacramento, California, USA.
[kk]Also at Département de Physique Nucléaire et Corpuscular, Université de Genève, Genève, Switzerland.
[ll]Also at Fakultät für Mathematik und Naturwissenschaften, Fachgruppe Physik, Bergische Universität Wuppertal, Wuppertal, Germany.
[mm]Also at Institute for Nuclear Research and Nuclear Energy (INRNE) of the Bulgarian Academy of Sciences, Sofia, Bulgaria.
[nn]Also at Washington College, Chestertown, Maryland, USA.
[oo]Also at School of Physics and Astronomy, University of Birmingham, Birmingham, United Kingdom.

[pp]Also at Institut für Experimentalphysik, Universität Hamburg, Hamburg, Germany.

[qq]Also at Institute of Applied Physics, Mohammed VI Polytechnic University, Ben Guerir, Morocco.

[rr]Also at Institute of Physics and Technology, Mongolian Academy of Sciences, Ulaanbaatar, Mongolia.

[ss]Also at Department of Physics and Astronomy, Michigan State University, East Lansing, Michigan, USA.